IDENTIFICATION OF INTERFERON REGULATORY FACTOR 4 (IRF4) - INTERACTING PROTEINS IN MELANOMA CELL LINES

by
Ekin Ece Erkan
B.S., Molecular Biology and Genetics, Boğaziçi University, 2012

Submitted to the Institute for Graduate Studies in
Science and Engineering in partial fulfillment of
the requirements for the degree of
Master of Science

Graduate Program in Molecular Biology and Genetics
Boğaziçi University
2015

IDENTIFICATION OF IRF4-INTERACTING PROTEINS
IN MELANOMA CELL LINES

APPROVED BY:

Assoc. Prof. N. C. Tolga Emre ……
(Thesis Supervisor)

Prof. Nesrin Özören ……

Assist.Prof. Elif Nur Fırat Karalar ……

DATE OF APPROVAL: 17.09.2015

ACKNOWLEDGEMENTS

I would like to express deepest gratitude to my supervisor, Assoc. Prof. Tolga Emre for his endless support and guidance throughout my thesis studies. He accepted me to his lab when I was an undergraduate student, from the day I started to work with him, his motivation made me more and more curious towards science and he has been the reason of my decision to get a master's degree. Furthermore, along my master studies, he contributed too much on my improvement as a researcher.

I would like to thank Prof. Nesrin Özören for spending time on the evaluation of this thesis. She has been supportive along my undergraduate education and my master studies.

I would also like to thank my third jury member Assist. Prof. Elif Nur Fırat Karalar for evaluating this thesis. Besides, she contributed too much on this thesis by sharing her knowledge on BioID with me, most of the data in this thesis obtained thanks to her.

I appreciate my lab-mates Ulduz Sobhiafshar, Cansu Yerinde, Ahmet Buğra Tufan, Nalan Yıldız and Anna Öğmen for their practical contributions. I would like to emphasize my special thanks to my former lab-mates Erdem Yılmaz, Mustafa Can Ayhan and Begüm Alankuş, their scientific and moral support was always with me even after they graduated.

I am very thankful to Uğur Kaplan for his endless patience throughout the times I was very stressful and desperate. Besides his moral support, he also guided me scientifically and I am very grateful to have him in my life.

I would like to thank kindly the members of our sibling laboratory (AKİL) members, Aybüke Alıcı Garipcan, Mustafa Yalçınkaya and Ceren Saygı. They supported me

in all aspects. Their scientific contribution to this thesis can not be denied as well as their moral support.

Further I would like to honor to my closest friends; Güneş Tunçgenç, Vahap Kapıkıran, Pelin Aksoy Kapıkıran, Güner Kaçmaz, Ayşegül Kaçmaz, and Mehmet Ali Dalyan for their friendship and help whenever I needed them the most.

Finally, I would like to emphasize my strongest gratitude to my parents; Nurhan Erkan and Tayfun Erkan. This thesis is dedicated to them for their support throughout my life.

This study was supported by grants from EMBO - Integration Grant (IG) - 2338, TUBITAK- 1001-113Z103 and Boğaziçi Bilimsel Araştırma Projeleri (BAP – 6704, BAP – 9120).

ABSTRACT

IDENTIFICATION OF INTERFERON REGULATORY FACTOR 4 (IRF4)-INTERACTING PROTEINS IN MELANOMA CELL LINES

IRF4 is a member of interferon regulatory factor family of transcription factors. Previously, IRF4 was shown to have regulatory roles in immune cells and B-cell malignancies. In addition, IRF4 was recently shown to be expressed in cells other than immune related cells; such as adipocytes and melanocytes. Its expression in melanocytes and certain melanoma cell lines guided us to investigate the role of IRF4 in melanoma.

Proteins interact with other proteins in the cells to function properly. There are many identified interaction partners of IRF4 in immune cells and especially the interaction of IRF4 with some members of ETS family transcription factors was observed to have a critical role in B-cell malignancies. However, interaction partners of IRF4 are not identified in melanoma cell lines; identification of these proteins might shed a light on the role of IRF4 in melanoma cell progression. For this purpose, we used Tandem affinity purification (TAP) and BioID methods to identify the interaction partners of IRF4. The candidate IRF4-interacting proteins identified with mass spectrometry data from TAP and BioID, are mostly involved in pre-mRNA processing and splicing, suggesting a role for IRF4 in these processes; yet further studies should be conducted to conclude the role of IRF4 in pre-mRNA processing and splicing.

Two of the proteins, obtained from the mass spectrometry data of TAP and BioID, were studied further to validate their interaction with IRF4 and one of them was shown to interact with IRF4 in SKMEL28 melanoma cell line via other methods in addition to TAP and BioID. This transcription factor is a novel interaction partner of IRF4, which was not shown to be correlated with IRF4 in other studies.

ÖZET

INTERFERON REGULATORY FACTOR 4 (IRF4)'ÜN MELANOMA HÜCRE HATLARINDAKİ ETKİLEŞİM PARTNERLERİNİN BELİRLENMESİ

IRF4, interferon regulatory factor ailesinden bir transkripsiyon faktördür. IRF4, daha once sadece B-hücresi gibi bağışıklık hücreleri ve malignansileriyle ilişkilendirilmiştir. Ancak son zamanlarda, bağışıklık hücresi olmayan adiposit ve melanosit gibi hücre tiplerinde de IRF4 ekspresyonu gözlemlenmiştir. IRF4 proteinin melanosit ve melanoma hücrelerindeki ekspresyonu, bizi IRF4 proteinin melanoma hücreleri üzerindeki etkisini araştırmaya yönlendirdi.

Proteinler hücredeki fonksiyonlarını yerine getirmek için başka proteinlerle etkileşim içine girerler. IRF4'un da bağışıklık hücrelerinde tanımlanmış bir çok etkileşim partnerleri bulunmaktadır; özellikle ETS ailesine ait transkripsiyon faktörleriyle olan etkileşiminin B hücresi malignansilerinde önemli bir role sahip olduğu gözlenmiştir. IRF4'ün melanoma hücrelerindeki etkileşim partnerleri henüz tanımlanmamıştır ve bunların tanımlanması IRF4'ün melanoma progresyonu üzerindeki etkisine de ışık tutacaktır. Bu amaçla, biz de Tandem affinity purification (TAP) ve BioID metodlarını kullanarak IRF4 ile etkileşime giren proteinleri tanımlamayı amaçladık. TAP ve BioID metodları ile elde edilen kütle spektrometresi dataları sonucunda tanımlanan IRF4'ün muhtemel etkileşim partnerlerinin çoğunun RNA'nın işlenmesi ve RNA uçbirleştirme fonksiyonlarında görev alması IRF4'ün de böyle bir fonksyionu olabileceğini göstermektedir; ancak böyle bir çıkarım yapabilmek için daha fazla çalışmaya ihtiyaç vardır.

TAP ve BioID metodları sonucunda kütle spektrometrisinden elde edilen proteinlerden ikisi, IRF4 ile etkileşimlerinin konfirmasyonu için başka çalışmalarda kullanılmıştır ve bunlardan bir tanesinin SKMEL28 melanoma hücre hattında IRF4 ile etkileşimi TAP ve BioID metodlarına ek olarak başka metodlarla da gösterilmiştir. Bu transkripsiyon faktörü IRF4'ün yeni bir etkileşim partneridir ve daha once başka çalışmalarda gösterilmemiştir.

TABLE OF CONTENTS

LIST OF FIGURES

LIST OF TABLES

LIST OF SYMBOLS

bp	Base Pairs
g	Gravity
gr	Gram
kb	Kilobase
kDa	Kilodalton
L	Liter
M	Molar
mA	Milliamper
mg	Milligram
min	Minute
ml	Milliliter
mm	Millimeter
mM	Millimolar
ng	Nanogram
s	Second
V	Volt
^{o}C	Centigrade degree
µg	Microgram
µl	Microliter
β	Beta

LIST OF ACRONYMS / ABBREVIATIONS

ABC-DLBCL	Activated B-cell like diffuse large B-cell lymphoma
AKT	V-Akt Murine Thymoma Viral Oncogene / Protein Kinase B
ALCL	Anaplastic Large Cell Lymphoma
APS	Ammonium persulfate
BAT	Biotin acceptor tag
BCL	B-cell lymphoma
BCLAF1	Bcl-2 Associated Trasncription Factor 1
BirA	Biotin protein ligase
BirA*	R118G mutant of biotin protein ligase
BRAF	V-raf murine sarcoma viral oncogene homolog B
BSA	Bovine serum albumin
$CaCl_2$	Calcium chloride
CDK4	Cyclin dependent kinase 4
CDKN2A	Cyclin dependent kinase inhibitor 2A
CO_2	Carbon dioxide
C-terminal	Carboxy terminal
DBD	DNA binding domain
ddH_2O	Double-distilled water
DMEM	Dubecco's modified eagle medium
DMSO	Dimethyl sulfoxide
DNA	Deoxyribonucleic acid
E47	Transcription factor E2-alpha
ECL	Enhanced chemiluminescent solution
EDTA	Ethylenediaminetetraacetate
EtOH	Ethanol
FBS	Fetal bovine serum
FC	Fold change
FOXP3	Forkhead box protein P3
F/T	Flowthrough
GCB-DLBCL	Germinal center B-cell like diffuse large B-cell lymphoma

GFP	Green fluorescent protein
GO	Gene ontology
HEPES	4-(2-hydroxyethyl)-1-piperazineethanesulfonic acid
HRP	Horseradish peroxidase
IAD	IRF association domain
IRF4	Interferon regulatory factor 4
LB	Luria-Bertani broth
MAPK	Mitogen activated protein kinase
$MgCl_2$	Magnesium chloride
MITF	Microthalmia-associated transcription factor
MM	Multiple myeloma
mRNA	Messenger RNA
MS	Mass spectrometry
N-terminal	Amino terminal
NF-κB	Nuclear factor kappa B
NFAT	Nuclear factor of activated T-cells
NONO	Non-POU domain containing octamer binding protein
NRAS	Neuroblastoma v-ras oncogene homolog
NSAF	Normalized spectral abundance factor
PAGE	Polyacrylamide gel electrophoresis
PBS	Phosphate buffered saline
PCR	Polymerase chain reaction
PI3K	Phosphoinositide-3-OH kinase
PIP_2	Phosphatidylinositol (4,5)-bisphosphate
PIP_3	Phosphatidylinositol (3,4,5)-triphosphate
PSPC1	Paraspeckle component 1
PU.1	Transcription factor PU.1
PTEN	Phosphate and tensin homologue
PVDF	Polyvinylidene fluoride
Q61R	Glutamine to arginine substitituon
Q61K	Glutamine to lysine substitituon
RNA	Ribonucleic acid
rpm	Revolution per minute

RT	Room temperature
SDS	Sodium dodecyl sulfate
SFPQ	Splicing factor, proline- and glutamine-rich
shRNA	Short hairpin RNA
shLuc	Short hairpin RNA against Luciferase
SNP	Single nucleotide polymorphism
SPI-B	Trancription factor SPI-B
SRSF10	Serine/arginine-rich splicing factor 10
STAT3	Signal transducer and activator of transcription 3
STAT6	Signal transducer and activator of transcription 6
TAD	Transactivation domain
TAP	Tandem affinity purification
TBS	Tris-buffered saline
TBS-T	Tris buffered saline with tween
TEMED	Tetramethylethylenediamine
TFAP2A	Activating enhancer binding protein 2 alpha
Tris	Tris (hydroxylmethyl) aminomethane
Tween	Polysorbate
TYR	Tyrosinase
Unt	Untransfected
UV	Ultraviolet
V600E	Valine to glutamic acid substitituon

1. INTRODUCTION

1.1. Melanoma

Cancer cells are characterized by the defective regulation of cell proliferation and homeostasis. Transformation of normal human cells into cancer cells is a multistep process, involving the acquisition of different traits by the cells. The different traits that provide the malignant physiology of cancer cells can be grouped into six primary categories; which are self-sufficiency in growth signals, insensitivity to growth inhibitory signals, evasion of programmed cell death, limitless replicative potential, sustained angiogenesis, and tissue invasion and metastasis. (Hanahan and Weinberg, 2000)

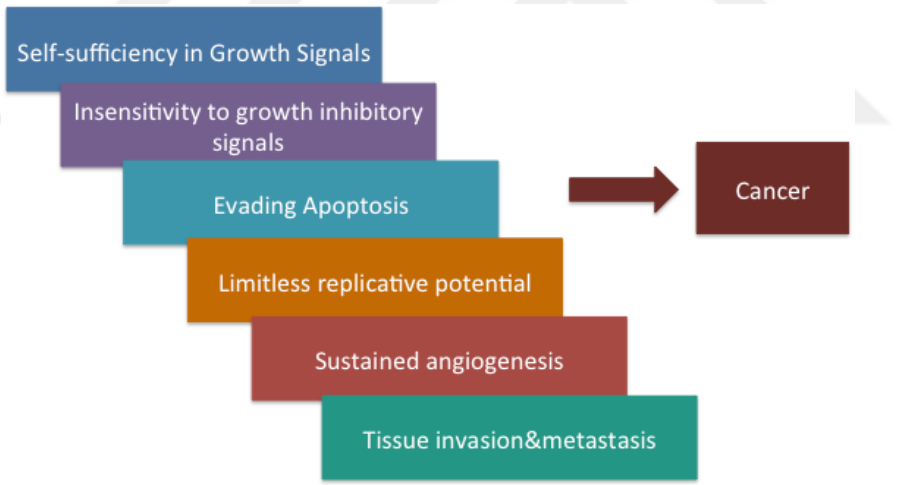

Figure 1.1 Major traits required for the transformation of normal cells into cancerous cells (adapted from Hanahan and Weinberg, 2000).

Melanoma is a type of skin cancer, originating from pigment producing cells of the epidermis layer (melanocytes). Melanoma is the most aggressive among skin cancers. Eventhough it constitutes 4% of skin cancers, it causes 80% of the mortality from skin cancers. If melanoma is diagnosed at an early stage, it can be cured via surgical dis-

section of the tumor. However, for patients with stage III and stage IV metastatic melanoma, 5-year survival rate is less than 10% (Kuphal and Bosserhoff, 2009).

Although the primary site of melanoma is skin, it can also arise in other parts of body, again with the transformation of melanocytes, such as in the eye (uveal melanoma), vulva (vulval melanoma) or vagina (vaginal melanoma). Still the most common type is cutaneous malignant melanoma that arises in the skin (Costin and Hearing, 2007).

Tranformation of melanocytes into melanoma cells is a multistep process, requiring genetic alterations that cause abnormal cell proliferation and homeostasis (Vultur and Herlyn, 2013). Most common mutation observed in melanoma cells is BRAF mutation (V600E) with a percentage of 66%. NRAS mutation (Q61R and Q61K) is also common with a percentage of 15% (Ch'ng and Tan, 2009). However, BRAF and NRAS mutations are mutually exclusive as the presence of double mutation results in a senescent phenotype in melanoma cells, indicating natural selection against double mutant cells (Yang *et al.*, 2013). Oncogenic BRAF and NRAS regulates MAPK and PI3K-AKT pathways; their mutations results in hyperactivation of MAPK and PI3K-Akt pathways, leading to increased cell proliferation, survival, invasion and migration (Ch'ng and Tan, 2009).

PTEN is a tumor suppressor gene, it inhibits MAPK and PI3K-Akt pathways (Slipicevic *et al.*, 2005; Wu *et al*., 2003; Chin *et al.*, 2006), causes cell cycle arrest and activates apoptotic pathways by the upregulation of pro-apoptotic proteins. Loss of PTEN expression is observed in 5-20% of melanomas; when it occurs synergistically with p53 inactivation, malignancy of melanoma cells are highly activated. Cyclins and CDKs are also important proteins for the cell-cycle control mechanism. CDK inhibitors, $p16^{INK4a}$ and p21 supresses cell proliferation and can cause cell cycle arrest, thus they are critical for tumor supression. In 75% of melanomas, decreased expression of $p16^{INK4a}$ is observed, correlating with the neoplastic characteristic of melanoma cells. (Ch'ng and Tan, 2009)

MITF is an amplified oncogene in melanoma and the master regulator of melanocyte development. MITF regulates melanocyte differentiation, pigmentation, cell-cycle progression and survival; in addition it has a role in melanocyte to melanoma transformation. Two of the critical target genes of MITF are CDK2 and BCL2, and the aberration of MITF gene results in increased cell proliferation and inhibited apoptosis in melanoma (Levy *et al*., 2006)

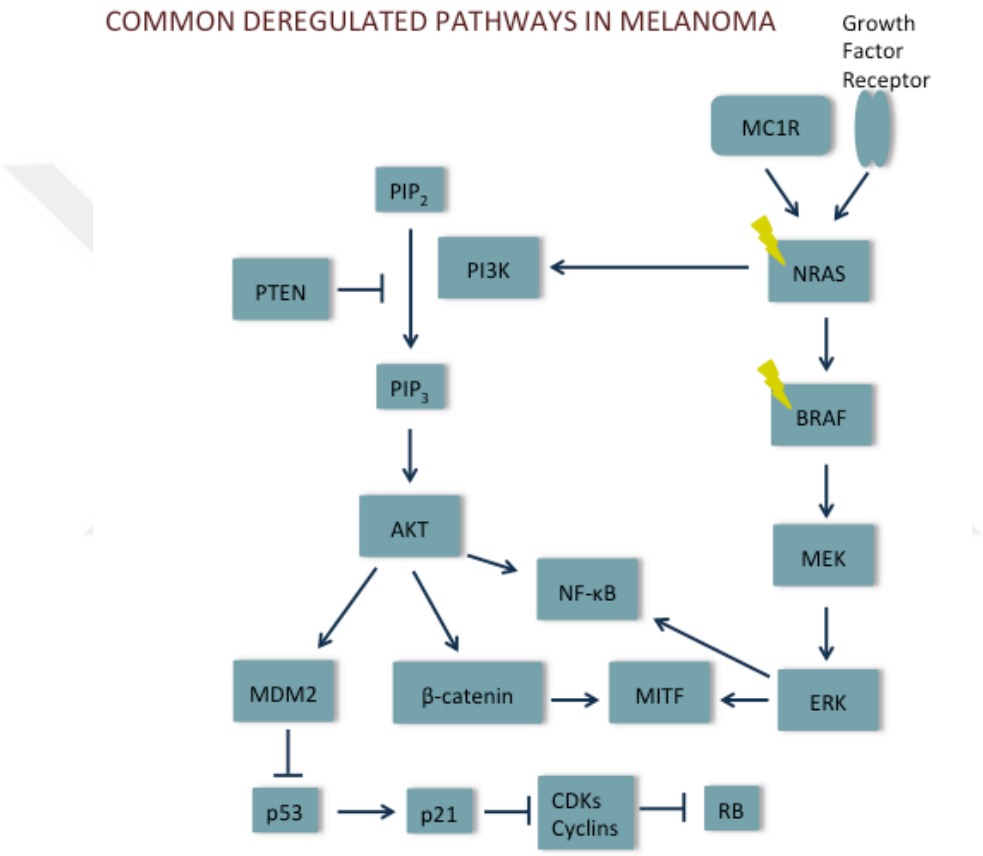

Figure 1.2 Deregulated pathways in melanoma cells. The most commonly observed deregulations in melanoma cells involve MAPK, PI3K-Akt pathways and the most commonly occurring mutations are BRAF and NRAS point mutations, loss of PTEN, suppression of $p16^{INK4a}$ and amplification of MITF (adapted fromVultur and Herlyn, 2013).

Commonly, with the acquisition of BRAF or NRAS mutations, melanocytes transform into benign nevi. Accumulation of other mutations changes the activity of some genes, mostly causing activation of MITF, CDK4 and CCND1 and inactivation of

CDKN2A and PTEN. The combination of some of these mutations brings the cells the ability of radial growth and vertical growth, leading to abnormal formation of cell populations that are divided in an uncontrolled manner. If the cells gain the ability to invade the surrounding tissue in the tumor microenvironment, and can survive in the new tissue which also requires angiogenic capability of the cells; then they become metastatic melanoma cells (Vultur and Herlyn, 2013).

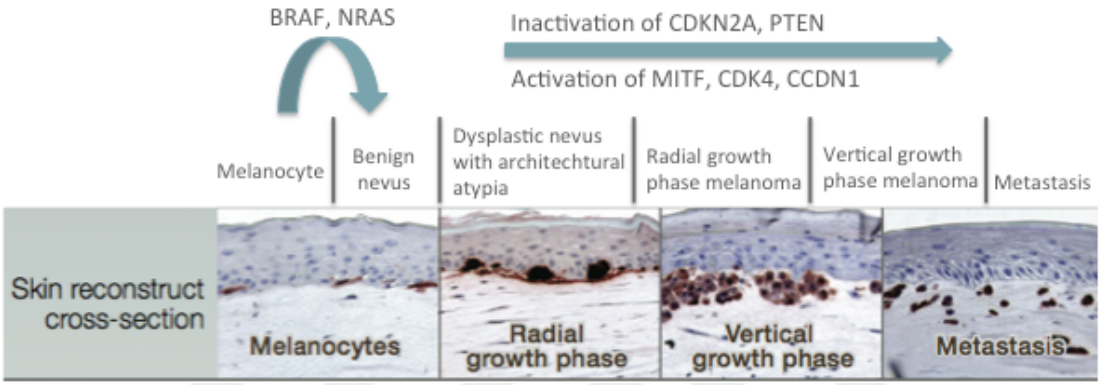

Figure 1.3 The stages of melanocyte to melanoma transformation. Melanocytes first transform into benign nevi, mostly via acquisiton of BRAF or NRAS mutations. With the deregulation of some genes melanocytes acquire the ability of radial growth and vertical growth, and at the final step they transform into malignant melanoma (Adapted from Vultur and Herlyn 2013).

1.2. Interferon Regulatory Factor 4 (IRF4)

1.2.1. IRF4: Overview

Interferon Regulatory Factor family of transcription factors has 9 members and IRF4 is one of them. IRF4 was originally identified to have roles in lymphoid-, myeloid-, and dendritic-cell development; hence it is also called as MUM1 (Multiple Myeloma Oncogene 1), LSIRF (Lymphocyte specific interferon regulatory factor) and ICSAT (Interferon consensus sequence binding protein for activated T-cells). IRF4 was also shown to bind to the DNA through its interaction with PU.1, which is an ETS family transcrip-

tion factor. Therefore, another annotation for IRF4 is PIP (PU.1 interacting protein) (Shaffer *et al*., 2009)

1.2.2. Role of IRF4 in Immune Cells and Related Malignancies

IRF4 is mainly expressed in immune-related cells, eventhough its expression was also observed in non-immune cells recently. As distinct from other members of interferon regulatory factor family, IRF4 is not induced by interferons in immune cells. Different mitogenic stimuli, such as antigen-receptor engagement, lipopolysaccharides and CD40 signaling can induce IRF4, depending on the cell type. For instance in B-cells all of these stimuli that has a role in the induction of IRF4, activates NF-kB pathway and in turn NF-kB pathway activates the transcription of IRF4. Moreover, IRF4 is induced by IL-4, through STAT6 transcription factor. IL-4 cytokine is an important factor for the differentiation and stimulation of lymphocytes (Gupta *et al*., 1999; Grumont *et al*., 2000).

IRF4 shows different expression levels at different stages of B-cell development. While IRF4 is expressed in early (immature) B-cells, it is not expressed during germinal center reaction, yet upon the exit of cells from the GC reaction, IRF4 is upregulated. So far, IRF4 was verified for its function in the termination of the GC-B cell transcriptional program, immunoglobulin (IgG) class switch recombination (CSR) and plasma cell development (De Silva *et al*., 2012). The highest expression of IRF4 is observed in terminally differentiated plasma cells. (Shaffer *et al*., 2009).

Studies demonstrated that genetic aberrations of IRF4 is rare in B-cell malignancies, mostly the transcriptional program controlled by IRF4 is deregulated. IRF4 plays diverse roles in B-cell malignancies; as a pro-survival factor in DLBCL and Hodgkin lymphoma (HL), as an oncogene in multiple myeloma (MM), as a tumor suppressor in B-cell acute lymphoblastic leukemia (B-ALL) and chronic lymphocytic leukemia (CLL). ABC DLBCL originates from plasmablast (late GC B cell that is committed to differentiate into a plasma cell), which are incapable of terminal differentiation. In ABC

DLBCL, B cell differentiation program controlled by IRF4 is disrupted. (De Silva *et al*., 2012)

IRF4 knockdown was shown to reduce the competitive fitness of multiple myeloma and ABC DLBCL cells, pointing the requirement of IRF4 expression in ABC DLBCL and MM. However, IRF4 knockdown did not have an effect on GCB DLBCL, consistent with the absence of IRF4 expression in GC B cells (Yang *et al.*, 2012).

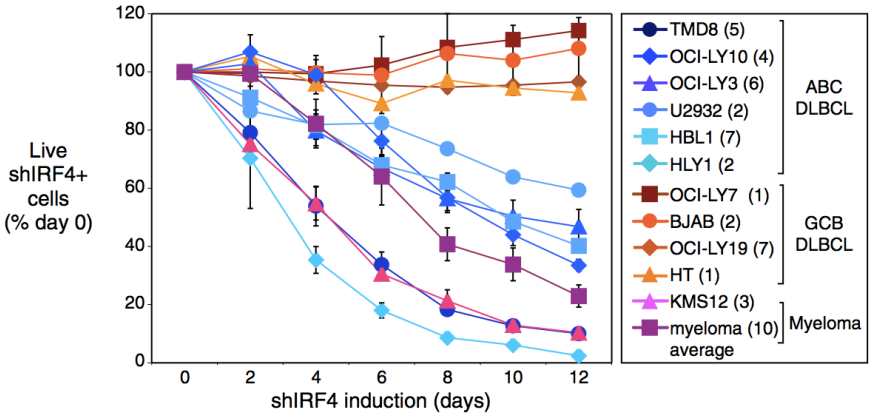

Figure 1.4 Effect of IRF4 knockdown on ABC DLBCL, MM and GCB DLBCL. ABC DLBCL and MM cells show reduced competitive fitness upon IRF4 knockdown, whereas GCB DLBCL cells are not affected (Yang *et al.*, 2012).

1.2.3. IRF4 in Non-immune Cells

Recently, IRF4 expression was identified in non-immune cells; such as adipocytes (Eguchi *et al*., 2008), cardiac tissue (Jiang *et al*., 2013), CNS (central nervous system) neurons (Jiang *et al*., 2013, Guo *et al*., 2014) and melanocytes (Grossman *et. al*, 1996, Praetorius *et al.,* 2013). IRF4 expression in melanocytes and melanoma samples can be found in some online databases such as Oncomine (Rhodes *et al*., 2004), Gene Expression Omnibus (GEO) (Edgar *et al*., 2002) and Cancer Cell Line Encyclopedia

(Barretina *et al*., 2012). High IRF4 mRNA level was observed for melanoma and it was comparable to the IRF4 mRNA levels in lymphoma and myeloma.

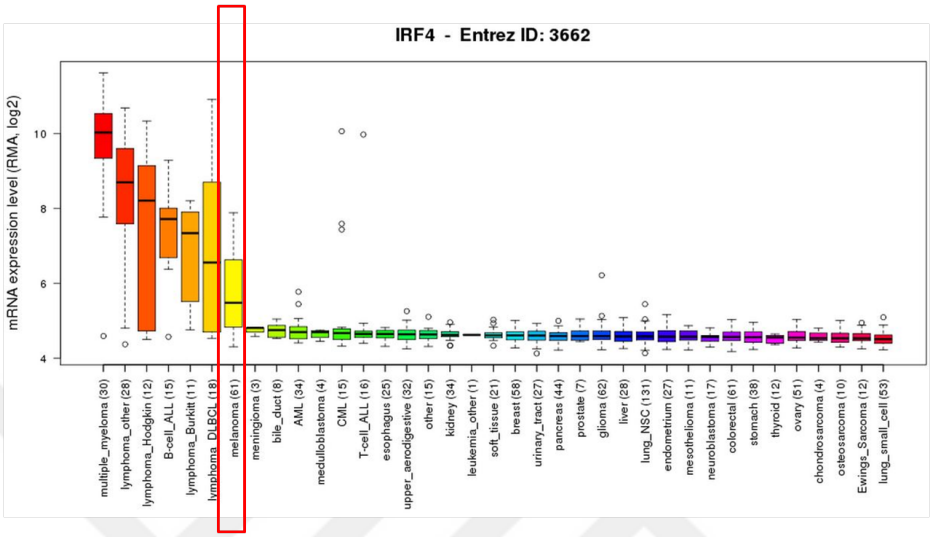

Figure 1.5 mRNA level of IRF4 in melanoma from cancer cell line encyclopedia database. IRF4 level in approximately one thousand cancer types were shown, from highest to lowest. Sample numbers were indicated in brackets and melanoma is highlighted with the red box (Barretina *et al*., 2012).

Also comparison of IRF4 mRNA levels between skin cells were performed, using UCSC Genome Browser, with the data from a previous study (Bernstein *et al*., 2010). Melanocytes show the highest IRF4 mRNA levels among skin cells.

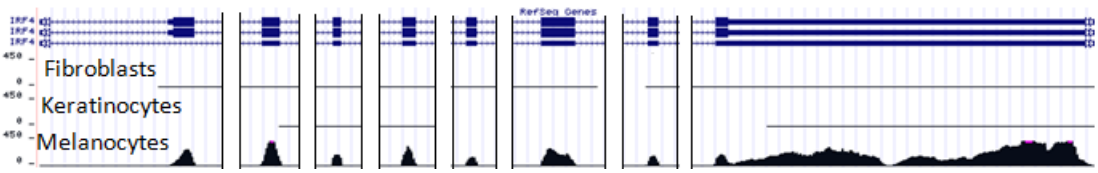

Figure 1.6 IRF4 expression level in fibroblasts, keratinocytes and melanocytes,from NIH Roadmap Epigenomics Project data, visualized by UCSC Genome Browser. The top shows three IRF4 transcripts from RefSeq. Exonic regions are represented with thick bars.

IRF4 protein expression is high in melanoma cells. First high IRF4 protein expression is observed in G361 melanoma cell line (Grossman *et al*., 1996). In the study of Sundram *et al.*, 2003, immunohistochemical analysis showed strong nuclear and weak to moderate cytoplasmic IRF4 staining in melanoma cells.

In addition to high expression level, genetic aberrations of IRF4 were linked to skin and melanoma related predispositions. A germline SNP in IRF4 (rs12203592) is related to melanoma, squamous cell carcinoma and basal cell carcinoma predispositions (Han *et al.*, 2011; Duffy *et al*., 2010; Nan *et al.*, 2009; Gathany *et al*., 2009). In a more recent study, it was found that MITF and TFAP2A cooperatively activate IRF4 expression, in turn IRF4 cooperates with MITF to regulate the expression of TYR (an enzyme that controls the production of melanin). A SNP in the enhancer region of IRF4 negatively affects binding of TFAP2A and it is associated with sensitivity of the skin to melanoma risk factors; such as sun exposure, freckles, blue eye and brown hair (Praetorius *et al*., 2013).

In the light of these previous studies, the potential role of IRF4 in melanoma has become the main focus of our studies.

1.3. IRF4-Interacting Proteins

IRF4 protein has a single polypeptide chain. The polypeptide chain can be mainly disrubuted into three parts: DNA binding domain, functional regulatory domain and intermediary linker domain. The N-terminal DNA binding domain (DBD) has five conserved tryptophan residues and IRF4 protein binds to DNA via this domain. The functional regulatory domain includes two transactivation domains (TAD) and the regions for ternary complex formation and auto inhibition. The functional regulatory domain controls the activity of the protein, inhibits its activity in the absence of co-factors and enables its activation when the protein is interacting with its co-factors. The intermediary linker domain is responsible for the conformational changes of the protein, required for the proper fucntioning (De Silva *et al*., 2012).

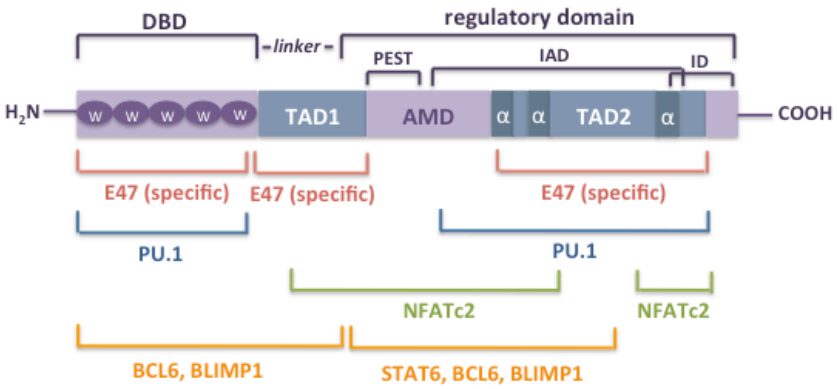

Figure 1.7 Functional domains of IRF4. IRF4 has DBD, TAD and intermediary linker domains, within these domains different regions of the protein enable its interaction with different factors leading to the proper functioning of the protein (Adapted from De Silva *et al*., 2012).

IRF4 functions in immune cells through its interaction with many other factors. When IRF4 is not interacting with a cofactor, IRF association domain (IAD) masks the DBD of IRF4 and prevents the DNA binding or ternary complex formation capabilities of IRF4 (De Silva *et al*., 2012). ETS family transcription factors are important cofactors for the function of IRF4. PU.1 was the first one to be identified to bind to the DNA together with IRF4, leading to transcriptional activation (Pongubala *et al.*, 1992). In the paper of Yang *et al*., 2012, a mutant form of IRF4 that is unable to interact with ETS domain of ETS family transcription factors was generated. ETS domain is highly conserved among ETS family transcription factors, thus the ETS interaction negative IRF4 can not interact with most of the members of this family. With this mutant, interaction of IRF4 with an ETS family transcription factor SPI-B was identified; without the interaction of IRF4 with SPIB, target gene transcription is prevented via IAD of IRF4 protein (see Figure 1.7, De Silva *et al.*, 2012), further indicating the importance of cofactors in the function of IRF4. In addition to ETS family transcription factors, many other transcription factors were identified to interact with IRF4 in immune cells and the interaction of IRF4 with these cofactors is dependent on the cell type. IRF4 interacts with PU.1, E47, SPI-B, STAT3 and STAT6 in B lymphocytes, also with PU.1 in macrophages and with NFAT, FOXP3 and STAT3 in T lymphocytes (Nagulapalli *et al*., 1998; Ettinger *et*

al., 2005; Kwon *et al*., 2009; Rengarajan *et al*., 2002; Hu *et al*., 2002; Zheng *et al*., 2009).

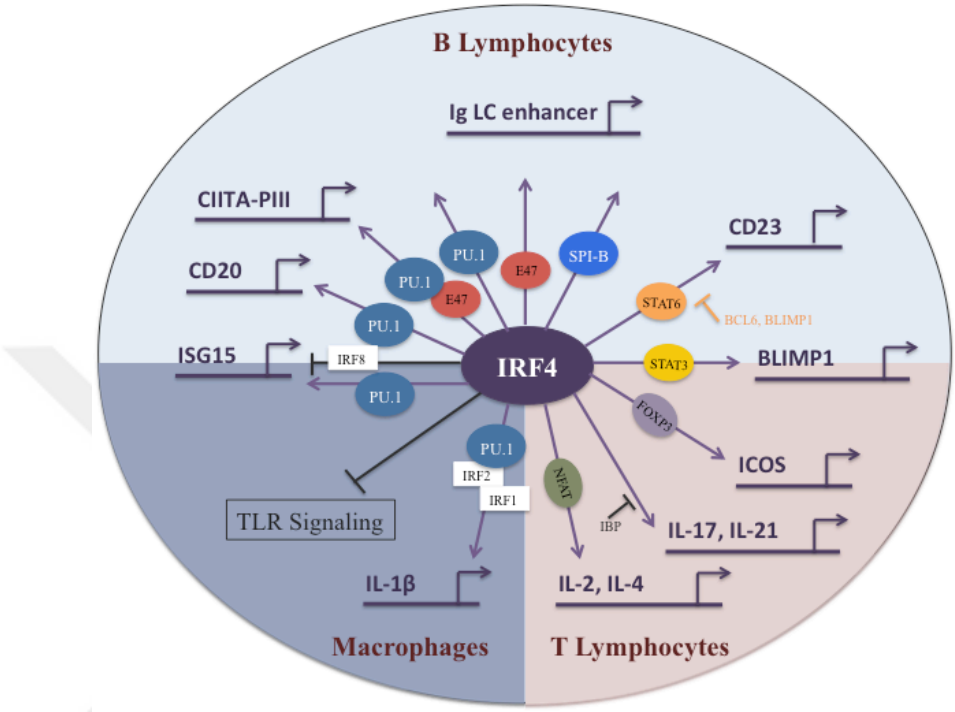

Figure 1.8 Interaction partners of IRF4 in different cell types. Interaction of IRF4 with different factors regulate the transcription of mostly different target genes, in many cell types (Adapted from De Silva *et al*., 2012).

As it is depicted from the literature, there are several interaction partners of IRF4 identified in immune cells. In B lymphocytes, T lymphocytes and macrophages conjunction of IRF4 with other transcription factors is critical for its function. However IRF4-interacting proteins in melanoma cells are not yet identified.. As for the other cells types, function of IRF4 in melanoma cell lines must also be dependent on its interaction partners. Therefore, identification of the IRF4-interacting proteins in melanoma cells is expected to reveal the significance of IRF4 in melanoma. As a consequence, different methods for the identification of protein-protein interactions were used to identify IRF4-interacting proteins in melanoma cell lines.

1.4. Methods for The Identification of Protein-Protein Interactions

1.4.1. Overview

Protein-protein interactions have a critical importance on many cellular processes such as DNA replication, transcription, translation, splicing, secretion, cell cycle control, signal transduction, and intermediary metabolism (Phizicky and Fields, 1995). As a result, identification of protein-protein interactions might reveal many mechanisms in the cell, which is the underlining reason for the improvement of new techniques in this field.

There are many developed methods for the identification of interaction partners of a specific protein. Yeast-two hybrid system (Y2H) is one of the oldest and most widely used one (Bruckner *et al.*, 2009). This system takes the advantage of most eukaryotic transcription factors having distinct functional domains. For example; yeast transcription factor Gal4 has two distinct functional domains; one domain is required for DNA binding and the other one is required for transcriptional activation. Without these domains cluster, transcription of the target genes can not occur. In Y2H system, bait protein and target protein each are fused to distinct functional domains, and transcriptional activation indicates there is an interaction between the bait and the target protein (Osman A., 2004). This method is advantegous for the identification of weak interactions. However, it is only proper for the identification of binary interactions and it also gives too much false positive results (Bruckner *et al*., 2009). Consequently, other methods were developed for the identification of protein interactions. One of them is Co-IP; in which target protein is captured, from the cell lysate, by the specific antibody of the target protein which is immobilized to beads or a resin. Then the target protein is eluted from the beads or resin, together with its interaction partners, and the interaction partners can be verified with mass spectrometry or western blotting. In this method, complex interactions, including more than two proteins, can also be determined, but this method also is known to suffer from high background (Berggård *et al*., 2007).

Tandem affinity purification and BioID, which will be discussed in detail, are newly developed methods for interacting protein identification.

1.4.2. Tandem Affinity Purification (TAP)

TAP method, as its name depicts, includes two purification steps. TAP tag includes two tandem epitope tags separated by a sequence that can be cleaved. This TAP tag is fused to the target protein and then the target protein from the cell lysate is pulled down, using the affinity of one of the tags. Mostly with the cleavage of the sequence between the tags, or using small molecules that show higher affinity to the beads than the tagged proteins, proteins are eluted from the beads and the protein of interest is pulled down again, this time using the affinity of the second tag. Then the eluate from the second step of purification is analyzed using mass spectrometry. The biggest advantage of this method is the reduced background, contaminant proteins that can negatively affect the analysis of interaction partners of target protein is reduced due to two steps of purification; therefore the probability of false negatives are diminished. However, the possibility of losing weak interacting partners of the target protein is relatively high (Puig *et al*., 2001).

Two of the tags that can be used for TAP method are FLAG and MAT tags. MAT tag is very similar to His tag, which is a more commonly used tag than MAT tag. His tag constitutes histidine residues and imidazole ring of the histidine shows high affinity for nickel ions. As a result of histidine residues, MAT tag as well as His tag has an affinity for nickel ions (Watson *et al*., 2007). FLAG tag is a small peptide with the sequence AspTyrLysAspAspAspAspLys (Einhauer *et al*., 2001) that is commercially available and also its specific antibody is commercially available. The system includes the pulldown of proteins, using nickel beads or a resin that is charged with nickel ions at the first step. In our system, FLAG and MAT tags have an enterokinase cleavage site between them which enables the elution of proteins from nickel beads, using enterokinase enzyme. However, elution with imidazole showed higher efficiency than enterokinase cleavage, thus in our system proteins were eluted from nickel beads with imidazole. The smaller size of free imidazole than histidine causes higher affinity of imidazole to nickel ions, enabling the elution of MAT tagged proteins from the beads (Bornhorst and Falke, 2000). At the second step, the eluate from the first step is pulled down, this time using anti-FLAG antibody conjugated beads.

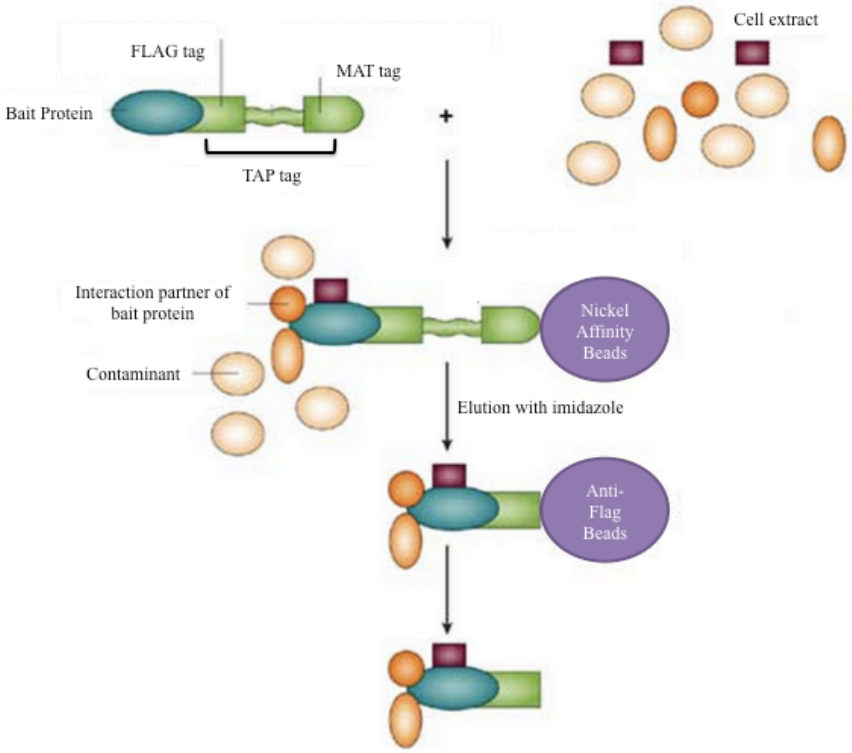

Figure 1.9 Schematic representation of TAP. Cell lysate containing the TAP-tagged protein is prepared and target protein is pulled down with the interaction partners, using Nickel beads and eluted from the beads with imidazole. Then the eluate from the first step is pulled down with Anti-FLAG conjugated beads (Adapted from Huber, 2003).

1.4.3. BioID

This method takes the advantage of a promiscuous prokaryotic biotin ligase (BirA*). BirA is a 35 kDa DNA-binding biotin protein ligase in *Esscheria coli*. It is the transcriptional repressor of the biotin biosynthetic operon. In *E. coli*, BirA biotinylates a subunit of acetyl-CoA carboxylase and it has high specificity for its substrate peptide, which is called biotin acceptor tag (BAT). Biotinylation by BirA has two steps; in the first step biotin and ATP are combined and form biotinoyl-5'-AMP (bioAMP). BirA active site holds this activated biotin until its reaction with a specific lysine residue of the BAT sequence (Roux *et al*., 2012).

Biotinylation is very rare in mammalian cells: only a few carboxylases show biotinylation. High specificity of BirA to its substrate poses a problem in mammalian cells if it is to be used as a proteomic tool. For this purpose, a mutant form of BirA was genereated (R118G, BirA*). The ability of DNA binding and self association are diminished in this mutant and it shows less affinity for BioAMP than the wild-type enzyme. Thus BirA* releases BioAMP easily and this activated BioAMP can react with primary amine of lysine residues. Reduction of the specificity provides an advantage for the usage of biotinylation to detect the protein-protein interactions in mammalian cells (Roux *et al*., 2012).

In BioID method, BirA* is fused to the target protein and BirA* fused protein is expressed in the cells. With the administration of biotin to the cells, BirA* fused target protein can biotinylate the proteins that are in proximity as well as itself. Then the biotinylated proteins are pulled down, using the affinity of biotin to streptavidin. This method is also suitable for the identification of weak protein interactions. However, this method does not only identifiy the direct interaction partners of the target protein, but also the proteins that are proximal to the target protein (Roux *et al*., 2012).

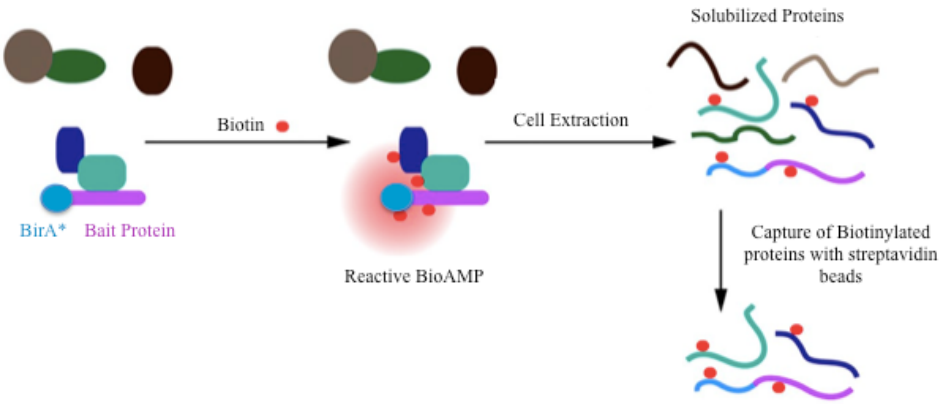

Figure 1.10 Schematic representation of BioID. BirA*-fused target protein is expressed in the cells and biotinylates the proteins in its proximity with the administration of biotin to the cells. Then the biotinylated proteins are pulled down with streptavidin beads. (Adapted from Roux *et al*., 2012)

In the comparative study of AP-MS (Affinity Purification-Mass Spectrometry) and BioID by Lambert *et al*., 2014, it was concluded that AP-MS and BioID are complementary approaches for the interactome studies. These two methods identified some overlapping but largely different interaction partners of the target protein, which were involved in different biological processes and also differed in their abundance. Therefore; rather than relying on one of these methods for interactome studies, both AP-MS and BioID could be applied in order to get a larger pool of proteins. This larger pool of interaction partners could lead to a broader perspective of the function of the protein-of-interest in different metabolic pathways.

1.4.4. Mass Spectrometry

After the purification of the target protein together with its interaction partners, identity of these target protein-interacting proteins need to be determined, which is possible via mass spectrometry (MS; "mass spec"). As intact proteins are too large to be analyzed with mass spectrometry, mass spectrometric analysis first requires the digestion of proteins into peptides, usually with the proteolytic enzyme trypsin. Basically all mass spectrometers have an ion source, mass analyser and a detector. Ion source enables the ionization of peptides to be analyzed; by this way ionized analytes can travel towards the mass analyser. Mass analyser contains electric and magnetic fields which affects the speed and direction of the ionized particles and accordingly measures the mass-to-charge (m/Z) ratio of the particles. After the mass analyser, analytes pass through the detector which measures the abundance of ions in the sample population (Aebersold and Mann, 2003).

Different methods, such as TAP and BioID in our case, could be applied for the purification of target protein and its interaction partners. The number of purified proteins is large in most cases, and mass spectrometry is the convenient way for the high-throughput identification of these proteins. Mass spectrometer analysis gives the amino-acid sequences of the peptides, relying on the m/Z ratio (Dingar *et al*., 2014). Then the peptide sequences are matched to the human database, using different softwares, com-

monly Mascot, (Alves and Yu, 2014). By this way, the interaction partners of the target protein could be identified.

2. PURPOSE

The role of IRF4 in hematopoietic cells and hematologic malignancies has already been investigated, leading to the observation that IRF4 has a critical role especially in multiple myeloma and ABC DLBCL. Besides, publicly available expression databases show high expression of IRF4 in melanoma, and our group has also observed high expression of IRF4 protein in certain melanoma cell lines. In addition to that, by our group IRF4 knockdown was shown to reduce the competitive fitness of some melanoma cell lines, indicating the dependence of these cell lines to IRF4.

Some critical interaction partners of IRF4 were explored in multiple myeloma and ABC DLBCL and shown to conribute critically to IRF4 function. The purpose of this thesis is to identify the IRF4-interacting proteins in melanoma cell lines to help reveal the important mechanisms that IRF4 partake in melanoma. In order to achieve our goal, BioID and tandem affinity purification methods were performed. These two methods are complementary for the identification of interaction partners of a target protein.

3. MATERIALS

3.1. General Kits, Enyzmes and Reagents

Table 3.1. List of kits, enzymes and reagents.

BCA Protein Assay Kit	Life Technologies, USA
DMEM	Gibco, LifeTechnologies, USA
IMDM	Gibco, LifeTechnologies, USA
RPMI 1640	Gibco, LifeTechnologies, USA
FBS	Gibco, LifeTechnologies, USA
Non Essential Amino Acids	Gibco, LifeTechnologies, USA
Penicillin / Streptomycin	Gibco, LifeTechnologies, USA
Trypsin	Gibco, LifeTechnologies, USA
Plasmid Miniprep Kit	Roche, Switzerland Macherey Nagel, Germany
EndoFree Plasmid Maxi Kit	Qiagen, Germany Macherey Nagel, Germany
PCR Product Purification Kit	Roche, Switzerland
Qiaquick Gel Extraction Kit	Qiagen, Germany
Phusion High Fidelity DNA Polymerase	New England Biolabs, USA
Deoxynucleotide (dNTP) Solution Mix	New England Biolabs, USA
Quick-Load 1 kb DNA ladder	New England Biolabs, USA
EcorI	New England Biolabs, USA
SalI	New England Biolabs, USA
BamHI	New England Biolabs, USA
HpaI	New England Biolabs, USA
Protease Inhibitor Coctail Tablets	Roche, Switzerland
Phosphatase Inhibitor	Roche (PhosStop), Switzerland
PageRuler Prestained Protein Ladder	Thermo Scientific, USA (26616)
K2 Transfection Reagent	Biontex Laboratories, Germany
Dynabeads His-Tag Isolation&Pulldown	Life Technologies, AS, Oslo (10103D)
Anti-FLAG M2 Magnetic Beads	Sigma Aldrich, USA
Dynabeads MyOne Streptavidin C1	Life Technologies, AS, Oslo (65001)
Dynabeads Protein G	Life Technologies, AS, Oslo (10004D)
BS3 (bis(sulfosuccinimidyl) suberate)	Pierce Biotechnology (21580)
37.5% Acrylamide/Bisacrylamide mix	Fisher Scientific, USA

3.2. Biological Materials

3.2.1. Bacterial Strains

For the transformation; competent cells from *Escherichia coli* STBL3 strain, which has the genotype of F– mcrB mrr hsdS20 (rB–, mB–) recA13 supE44 ara-14 galK2 lacY1 proA2 rpsL20 (StrR) xyl-5 λ– leu mtl-1, was used. This strain was testified for the minimal possibility of the recombination of lentiviral vectors.

3.2.2. Cell Lines

SKMEL-28, G-361 (human melanoma cell lines; kindly provided by Dr. Marisol Soengas), SKMEL-5 (human melanoma cell line; kindly provided by Yetiş Gültekin, M.Sc and Dr. David M. Sabatini), HBL-1 and OCI-LY3 (human ABC-DLBCL cell lines; kindly provided by Prof. Georg Lenz), FEPD (human ALCL cell line, kindly provided by Prof. Georg Lenz) were used in the experiments.

3.2.3. Plasmids

The coding sequence of IRF4 was derived from IRF4_pDONR221 plasmid (PlasmID database, Harvard (Clone ID: HsCD00040446))

For tandem affinity purification method, IRF4 coding sequence was cloned into PCMV-FLAG-MAT-Tag-2 plasmid (Sigma Aldrich, USA, C6114) and then IRF4 coding sequence fused to TAP tag and Only_TAP tag were cloned into pIRES2-eGFP plasmid (kindly provided by Assist. Prof. Necla Birgül and Tuncay Şeker, M.Sc).

For BioID method, IRF4 coding sequence was cloned into PCDNA3.1 MCS-BirA(R118G)-HA plasmid (kindly provided by Assist. Prof. Elif Nur Fırat Karalar).

3.2.4. Primers

Table 3.2. Primers used in this study.

Primer ID	Sequence	Application
IRF4_PCMV-FLAG-MAT-Tag2	Forward: 5' GACTGAATTCATGAAC-CTGGAGGG Reverse: 5' GACTGGATCCCAATTCTT-GAATAGAGG	PCR
IRF4_TAP_pIRES2-eGFP	Forward: 5' GACTGAATTCGAATTCATGAACCTGG Reverse: 5' GACTGTCGACTTAGTGCTT-GTGGC	PCR
Only_TAP_pIRES2-eGFP	Forward: 5' GACTTCTAGAATGGAC-TACAAAGACG Reverse: 5' GACTGTCGACTTAGTGCTT-GTGGC	PCR
IRF4_PCDNA3.1 MCS-BirA(R118G)-HA	Forward: 5' GACTGTTAACATGAAC-CTGGAGGG Reverse: 5' GACTGGATCCCAATTCTT-GAATAGAGG	PCR

3.3. Chemicals

Table 3.3. Chemicals used in this study.

Ethidium Bromide	Merck, USA
EDTA	Merck, USA
EGTA	Merck, USA
Hydrochloric Acid	Merck, USA
Sodium Chloride	Merck, USA
Bromophenol Blue Indicator	Merck, USA
Tween 20	Merck, USA
Methanol	Merck, USA
Acetic Acid	Merck, USA
LB Broth	Merck, USA
Glycine	Merck, USA
DMSO	Merck, USA
Ethanol	Merck, USA
Nonidet P40	Fluka, USA
Triton-X-100	Sigma Aldrich, USA
SDS	Applichem, Germany Sigma Aldrich, USA
Ampicilllin	Applichem, Germany
Acrylamide	Sigma Aldrich, USA
Sodium Deoxycholate	Sigma Aldrich, USA
N,N'-Methylenbisacrylamide	Sigma Aldrich, USA
Agarose	Sigma Aldrich, USA
Kanamycin	Applichem, Germany
Glycerol	Merck, USA
Sucrose	Sigma Aldrich, USA
Formaldehyde	Sigma Aldrich, USA
Glutardialdehyde	Merck, USA
2-Mercaptoethanol	Merck, USA
TEMED	Merck, USA
Tris-Cl	Merck, USA
Calcium Chloride	Merck, USA
Potassium Chloride	Merck, USA
BSA	Applichem, Germany
Tris-Base	Sigma Aldrich, USA
Isopropanol	Merck, USA
HEPES	Gibco Invitrogen, USA
Silver Nitrate	Merck, USA
Sodium Carbonate	Merck, USA
Imidazole	Sigma Aldrich, USA (I5513)
Biotin	Sigma Aldrich, USA (B4501)

3.4. Buffers and Solutions

Table 3.4. Buffers and solutions used in this study.

10X SDS Running Buffer	1% SDS 1.92 M Glycine 250 mM Tris-Base
10X Transfer Buffer	1.92 M Glycine 250 mM Tris-Base
1X Transfer Buffer	10% 10X Transfer Buffer 20% Methanol
12% SDS-PAGE gel, resolving part (20 ml)	8.4 ml dH_2O 6 ml 37.5% Acrylamide/Bisacrylamide mix 5.2 ml 1.5 M Tris-Cl (pH: 8.8) 200 µl 10% SDS 200 µl 10% APS 20 µl TEMED
12% SDS-PAGE gel, stacking part (10 ml)	7.54 ml dH_2O 1 ml 37.5% Acrylamide/Bisacrylamide mix 1.25 ml 1 M Tris-Cl (pH: 6.8) 100 µl 10% APS 10 µl TEMED
10X TBS	200 mM Tris-Cl (pH: 7.4) 1.5 M NaCl
TBS-T	10% 10X TBS 0.1% Tween-20
50X Tris acetic acid (TAE)	2M Tris-acetate 50 mM EDTA (pH: 8.5)
His-Tag Binding/Wash Buffer	50 mM Sodium Phosphate (pH: 8.0) 300 mM NaCl 0.01% Tween-20
0.5% Triton-X His-Tag Binding/Wash Buffer	50 mM Sodium Phosphate (pH: 8.0) 300 mM NaCl 0.01% Tween-20 0.5% Triton-X-100
Harvest Buffer	10 mM HEPES (pH: 7.9) 50 mM NaCl 0.5 M Sucrose 0.1 mM EDTA 0.5% Triton-X-100
Buffer A	10 mM HEPES (pH: 7.9) 10 mM KCl 0.1 mM EDTA 0.1 mM EGTA

Table 3.4 Buffers and solutions used in this study (cont.).

Buffer C	10 mM HEPES (pH: 7.9) 500 mM NaCl 0.1 mM EDTA 0.1 mM EGTA 0.1% NP-40
Freezing medium	1X DMEM 20% FBS 1X Pen/Strep 100 µM MEM-NEAA 10% DMSO
0.1 M Glycine, pH3 Buffer	0.75 g Glycine 100 ml distilled water pH adjusted with HCl
TBS Buffer	50 mM Tris HCl (pH: 7.4) 150 mM NaCl,
PBS-T	PBS (pH: 7.4) 0.01% Tween-20
Wash Buffer 1	2% SDS
Wash Buffer 2	0.2% deoxycholate 1% Triton-X-100 500 mM NaCl 1 mM EDTA 50 mM HEPES (pH: 7.5)
Wash Buffer 3	10 mM Tris (pH: 8.1) 250 mM LiCl 0.5% NP-40 0.5% deoxycholate 1% Triton-X-100 500 mM NaCl 1 mM EDTA
Wash Buffer 4	50 mM Tris (pH: 7.4) 50 mM NaCl
BS3 Conjugation Buffer	100 mM Sodium Phosphate (pH: 8.0) 0.15M NaCl
Crosslinking Solution	10% Glutardialdehyde
Silver Nitrate Solution	0.1% (w/v) Silver Nitrate
Developing Solution	3% (w/v) Sodium Carbonate 0.019% (v/v) Formaldehyde
Destain I Solution	40% (v/v) Methanol 7% (v/v) Acetic Acid
Destain II Solution	5% (v/v) Methanol 7% (v/v) Acetic Acid

3.5. Antibodies

Table 3.5. Antibodies used in this study.

Name	Species	Dilution	Source
Anti-Actin	Rabbit	1:2500	4967S, Cell Signaling
Anti-IRF4 X (M-17)	Goat	1:5000	Sc-6059, Santa Cruz
Anti-FLAG	Mouse	1:1000	F1804, Sigma Aldrich
Anti-HA (HA.C5)	Mouse	1:1000	Ab18181, Abcam
Streptavidin, horseradish peroxi-dase conjugate		1:4000	s-911, Life Technologies
Anti-Rabbit-HRP	Mouse	1:2500	7074S, Cell Signaling
Anti-Goat-HRP	Rabbit	1:2500	Sc-2768, Santa Cruz
Anti-Mouse-HRP	Horse	1:2500	7076S, Cell Signaling
Anti-BTF	Rabbit	1:1000	Ab90466, Abcam
Anti-nmt55/p54nrb	Rabbit	1:1000	Ab70335, Abcam
Anti-Histone H3 (tri-methyl K9)	Rabbit	1:1000	Ab8898, Abcam

3.6. Disposable Labware

Table 3.6. List of disposable labwares used in this study.

Western Blotting Paper	Whatman, UK
Parafilm	Brand, Germany
Scalpel	Swann-Morton, UK
Centrifuge Tubes, 15 ml	Vwr, USA
Centrifuge Tubes, 50 ml	Vwr, USA
Serological pipette, 5ml	Tpp, Switzerland
Serological pipette, 10ml	Tpp, Switzerland
Serological pipette, 25ml	Tpp, Switzerland
Pipette Tips, filtered	Biopointe, USA
Pipette Tips, bulk	Biopointe, USA
Microcentrifuge tubes	Axygen, USA
PCR Tubes, 0.2 ml	Axygen, USA
Medical Gloves	Vwr, USA
Syringe Filters	Sartorius, Germany
Cryovial	Tpp, Switzerland

Table 3.6 List of disposable labwares used in this study (cont.).

Cell Culture Flasks, 75cm^2	Tpp, Switzerland
Cell Culture Plates, 6-well	Tpp, Switzerland
Insulin Syringes, 1 ml	Vwr, USA
Syringe, 10ml	Becton Dickinson, USA
PS Test Tubes, 5 ml	Becton Dickinson, USA Isolab, Germany
Glass Pasteur Pipette, 230 mm	Witeg, Germany
Chemiluminescent Detection Film	Roche, Switzerland

3.7. Equipments

Table 3.7. List of equipment used in this study.

Beaker, 100 ml	Duran, Germany
Beaker, 600 ml	Duran, Germany
Erlenmeyer, 250 ml	Duran, Germany
Erlenmeyer, 500 ml	Duran, Germany
Bottle, 1000 ml	Vwr, USA
Bottle, 500 ml	Vwr, USA
Bottle, 100 ml	Vwr, USA
Forceps	RSG Solingen, Germany
Magnetic Stirring Bar	Vwr, USA
Cryobox	Tenak, Denmark
Autoclave Indicator Tape	Llg, Germany
Measuring Cylinder 100 ml	Kartell, Italy
Measuring Cylinder 250 ml	Kartell, Italy
Measuring Cylinder 1000 ml	Kartell, Italy
pH Meter	Hanna, USA
Microtube Racks	Vwr, USA
Electronic Balance	Sartorius AY123, Germany
Microcentrifuge	Vwr Galaxy Ministar, USA
Horizontal Electrophoresis	Cleaver Scientific Multi Sub Mini, UK

Table 3.7 List of equipment used in this study (cont.).

Micropipettes	Cleaver Scientific, UK Gilson Pipetman Neo PCR Kit, USA Axygen, USA
Heat Block	Cleaver Scientific EL-01, UK
Pipettor	Greiner Labopet 240, Germany
Vortex	Vwr, USA
Vertical Electrophoresis	Cleaver Scientific Omni-page Mini, UK
Centrifuges	J2-21, Beckman Coulter, USA Allegra X-22, Beckman Coulter, USA 5415R, Eppendorf, USA
Rotor	Beckman Coulter JA-14, USA
Cell Culture Incubator	Binder C-150, Germany
Documentation System	GelDoc XR System, Bio-Doc, Italy
Flow Cytometer	FACSCalibur , Becton Dickinson, USA
Freezers	-20°C, Ugur UFR 370 SD, Turkey -80°C, Thermo Scientific TS368, USA -150°C, Sanyo MDF1156, Japan
Microplate Reader	680, Biorad, USA
Microscopes	Inverted Microscope, Nikon Eclipse TS100, Japan Fluoroscence Microscope, Observer Z1, Zeiss, Germany
Thermal Cycler	Antarus MyCube ANT101, USA
Power Supply	Vwr, USA
Shaker	VIB Orbital Shaker, InterMed, Denmark Vwr Mini Orbital Shaker, USA
Spectrophotometer	NanoDrop 1000, USA
Stirrer - Heater	Dragonlab MS-H-S, China
Rotator	Grant Bio Multifunctional Rotator PTR-35, UK
Refrigerator	4°C, Ugur USS 374 DTKY, Turkey
Refrigerated Vapor Trap	Thermo Scientific SPD111V, USA
Oil-free Gel Pump	Thermo Scientific Savant VLP110, USA
Vacuum Pump Oil Filter	Thermo Scientific VPOF110, USA
Carbon dioxide Tank	Genc Karbon, Turkey
Ice Maker	Brema, Italy Scotsman Inc. AF20, Italy
Autoclave	Model ASB260T, Astell, UK
Dishwasher	Miele Mielabor G7783, Germany
Stella	Raytest, Germany
Freezing Container	Nalgene, USA
Oven	Nüve KD200, Turkey

4. METHODS

4.1. Cell Culture

4.1.1. Maintenance of Cell Lines

SKMEL28, SKMEL5 and G361 cell lines were grown in DMEM-high glucose, additionally containing 10% FBS, 1% penicillin/streptomycin and 1% non-essential aminoacids. FEPD and HBL-1 cell lines were grown in IMDM, additionally containing 20% FBS, 1% penicillin/streptomycin and 1% non-essential aminoacids. OCI-LY3 cell line was grown in RPMI1640, additionally containing 20% FBS, 1% penicillin/streptomycin and 1% non-essential aminoacids. Cells were incubated in an incubator which is calibrated to 37°C and 5% CO_2. For the maintenance of the cells, cells were passaged approximately every 3 days. For adhesive cell lines, SLMEL28, SKMEL5 and G361, first their medium was aspirated and cells were washed with 1X PBS. After the aspiration of the PBS, 0.05% trypsin was added onto the cells and cells were incubated at 37°C for 3 minutes. When the cells completely detached from the surface, medium which was equal in amount with trypsin was added to the cells, to deactivate trypsin. Cells were transferred into a falcon and centrifuged at 2000 rpm for 2 minutes. Cell pellet was resuspended in DMEM and seeded to the proper surface again. For suspension cell lines, HBL-1, FEPD, OCI-LY19, OCI-LY3, cells were transferred into a falcon and centrifuged at 2000 rpm for 2 minutes. Cell pellet was resuspended in IMDM or RPMI 1640 and seeded to the proper surface again.

For the stocking of the cell lines SKMEL5, SKMEL28 and G361; cells were detached with the trypsin and centrifuged. Cell pellet was resuspended in the freezing medium, which is shown in Table 3.4. 100% confluent cells in a 75 cm flask were divided into 5 cyrovials; 1 ml cell-freezing medium mix to each. Cells were freezed first in Nalgene Freezing Container filled with isopropanol, which was placed into -80°C refrigerator, then cells were transferred to -150°C refrigerator.

Cells that are kept at -150°C refrigerator were thawed by placing the cryovial into the water bath at 37°C. When the cells were completely thawed, they were transferred into falcon tubes and centrifuged at 2000 rpm for 2 minutes. After the aspiration of DMSO containing medium, cell pellet was resuspended in the proper medium.

4.1.2. Transient Transfection of The Cells, using K2 Transfection System

K2 transfection system has two components; K2 transfection reagent and K2 multiplier. K2 transfection reagent enables cationic lipids to form liposomes around DNA, which can be taken up by the cells. K2 multiplier enables DNA not to be detected by transfected cells, by this way liposome-DNA complex can not be targeted by the immune reactions inside the cells.

For the transfection of the desired plasmids into the cells, 40 µl K2 Multiplier diluted in 2 ml of DMEM was added onto the cells in a 6-well plate and cells were placed into the incubator for 2h, prior to transfection. 30 minutes before transfection, transfection solutions were prepared; solution A contains 2 µg of the desired plasmid diluted in 144 µl serum-free medium, and solution B contains 12 µl K2 transfection reagent diluted in 144 µl serum-free medium. Solution A was added onto solution B dropwise and solutions were mixed by pipetting. The mixed solution was incubated for 20 min. and added onto the cells dropwise. After 6-24 hours of transfection, medium of the cells were refreshed with serum containing-DMEM. 1 or 2 days after the transfection, cells were examined under fluorescence microscope and analyzed through flow cytometry, for their transfection efficiency.

4.2. Molecular Biological Techniques

4.2.1. Plasmid Isolation

Plasmids were isolated for different purposes. Plasmids to be used for cloning experiments were isolated using Roche High Pure Plasmid Isolation kit. And plasmids to

be administered to the cells were isolated with either QIAGEN EndoFree Plasmid Maxi Kit or Macharey-Nagel NucleoBond Xtra MaxiPlus EF; as these plasmids were administered to the cells, they need to pure, which is provided by the endo-free kits. The kits were used according to the manufacturer's instructions.

4.2.2. Cloning

IRF4 coding sequence was amplified from IRF4_pDONR221 plasmid, with primers that adds the desired restriction sites to the PCR product. Phusion High-Fidelity DNA polymerase, which has high proofreading capacity was used for PCR reactions. 1 µl 100 ng IRF4_pDONR221 plasmid, 10 µl 5X Phusion HF buffer, 2 µl 50 mM $MgCl_2$, 5 µl of forward and reverse primers (shown in Table 3.2), 1 µl Phusion DNA polymerase and dH_20 to complete the reaction volume to 50 µl were added to the PCR mix. PCR reaction was conducted as the following:

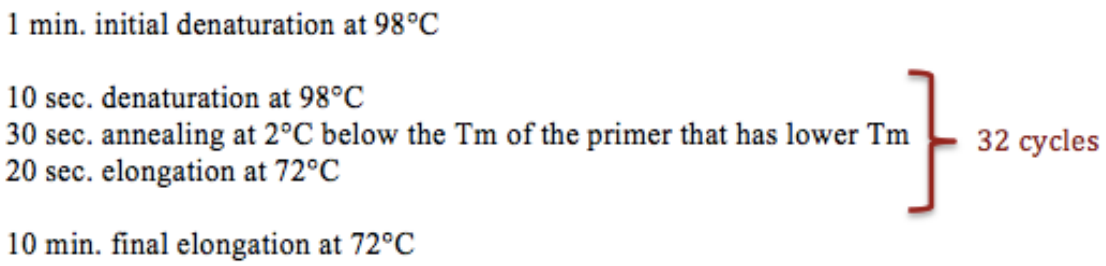

Figure 4.1 Schematic representation of the PCR reaction, that shows the cycles.

After the PCR reaction was performed, PCR product was loaded to 1% Agarose gel, and the band that has the proper size was extracted from the gel. Extracted PCR product was digested with endonucleases, overnight at 37°C. Meanwhile the plasmid that the PCR product will be cloned into, was digested with the same endonucleases, 2 h at 37°C. Digested PCR product was purified, using Roche High Pure PCR Product Purification Kit; digested plasmid was loaded to 1% agarose gel and extracted from the gel. Digested plasmid and digested PCR product were ligated. For the ligation reaction, 50 ng vector was used, the amount of insert was calculated to get 1:3 molar vector-to-insert

ratio in the reaction, also 2 µl 10X T4 DNA ligase buffer, 1 µl T4 DNA ligase and dH_2O to complete the reaction to 20 µl were added.

4.2.3. Agarose Gel Electrophoresis

For the preparation of 1% Agarose gel; 1% weight to volume ratio of agarose was added to 1X TAE buffer and the solution was placed into the microwave to dissolve the agarose in TAE buffer. 5 µl of ethidium bromide was added to 80 ml of 1% agarose and the mix was freezed. Samples were mixed with 6X loading dye to get a final concentration of 1X and then they were loaded to the gel. The gel was run at 120V for 30 min. The image of the gel was obtained by Bio-Rad GelDoc XR System under UV.

4.3. Western Blotting

4.3.1. Cell Lysis and Protein Extraction

Medium of the cells were aspirated and cells were washed with PBS. Cells were detached from the surface with trypsin and detached cells were transferred to a falcon and centrifuged at 2000 rpm for 2 min. After discarding the medium of the cells, cells were washed twice with PBS. For the preparation of the total lysate, cell pellet was resuspended in RIPA buffer containing 1X protease inhibitor cocktail. Resuspended cell pellet was transferred to 1.5 ml tube, kept on ice for 30 min., vortexed every 10 min. Then the cells were syringed through 22-gauge needle and centrifuged at 14000 g for 15 min. at 4°C. The supernatant which includes the proteins were transferred to a new tube. For the nuclear fractionation, cell pellet was resuspended in Harvest buffer containing 1X protease inhibitor cocktail and resuspended cell pellet was transferred to 1.5 ml tube. Cell lysate was incubated on ice for 5 min. and afterwards centrifuged at 1000 rpm for 10 min. at 4°C. The supernatant was discarded and the pellet was washed with Buffer A containing 1X protease inhibitor cocktail and 1X phosphatase inhibitor cocktail and then centrifuged at 1000 rpm for 10 min. at 4°C. The pellet was dissolved in 0.5% Triton-X His-Tag Binding/Wash buffer or PBS-T, for TAP and BioID respectively, vortexed for

15 min. at 4°C and centrifuged at 14000 rpm for 10 min. at 4°C. The supernatant is the nuclear fraction and it was transfered to a new tube.

4.3.2. BCA Assay for The Determination of Protein Concentration

Protein concentrations of total cell lysates were determined with Pierce BCA Protein Assay Kit. BSA, included in the kit, was serially diluted in 1X PBS to obtain standards with the concentrations of 125, 250, 500, 750, 1000, 1500 and 2000 µg/ml. Cell lysates mostly diluted 1:4, not to exceed the OD range of the standards and dilutions were prepared as triplicates. 150 µl Reagent A and 3 µl Reagent B were mixed and 153 µl of the mix was added to each well of a 96-well plate. 5 µl of the standards and diluted samples were added onto the mix. Plate was incubated at 37°C for 30 min. and OD values were measured at 562 nm with the plate reader. Blank was the buffer that proteins were resuspended and blank of the standards was PBS. The median of the triplicates of diluted samples and standards were calculated, blanks were subtracted from them. Standard curve for the standards was prepared in Microsoft Excel; x axis shows the concentration and y axis shows the OD values. For the calculation of the concentrations of the samples, formula obtained from the standard curve was used and this result was multiplied with 4 to obtain the undiluted concentrations of the samples.

4.3.3. Preparation of Protein Samples and SDS Gel Electrophoresis

4X laemmli loading dye was added to protein lysates, at a final concentration of 1X and the mix were boiled at 95°C for 5 min. Protein lysates, mixed with laemmli and boiled, were loaded to the wells of SDS-PAGE gel, prepared at Bio-Rad Mini Protean Tetra System. The gel contains 12% resolving part at the bottom and stacking part at the upper part. For the running of the gel, tank was filled with 1X running buffer. The gel was run at 100V until the samples entered the resolving part of the gel, then it was run at 120V.

4.3.4. Transfer from SDS Gel to PVDF Membrane

Whatman papers and PVDF membrane were cut in the size of the gel. PVDF membrane was placed into methanol for the activation of the membrane, then washed in sterile water and kept in 1X transfer buffer. Blotting sandwich was prepared by placing gel and membrane on top of each other between two whatman papers and two blocking pads. Blotting sandwich was placed into the tank which was filled with 1X transfer buffer and transfer was achieved at 250 mA for 1h 45 min. At the end of the transfer, membrane was washed with TBS-T to remove methanol.

4.3.5. Blotting - Antibody Incubations

Before blotting of the membrane with antibody, membrane was blocked with 5% BSA dissolved in TBS-T, for 1h at room temperature. Then the membrane was incubated with primary antibody diluted in 5% BSA containing TBS-T, overnight at $4^{o}C$. The membrane was washed with TBS-T 3 times and incubated with HRP-linked secondary antibody for 2h at room temperature. After the secondary antibody incubation, membrane was washed 3 times with TBS-T again.

4.3.6. Chemiluminescence Detection

Enhanced chemiluminiscent solution (ECL) was used for the visualization of the proteins, ECL was prepared by mixing peroxide and substrate at a ratio of 1:1 and kept away from direct light. Membrane was incubated in ECL for a short time and then the image of the membrane was taken by Stella.

4.4. Tandem Affinity Purification (TAP)

SKMEL28 cells were seeded to 6-well plates at a confluency of 80%, the day before the transfection. Cells were transfected with IRF4_TAP-pIRES2-eGFP or On-

ly_TAP_pIRES2-eGFP, using K2 transfection system, 24 wells for each group. 36 hours after transfection, 800 µl of nuclear fractions in 0.5% Triton-X His-Tag Binding/Wash Buffer were prepared from each group; 50 µl from each group was stored as the input. The remaining 750 µl nuclear lysates were added onto 300 ul Dynabeads His-Tag Isolation&Pulldown beads and incubated on a rotater at room temperature for 15 minutes. 50 µl of the flowthroughs (F/Ts) were kept as control. Then the beads were washed three times with 750 µl of His-Tag Binding/Wash Buffer and the bound proteins were eluted from the beads, via incubation of the beads in His-Tag elution buffer at room temperature for 15 minutes. 50 µl of the eluates were stored as control. 300 ul of Sigma Anti-FLAG M2 magnetic beads were washed twice with TBS buffer and twice with His-Tag Elution Buffer without imidazole; the eluates from the previous step were added to Anti-FLAG M2 magnetic beads. Bead-protein suspensions were incubated on a rotater at room temperature for 2 hours. 50 µl of the F/Ts were stored as control. Beads were washed three times with TBS buffer. In the first replicate, for the elution of bound proteins, 75 µl 0.1 M Glycine pH: 3 solution was added onto the beads and incubated on a rotator at room temperature for 20 minutes. 50 µl of the eluates were stored to be tested with western blotting and to be visualized by silver staining. The remaining was stored to be sent to Mass Spectrometry analysis. After checking the efficiciency of TAP protocol with western blot and silver staining, IRF4_TAP_pIRES2-eGFP and Only_TAP_pIRES2-eGFP eluates from Anti-FLAG beads were sent to EMBL Proteomics Core Facility for Mass Spectrometry analysis. In the second replicate, 1/10 of the Anti-FLAG M2 magnetic beads were separated and boiled at 95°C for 5 minutes after the addition of 40 ul 4X laemmli buffer, to be used in western blotting. The remaining of the beads were stored in 50 µM ammonium bicarbonate solution and sent to UC Davis proteomics core facility for on-bead tryptic digestion.

4.5. BioID

SKMEL28 cells were seeded to 6-well plates at a confluency of 80%, the day before the transfection. Cells were transfected with IRF4_BirA*_PCDNA3.1 or Only BirA*_PCDNA3.1, using K2 transfection system, 24 wells for each group. 24 hours after transfection, cells were administered with 50 µM Biotin for 24 hours and 800 µl of nu-

clear fractions in PBS-T were prepared. 50 µl of each nuclear lysates were stored as inputs. 400 µl of Dynabeads MyOne Streptavidin C1 beads for each sample, were washed twice with PBS and calibrated twice with PBS-T; the remaining 750 µl of lysates were added onto beads. Bead-protein suspensions were incubated at room temperature on a rotator for 30 minutes. 50 µl of F/Ts were stored as control. Beads were washed with Wash Buffer 1, Wash Buffer 2, Wash Buffer 3 and Wash Buffer 4, respectively. 40 µl of beads were separated and boiled at 95°C for 5 minutes after the addition of 40 µl 4X laemmli buffer. The remaining beads were stored in 200 µl 50 µM ammonium bicarbonate solution. After the verificiation of BioID protocol with western blot and silver staining, IRF4_BirA*_PCDNA3.1 and Only_BirA*_PCDNA3.1 beads were sent to UC Davis Proteomics Core Facility. In the second and third replicate of BioID, also untransfected SKMEL28 cells, treated with 50 uM Biotin for 24 hours were added as an additional negative control and same BioID protocol was applied.

4.6. Endogenous IRF4 Pulldown

SKMEL28, SKMEL5, G361, FEPD, HBL-1, and OCI-LY3 cells were seeded to 75 cm^3 flasks at 100% confluency and nuclear lysates were prepared from the cells, resuspending the pellet in PBS-T at the final step. Dynabeads Protein G beads were conjugated with M-17 antibody or Goat IgG as the negative control; 50 µl of beads were incubated with 5 µg of M-17 antibody or Goat IgG diluted in 250 µl of PBS-T, for 30 minutes at room temperature. Also beads that were not conjugated with antibody or IgG were used as an additional negative control. Bead-antibody, bead-IgG conjugates and only beads were washed twice with BS3 conjugation buffer. Then 250 µl of 5 mM BS3 crosslinking reagent dissolved in BS3 conjugation buffer was added onto beads and incubated at toom temperature for 30 minutes. 12.5 µl Tris-Cl, pH 7.5 solution was added onto beads to quench the crosslinking reaction between beads and antibody or IgG and incubated at room temperature for 15 minutes. Then the beads were washed twice with PBS-T and 250 µl of nuclear cell lysate was added onto crosslinked beads and incubated at room temperature for 30 minutes. Then the beads were washed three times with PBS-T. In order to elute the proteins from the beads, 40 µl of leammli buffer was added onto beads and beads were boiled at 95°C for 5 minutes.

4.7. Endogenous nmt55/p54nrb/NONO Pulldown

SKMEL28 and G361 cells were seeded to 75 cm^3 flasks at 100% confluency and nuclear lysates were prepared from thes cells, resuspending the pellet in PBS-T at the final step. Dynabeads Protein G beads were conjugated with anti-nmt55/p54nrb antibody or Rabbit IgG as the negative control; 50 µl of beads were incubated with 5 ug of anti-nmt55/p54nrb antibody or Rabbit IgG diluted in 250 µl of PBS-T, for 1 hour at room temperature. Also beads that were not conjugated with antibody or IgG were used as an additional negative control. Bead-antibody, bead-IgG conjugates and only beads were washed twice with BS3 conjugation buffer. Then 250 µl of 10 mM BS3 crosslinking reagent dissolved in BS3 conjugation buffer was added onto beads and incubated at room temperature for 40 minutes. 30 µl Tris-Cl, pH 7.5 solution was added onto beads to quench the crosslinking reaction between beads and antibody or IgG and incubated at room temperature for 20 minutes. Then the beads were washed twice with PBS-T and 250 µl of nuclear cell lysate was added onto crosslinked beads and incubated at room temperature at room temperature for 1 hour. Then the beads were washed three times with PBS-T. In order to elute the proteins from the beads, 40 µl of leammli buffer was added onto beads and beads were boiled at 95°C for 5 minutes.

4.8. Endogenous BTF/BCLAF1 Pulldown

SKMEL28 cells were seeded to 75 cm^3 flasks at 100% confluency and nuclear lysates were prepared from thes cells, resuspending the pellet in PBS-T at the final step. Dynabeads Protein G beads were conjugated with anti-BTF antibody or Rabbit IgG as the negative control; 50 µl of beads were incubated with 5 µg of anti-BTF antibody or Rabbit IgG diluted in 250 µl of PBS-T, for 1 hour at room temperature. Also beads that were not conjugated with antibody or IgG were used as an additional negative control. Bead-antibody, bead-IgG conjugates and only beads were washed twice with BS3 conjugation buffer. Then 250 µl of 10 mM BS3 crosslinking reagent dissolved in BS3 conjugation buffer was added onto beads and incubated at room temperature for 40 minutes. 30 ul Tris-Cl, pH 7.5 solution was added onto beads to quench the crosslinking reaction

between beads and antibody or IgG and incubated at room temperature for 20 minutes. Then the beads were washed twice with PBS-T and 250 µl of nuclear cell lysate was added onto crosslinked beads and incubated at room temperature for 1 hour. Then the beads were washed three times with PBS-T. In order to elute the proteins from the beads, 40 µl of leammli buffer was added onto beads and beads were boiled at 95°C for 5 minutes.

4.9. Analysis of TAP Mass Spectrometry Data

First samples were median-median normalized; spectral counts of each protein in IRF4_TAP sample were divided by the median of IRF4_TAP spectral counts and the same applied to the spectral counts of each protein in Only_TAP sample by dividing by the median of Only_TAP spectral counts. The aim of median-median normalization is to eliminate the differences between samples, resulting from the different amounts of peptides identified in each sample. Then the normalized spectral abundance factor (NSAF) was calculated for each protein. NSAF is the normalization of spectral counts to the molecular weight of the protein (Zyballov *et al*., 2006). When the molecular weight of a protein is large, the count of peptides that are identified for this protein can be larger, this normalization is used to prevent the miscalculations when the abundance of two different proteins are compared. For the calculation of NSAF value, median normalized spectral counts of each protein in each sample group were divided by the molecular weight of the protein. The fold change between the IRF4_TAP proteins and Only_TAP proteins were calculated by the ratio of NSAF values of IRF4_TAP proteins to NSAF values of Only_TAP proteins. To be able to calculate fold change, 0 (zero) spectral counts in Only_TAP sample were replaced with 1. Proteins that show a fold change less than 1.5 were excluded from the table as we are interested in the proteins that show higher abundance in the IRF4_TAP sample (See Appendix G for the table of TAP analysis proteins).

4.10. Analysis of BioID Mass Spectrometry Data

Exclusive spectrum counts of each protein in each sample group was included to the analysis. Exclusive spectrum count means the number of spectra associated only with a specific protein, by this way spectra shared between proteins are excluded. Then the spectral counts were median-median normalized and NSAF value of each protein was calculated, as described in Section 4.9. For the calculation of fold change, 0 values in Only_BirA* and Unt. negative control groups were replaced with 1 and mean values of median normalized NSAF values were calculated for IRF4_BirA*, Only_BirA* and Unt. groups, by taking the averages of the replicates of each group. The fold change between IRF4_BirA* and Only_BirA* and between IRF4_BirA* and Unt. were calculated, the smallest fold changes were included in the Table5.1. To measure statistical significance, highest value between Only_BirA* and Unt. groups were taken, as there is no Unt. control group for the 1st replicate, Only_BirA* group was taken as negative control of the 1st replicate. T-test was applied to three replicates of IRF4_BirA* group and three negative control groups with highest counts. Benjamini-Hochberg normalization (Diz *et al*., 2011) for multiple testing correction was applied to p-values in order to calculate q values (false discovery rate (FDR) estimations) for each protein. Proteins that show a fold change less than 1.5 and have a p-value higher than 0.05 were excluded from the Table 5.1.

5. RESULTS

5.1. Construction and Validation of IRF4_TAP protein in SKMEL28 cell line

For the tandem affinity purification (TAP) method; TAP-tagged protein and its negative control containing plasmids were constructed. IRF4_TAP fusion protein and its Only_TAP control were cloned into pIRES2-eGFP plasmid, which is an episomal vector with a green fluorescent protein marker (see Appendix A for the plasmid maps and the verifications of clonings). After the construction of IRF4_TAP fusion protein, expression of the protein in the cells were validated. SKMEL28 cells were transfected with IRF4_TAP_pIRES2-eGFP and Only_TAP_pIRES2-eGFP, using K2 transfection system (As described in 4.1.2). As the pIRES2-eGFP plasmid has green fluorescent protein marker, after 36 hours of transfection cells were examined under fluorescence microscope and GFP was observed for transfected cells, indicating successful transfection (Figure 5.1).

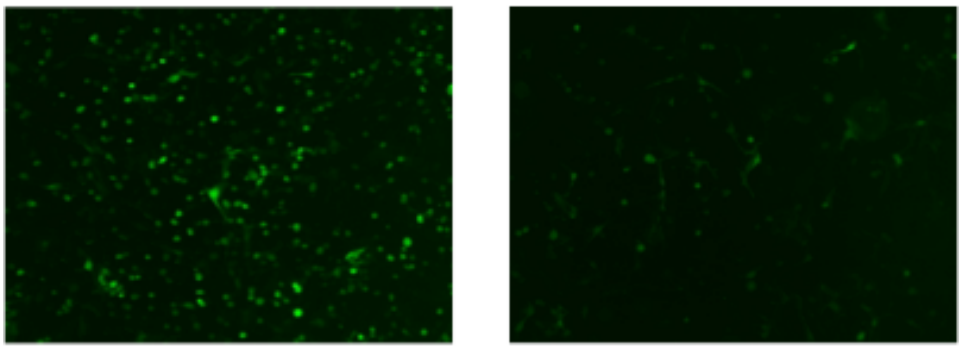

Figure 5.1 Images of IRF4_TAP_pIRES2-eGFP and Only_TAP_pIRES2-eGFP transfected SKMEL28 cells under fluorescence microscope, presence of GFP demonstrates that transfection was successful.

Then total lysates and nuclear fractions were prepared from the transfected and untransfected cells in order to validate the expression of IRF4_TAP both in nuclear fraction and total lysate (See Appendix B for the fidelity of nuclear fractionation). Western blot was performed with IRF4 (M-17) and Anti-FLAG M2 (Sigma Aldrich, USA) antibodies. IRF4 protein is 52 kDa and TAP tag is approximately 2 kDa; as a result IRF4_TAP protein has an approximate molecular weight of 54 kDa and due to small molecular weight of TAP tag, IRF4_TAP is indistinguishable from wild-type IRF4. Blotting of the lysates with antibodies showed a band between 58 kDa and 46 kDa bands of the protein marker. The presence of IRF4_TAP protein in nuclear lysate, in addition to total lysate, confirms the successful entrance of the protein into the nucleus. As the Only_TAP is only 2 kDa, it could not have been observed in the western blot (Figure 5.2).

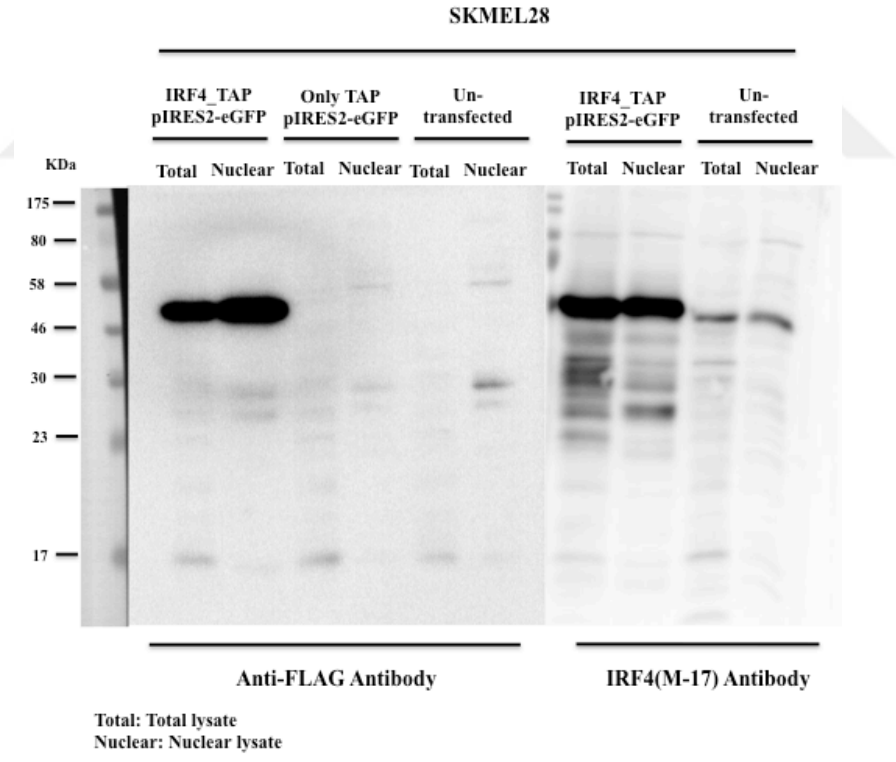

Figure 5.2 Blotting of nuclear and total lysates of IRF4_TAP_pIRES2-eGFP or Only_TAP_pIRES2-eGFP transfected and untransfected SKMEL28 cells, with anti-FLAG M2 and IRF4 (M-17) antibodies. IRF4_TAP protein was observed in both total and nuclear lysates.

5.2. Pull down of IRF4 and IRF4-Interacting Proteins with TAP

After the validation of IRF4_TAP fusion protein expression in SKMEL28 cells; four 6-well plates of SKMEL28 cells were transfected with IRF4_TAP_pIRES2-eGFP and Only_TAP_pIRES2-eGFP, to be able to purifiy as much as protein to be detected with Mass Spectrometry. Cells were examined under fluorescent microscope and GFP was traced through flow cytometry to obtain the percentage of GFP positive cells. IRF4_TAP_pIRES2-eGFP transfected SKMEL28 cells showed 84% transfection efficiency and Only_TAP_pIRES2-eGFP transfected cells showed 88% efficiency (Figure 5.3).

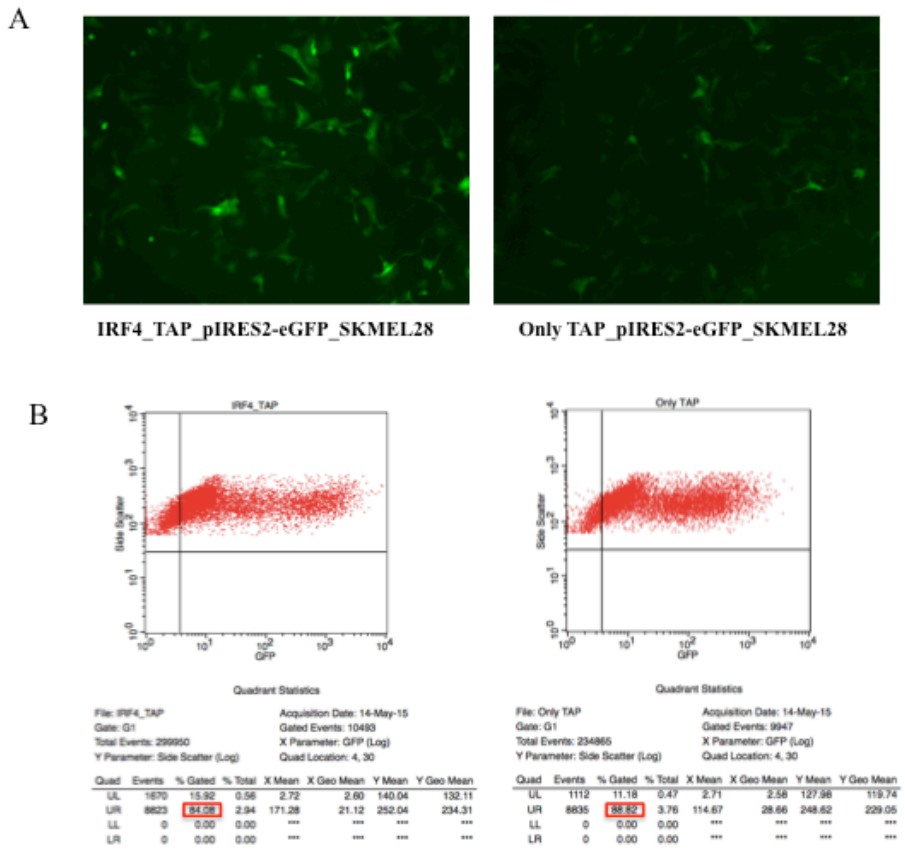

Figure 5.3 Images of IRF4_TAP_pIRES2-eGFP and Only_TAP_pIRES2-eGFP transfected SKMEL28 cells under fluorescence microscope (A) and their analysis through flow cytometer (B). IRF4_TAP_pIRES2-eGFP and Only_TAP_pIRES2-eGFP transfected cells show higher than 80% transfection efficiency.

As the transfection efficiencies of the cells are sufficient, nuclear lysates were prepared from the cells and TAP was performed (as described in 4.4). In order to check the efficiency of TAP protocol, inputs, flowthroughs (F/T) and eluates of TAP were blotted with IRF4 (M-17) and Anti-FLAG M2 (Sigma Aldrich, USA) antibodies (Figure 5.4). As TAP tag has a small molecular weight, IRF4_TAP fusion protein is indistinguishable from wild-type IRF4; however a much more bolder band was observed in the IRF4_TAP_pIRES2-eGFP input when compared to Only_TAP_pIRES2-eGFP input (Figure 5.4A). Some product loss is observable in the F/Ts of Dynabeads His-Tag Isolation and pulldown beads and Sigma Anti-FLAG M2 magnetic beads. Still, eluates from Dynabeads His-Tag Isolation and Pulldown beads and Sigma Anti-FLAG M2 magnetic beads show a band at the size of IRF4_TAP.

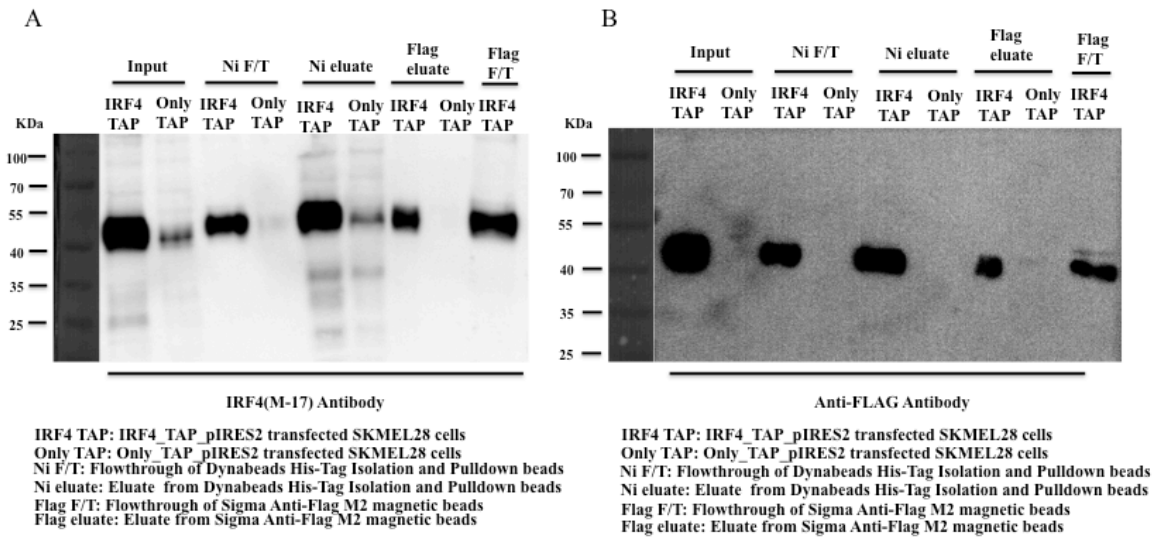

Figure 5.4 Confirmation of TAP protocol. Blotting of inputs, F/Ts and eluates of first replicate of TAP, with IRF4(M-17) (A) and Anti-Flag M2 (B) antibodies. As the final eluate of IRF4_TAP_pIRES2-eGFP transfected cells from Anti-FLAG M2 magnetic beads show a band at the size of IRF4_TAP, TAP protocol can be concluded to be successful.

Inputs and eluates of TAP were also silver stained. In the IRF4_TAP_pIRES2-eGFP eluate of Sigma Anti-FLAG M2 magnetic beads, a bold band at the size of IRF4_TAP is observable whereas it was absent in the Only_TAP_pIRES2-eGFP eluate.

Moreover, there were a few bands in the IRF4_TAP_pIRES2-eGFP eluate of Sigma Anti-FLAG M2 magnetic beads which are not present in Only_TAP_pIRES2-eGFP eluate (Figure 5.5) which points to elution of other proteins than IRF4 and as they are not present in the negative control, they might be IRF4-interacting proteins.

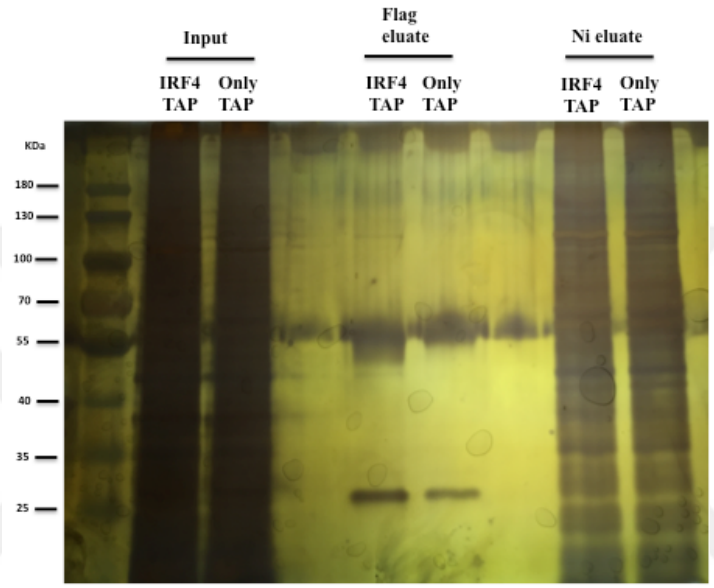

Figure 5.5 Silver staining of inputs and eluates of TAP. IRF4_TAP_pIRES2-eGFP eluate of Sigma Anti-FLAG M2 magnetic beads shows a band at the size of IRF4_TAP and there are other bands than IRF4_TAP which are not present in the negative control.

Second replicate of TAP purification was prepared as described in 4.4 (See Appendix C for the western blot and silver staining of second replicate of TAP).

5.3. Construction and Validation of IRF4_BirA* protein and biotinylation in SKMEL28 cell line

For the BioID experiment, IRF4_BirA* fusion protein containing plasmid was constructed. When this fusion protein is expressed in the cells, it can biotinylate the pro-

teins that are in proximity with IRF4 and IRF4 itself is also biotinylated. For this purpose, IRF4 coding sequence was cloned into PCDNA3.1 MCS-BirA(R118G)-HA plasmid which is an epsiomal plasmid, containing BirA* (see Appendix D for plasmid maps and verification of cloning). After the construction of IRF4_BirA* fusion protein, expression of the protein in the cells were validated. SKMEL28 cells were transfected with IRF4_BirA*_PCDNA3.1 and Only BirA*_PCDNA3.1, using K2 transfection system (As described in 4.1.2). Eventhough cells contain a basal level of biotin, excess biotin is required for the proper biotinylation of all proteins-in-proximity and IRF4 protein itself. In order to determine the optimum conditions for biotin treatment, transfected and untransfected cells were administered with 50 uM or 100 uM biotin and treated with biotin for 24, 48 and 72 hours. Total lysates were prepared for all conditions and blotted with IRF4 (M-17) antibody (Figure 5.6A). As the cells are transiently transfected with the plasmids, a decrease in the amount of IRF4_BirA* protein is observable at 48h and 72h time points. In consistent with the decrase in the amount of IRF4_BirA*, biotinylation decreases at 48h time point. Therefore, optimum condition for biotin treatment was decided to be 24 hours. When the samples were blotted with Streptavidin-HRP (Life Technologies, a significant difference between 50 uM or 100 uM biotin treatment was not observed (Figure 5.6B), thus 50 uM biotin was decided to be used.

IRF4 protein is 52 kDa and BirA* is approximately 35 kDa; as a result IRF4_BirA* protein has an approximate weight of 87 kDa and blotting of the lysates of IRF4_BirA*_PCDNA3.1 transfected SKMEL28 cells with IRF4 (M-17) showed a band between 100 kDa and 70 kDa bands of the protein marker. Moreover, the 35 kDa molecular weight of BirA* enables us to distinguish IRF4_BirA* fusion protein from wild-type IRF4. Both IRF4_BirA* and wild-type IRF4 is observed for IRF4_BirA*_PCDNA3.1 transfected cells, whereas only wild-type IRF4 was observed for Only BirA*_PCDNA3.1 and untransfected cells, as expected (Figure 5.6A).

When the lysates of IRF4_BirA*_PCDNA3.1 transfected SKMEL28 cells blotted with Streptavidin-HRP (Life Technologies) antibody, the amount of biotinylated proteins was too high that bands were indistinguishable. However, blotting of Only_BirA*_PCDNA3.1 transfected and untransfected cells show the basal biotinylation

level in the cells which is present in the absence of IRF4_BirA* protein. Also for the Only_BirA*_PCDNA3.1 transfected cells, a band at the size of BirA* is observable, indicating the success of negative control.

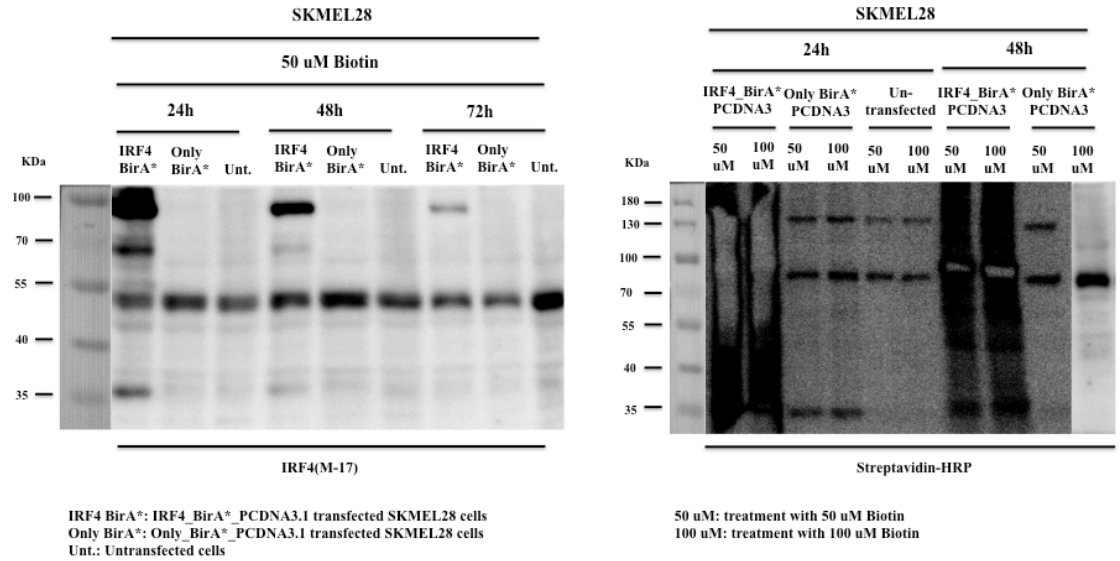

Figure 5.6 Blotting of total lysates of IRF4_BirA*_PCDNA3.1 and Only_BirA*_PCDNA3.1 transfected and untransfected SKMEL28 cells with IRF4(M-17) (A) and Streptavidin-HRP (B) antibodies, after different conditions of biotin treatment.

After optimum conditions for biotin treatment were determined, SKMEL28 cells were again transfected with IRF4_BirA*_PCDNA3.1 and Only BirA*_PCDNA3.1, using K2 transfection system. 24 hours after transfection, transfected and untransfected cells were administered with 50 uM Biotin or 50 uM DMSO as the vehicle for 24 hours, to see the the difference between biotin tretated and non-biotin treated cells. Nuclear fractions were prepared from the cells and blotted with IRF4 (M-17) and Streptavidin-HRP (Life Technologies) antibodies (Figure 5.7). It was observed that IRF4_BirA* protein is capable of nuclear entrance as a band at the size of IRF4_BirA* was observed for also nuclear fraction of IRF4_BirA*_PCDNA3.1 transfected cells (Figure 5.7A). Moreover, IRF4_BirA* is capable of biotinylation in the nucleus (Figure 5.7B). However, a band at the size of BirA* was not observed when Only_BirA*_PCDNA3.1 transfected

cells were blotted with Streptavidin-HRP (Life Technologies). In order to confirm the entrance of negative control Only_BirA* protein into the nucleus, nuclear lysates of IRF4_BirA*_PCDNA3.1 and Only_BirA*_PCDNA3.1 transfected cells were blotted with Anti-HA (Abcam) antibody, PCDNA3.1 MCS-BirA(R118G)-HA plasmid also contains HA tag at the C-terminal of BirA*, thus IRF4_BirA* and Only_BirA* proteins are also fused with HA tag. When blotted with Anti-HA (Abcam) antibody, Only_BirA* protein was observed in the nuclear fraction, indicating the convenience of Only_BirA* as a negative control (See Appendix E for the blotting of nuclear lysates with Anti-HA (Abcam) antibody).

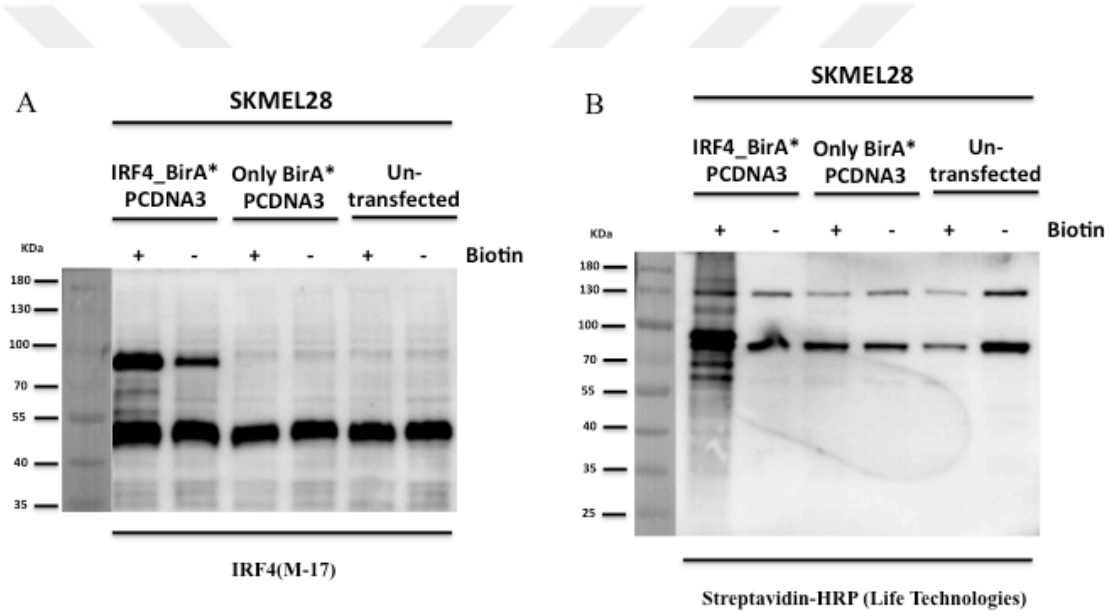

Figure 5.7 Blotting of nuclear lysates of IRF4_BirA*_PCDNA3 and Only BirA*_PCDNA3 transfected and untransfected SKMEL28 cells with IRF4 (M-17) (A) and Streptavidin-HRP (B) antibodies. IRF4_BirA* fusion protein is capable of nuclear entrance and it can perform biotin ligase function in the nucleus.

5.4. Pull down of Biotinylated Proteins with BioID

After the validation of IRF4_BirA* fusion protein expression in SKMEL28 cells and the optimization of biotin treatment; four 6-well plates of SKMEL28 cells were

transfected with IRF4_BirA*_PCDNA3.1 and Only BirA*_PCDNA3.1. IRF4_BirA*_PCDNA3.1 and Only BirA*_PCDNA3.1 and untransfected SKMEL28 cells were treated with 50 uM biotin for 24 hours. After the preparation of the nuclear fractions from the cells, BioID was performed (As described in 4.5).

In order to check the efficiency of the protocol, 1/10 of the beads were set aside to be used in western blotting and silver staining. In the western blot with IRF4 (M-17) antibody, a band at the size of IRF4_BirA* was observed in the IRF4_BirA*_PCDNA3.1 input. Some product loss is observable in the IRF4_BirA*_PCDNA3.1 F/T; however a relatively high amount of IRF4_BirA* is observable in IRF4_BirA*_PCDNA3.1 eluate (Figure 5.8A). Inputs were also blotted with Streptavidin-HRP (Life Technologies), for IRF4_BirA*_PCDNA3.1 input the amount of biotinylated proteins was too high that bands were indistinguishable. There was a band at the size of Only_BirA* in the input of Only_BirA*_PCDNA3.1, which was not present for the input of untransfected cells (Figure 5.8B).

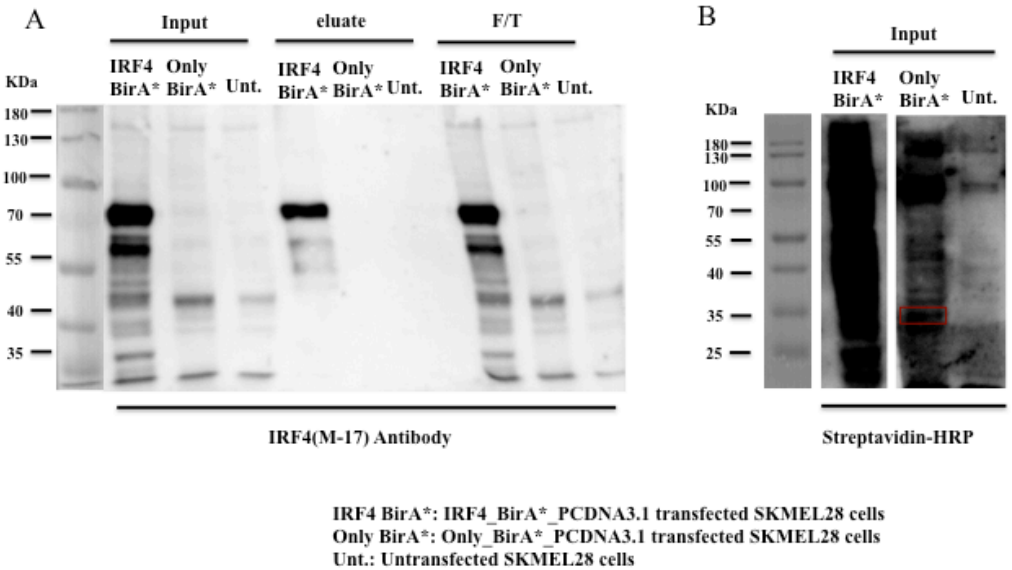

Figure 5.8 Confirmation of BioID protocol. Blotting of inputs, F/Ts and eluates of BioID with IRF4 (M-17) antibody (A) and blotting of inputs with Streptavidin-HRP (B). With IRF4 (M-17) blotting, success of the BioID was confirmed and with Streptavidin-HRP convenience of Only_BirA* negative control was confirmed.

BioID samples were also silver stained. In the silver staining of inputs and eluates, a band at the size of IRF4_BirA* was observed in IRF4_BirA*_PCDNA3.1 eluate. Also there were a few bands in the IRF4_BirA*_PCDNA3.1 eluate which are not present in Only BirA*_PCDNA3.1 and untransfected eluates, indicating the presence of proteins in proximity with IRF4 (Figure 5.9).

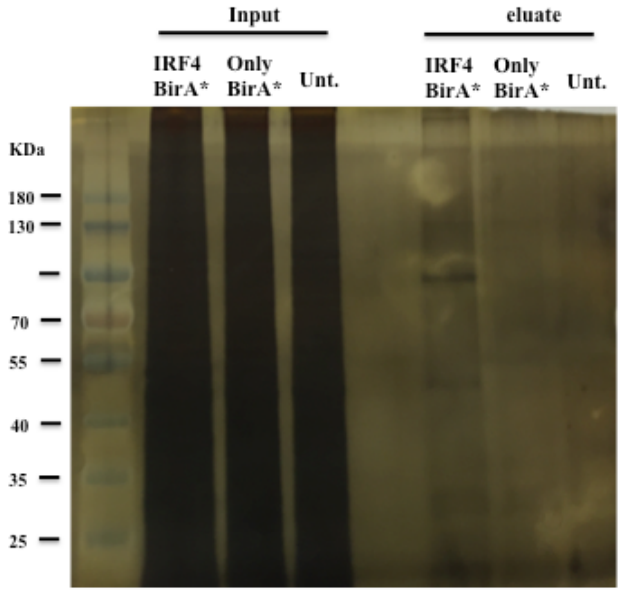

Figure 5.9 Silver Staining of BioID samples. A band at the size of IRF4_BirA* was observed in the eluate of IRF4_BirA*_PCDNA3.1. in addition to few bands other than IRF4_BirA* and these bands were absent in the negative controls.

First and third biological replicates of BioID were prepared similarly. (See Appendix F for the western blot and silver staining of first and third replicates of BioID.).

5.5. Mass Spectrometry Analysis

5.5.1. Provisional Analysis of TAP Mass Spectrometry Data

TAP mass spectrometry data was analyzed as described in Section 4.9. The mass spectrometry data of second replicate of TAP is contradictory to the first replicate of TAP and it was also inconsistent with the mass spectrometry data of BioID, therefore it is not included in TAP analysis and no statistical significance test could have been applied in TAP mass spectrometry analysis (See Appendix G for the list of TAP proteins).

The proteins from TAP analysis were functionally annotated via DAVID Functional Annotation Tool (DAVID Bioinformatics Resources 6.7, NIAID/NIH). Uniprot accession numbers of the proteins from the list of TAP mass spectrometry analysis (Appendix G) were uploaded to DAVID program, after the selection of UNIPROT_ACCESSION as the identifier and gene list as the list type, the list of proteins were submitted. Then Go_TERM BP (BP depicts for biological process) was selected from Gene Ontology part and functional annotation chart was selected to see the functions assigned to the proteins in the list, with highest significance scores (Figure 5.10). This analysis suggests that proteins from TAP mostly have functions in RNA processing and splicing.

	Annotation Cluster 1	Enrichment Score: 34.78			Count	P_Value	Benjamini
☐	GOTERM_BP_FAT	mRNA metabolic process	RT		46	4.0E-39	2.7E-36
☐	GOTERM_BP_FAT	mRNA processing	RT		44	4.1E-39	1.4E-36
☐	GOTERM_BP_FAT	RNA splicing	RT		42	1.4E-38	3.1E-36
☐	GOTERM_BP_FAT	RNA processing	RT		49	4.0E-35	6.7E-33
☐	GOTERM_BP_FAT	RNA splicing, via transesterification reactions	RT		31	3.3E-32	4.4E-30
☐	GOTERM_BP_FAT	RNA splicing, via transesterification reactions with bulged adenosine as nucleophile	RT		31	3.3E-32	4.4E-30
☐	GOTERM_BP_FAT	nuclear mRNA splicing, via spliceosome	RT		31	3.3E-32	4.4E-30

Figure 5.10 Functional clustering of TAP proteins by DAVID Functional Annotation Tool (Only the highest ranked functional clusters are shown.).

5.5.2. Analysis of BioID Mass Spectrometry Data

BioID mass spectrometry data was analyzed as described in Section 4.10. Proteins identified with BioID were organized according to fold changes in a descending manner, after filtering of the proteins with fold change less than 1.5 and p-value higher than 0.05. IRF4 was also observed in the list, observation of the target protein in the analysis further confirms the success of BioID method (Table 5.1). Raw spectral counts of the proteins for each sample group of each replicate are shown in Appendix H.

Table 5.1 List of the proteins obtained from BioID analysis.

Identified Proteins	Gene Symbol	Molecular Weight (kDa)	Fold Change	p-value	q value
Interferon regulatory factor 4	IRF4	52	524	0.048	0.25
Far upstream element-binding protein 2	FUBP2	73	31	0.003	0.20
Splicing factor 1	SF01	68	25	0.050	0.25
Host cell factor 1	A6NEM 2	213	19	0.016	0.25
Synemin	SYNEM	173	18	0.009	0.25
Bcl-2-associated transcription factor 1	BCLF1	106	17	0.032	0.25
T-complex protein 1 subunit theta	TCPQ	60	15	0.037	0.25
Splicing factor, proline- and glutamine-rich	SFPQ	76	13	0.009	0.25
E3 SUMO-protein ligase RanBP2	RBP2	358	13	0.018	0.25
Importin-7	IPO7	120	11	0.004	0.20
Eukaryotic initiation factor 4A-III	IF4A3	47	11	0.006	0.22
Calcium-binding mitochondrial carrier protein Aralar2	CMC2	74	10	0.017	0.25
Importin subunit beta-1	IMB1	97	10	0.001	0.11
Stomatin-like protein 2, mitochondrial	STML2	39	10	0.020	0.25
Paraspeckle component 1	PSPC1	59	10	0.027	0.25
Cluster of Nuclear receptor corepressor 1	NCOR1	270	10	0.014	0.25
RNA-binding protein 14	RBM14	69	9	0.037	0.25
Activity-dependent neuroprotector homeobox protein	ADNP	124	9	0.008	0.25
Heterogeneous nuclear ribonucleoprotein M	HNRPM	78	8	0.001	0.11
Paired amphipathic helix protein Sin3a	SIN3A	145	8	0.001	0.11
Myocyte-specific enhancer factor 2D	MEF2D	56	8	0.018	0.25
Chromome alignment-maintaining phphoprotein 1	CHAP1	89	8	0.017	0.25

Table 5.1 List of the proteins obtained from BioID analysis.

AT-rich interactive domain-containing protein 1A	ARI1A	242	7	0.045	0.25
Thyroid hormone receptor-associated protein 3	TR150	109	7	0.010	0.25
U4/U6 small nuclear ribonucleoprotein Prp3	PRPF3	78	7	0.016	0.25
Cluster of Bromodomain-containing protein 3	BRD3	80	6	0.000	0.02
Tubulin alpha-1B chain	TBA1B	50	6	0.006	0.22
Cluster of Zinc finger CCCH domain-containing protein 4	ZC3H4	140	6	0.015	0.25
Transcription factor SOX-13	SOX13	69	6	0.020	0.25
Coronin-1B	COR1B	54	5	0.047	0.25
Transcriptional repressor p66-beta	P66B	65	5	0.029	0.25
Eukaryotic initiation factor 4A-I	IF4A1	46	5	0.030	0.25
Uveal autoantigen with coiled-coil domains and ankyrin repeats	UACA	163	5	0.036	0.25
Cluster of Filamin-A	FLNA	281	5	0.014	0.25
5'-3' exoribonuclease 2	XRN2	109	5	0.009	0.25
Bromodomain-containing protein 4	BRD4	152	5	0.000	0.03
Non-POU domain-containing octamer-binding protein	NONO	54	5	0.001	0.11
Transcriptional repressor p66-alpha	P66A	68	5	0.009	0.25
Heterogeneous nuclear ribonucleoproteins A2/B1	ROA2	37	5	0.031	0.25
ADP/ATP translocase 2	ADT2	33	5	0.027	0.25
Cluster of Heterogeneous nuclear ribonucleoprotein A1	ROA1	39	5	0.018	0.25
Leucine-rich repeat-containing protein 47	LRC47	63	4	0.020	0.25
RNA-binding protein 27	RBM27	119	4	0.009	0.25
DNA repair protein RAD50	RAD50	154	4	0.025	0.25
Pyruvate kinase PKM	KPYM	58	4	0.043	0.25
Poly(rC)-binding protein 1	PCBP1	37	4	0.022	0.25
Prelamin-A/C	LMNA	74	4	0.046	0.25
Plectin	PLEC	532	4	0.029	0.25
Tubulin beta chain	TBB5	50	4	0.025	0.25
40S ribomal protein S7	RS7	22	4	0.041	0.25
Cullin-associated NEDD8-dissociated protein 1	CAND1	136	3	0.034	0.25
Cytoplasmic dynein 1 heavy chain 1	DYHC1	532	3	0.034	0.25
Filamin-A	FLNA	281	3	0.037	0.25
Sister chromatid cohesion protein PDS5 homolog A	PDS5A	151	3	0.005	0.21
PERQ amino acid-rich with GYF domain-containing protein 2	PERQ2	150	3	0.004	0.20

Table 5.1 List of the proteins obtained from BioID analysis.

Zinc finger CCCH domain-containing protein 11A	ZC11A	89	3	0.025	0.25
Cyclin-dependent kinase 12	CDK12	164	3	0.005	0.21
Golgin subfamily A member 2	GOGA2	113	3	0.040	0.25
Histone acetyltransferase p300	EP300	264	3	0.028	0.25
Splicing factor 3B subunit 1	SF3B1	146	3	0.030	0.25
Brain-specific angiogenesis inhibitor 1-associated protein 2-like protein 1	BI2L1	57	3	0.024	0.25
Kinesin-1 heavy chain	KINH	110	3	0.006	0.22
Tubulin beta-2A chain	TBB2A	50	3	0.003	0.20
Ataxin-2-like protein	ATX2L	113	2	0.022	0.25
Nuclear mitotic apparatus protein 1	NUMA1	238	2	0.031	0.25
Cluster of Splicing factor 3B subunit 2	SF3B2	100	2	0.039	0.25
Vigilin	VIGLN	141	2	0.029	0.25
Probable ATP-dependent RNA helicase DDX17	DDX17	80	2	0.043	0.25
Cluster of 40S ribomal protein S16	RS16	16	2	0.046	0.25
Eukaryotic initiation factor 4A-II	IF4A2	46	2	0.004	0.20

Proteins identified from BioID analysis, were functionally annotated via DAVID Functional Annotation Tool (DAVID Bioinformatics Resources 6.7, NIAID/NIH) as described in Section 5.5.1. Functions assigned to the proteins in the list, with highest significance scores are shown Figure 5.11. The proteins from BioID are also suggested to mostly function in RNA processing and splicing.

Annotation Cluster 1	Enrichment Score: 7.46			Count	P_Value	Benjamini
GOTERM_BP_FAT	RNA processing	RT		17	5.1E-10	3.0E-7
GOTERM_BP_FAT	mRNA processing	RT		14	5.7E-10	1.7E-7
GOTERM_BP_FAT	RNA splicing	RT		13	1.8E-9	3.4E-7
GOTERM_BP_FAT	mRNA metabolic process	RT		14	3.2E-9	4.7E-7
GOTERM_BP_FAT	RNA splicing, via transesterification reactions	RT		8	3.4E-6	4.0E-4
GOTERM_BP_FAT	RNA splicing, via transesterification reactions with bulged adenosine as nucleophile	RT		8	3.4E-6	4.0E-4
GOTERM_BP_FAT	nuclear mRNA splicing, via spliceosome	RT		8	3.4E-6	4.0E-4

Figure 5.11 Functional clustering of BioID proteins by DAVID Functional Annotation Tool (Only the highest ranked functional clusters are shown.).

5.5.3. Integration of TAP and BioID Mass Spectrometry Data

The proteins that are common in TAP and BioID mass spectrometry analysis are shown in Table 5.2.

Table 5.2 Common Proteins in TAP and BioID Mass Spectrometry Analysis.

Identified Proteins	Gene Symbol	Molecular Weight (kDa)
Interferon regulatory factor 4	IRF4	52
Splicing factor 1	SF01	68
Bcl-2-associated transcription factor 1	BCLF1	106
Splicing factor, proline- and glutamine-rich	SFPQ	76
Paraspeckle component 1	PSPC1	59
RNA-binding protein 14	RBM14	69
Heterogeneous nuclear ribonucleoprotein M	HNRPM	78
Thyroid hormone receptor-associated protein 3	TR150	109
U4/U6 small nuclear ribonucleoprotein Prp3	PRPF3	78
5'-3' exoribonuclease 2	XRN2	109
Non-POU domain-containing octamer-binding protein	NONO	54
RNA-binding protein 27	RBM27	119
Poly(rC)-binding protein 1	PCBP1	37
Splicing factor 3B subunit 1	SF3B1	146
Ataxin-2-like protein	ATX2L	113
Vigilin	VIGLN	141
Probable ATP-dependent RNA helicase DDX17	DDX17	80

Also proteins that are common in BioID and TAP analysis were functionally annotated via DAVID Functional Annotation Tool (DAVID Bioinformatics Resources 6.7, NIAID/NIH) as described in Section 5.5.1. Functions assigned to the proteins in the list, with highest significance scores are shown Figure 5.12. As expected, these proteins are suggested to mostly function in RNA processing and splicing.

Annotation Cluster 1	Enrichment Score: 7.27			Count	P_Value	Benjamini
GOTERM_BP_FAT	mRNA processing	RT		9	2.4E-10	4.5E-8
GOTERM_BP_FAT	RNA processing	RT		10	4.5E-10	4.2E-8
GOTERM_BP_FAT	mRNA metabolic process	RT		9	7.6E-10	4.7E-8
GOTERM_BP_FAT	RNA splicing	RT		8	5.1E-9	2.3E-7
GOTERM_BP_FAT	RNA splicing, via transesterification reactions	RT		5	1.4E-5	5.4E-4
GOTERM_BP_FAT	RNA splicing, via transesterification reactions with bulged adenosine as nucleophile	RT		5	1.4E-5	5.4E-4
GOTERM_BP_FAT	nuclear mRNA splicing, via spliceosome	RT		5	1.4E-5	5.4E-4

Figure 5.12 Functional clustering of common proteins in BioID and TAP analysis by DAVID Functional Annotation Tool (Only the highest ranked functional clusters are shown.).

After the analysis of BioID and TAP Mass Spectrometry data, we selected two candidate proteins, Bcl-2 associated transcription factor (BCLAF1 or BTF) and Non-POU Domain-Containing Octamer-Binding Protein (NONO/nmt55/p54nrb) as candidate interaction partners of IRF4. These two proteins are present in both TAP and BioID analysis (Table 5.2) and both of them have high fold changes and p-values less than 0.05 (Table 5.1). Moreover, the functions of these proteins can be related to IRF4, further supporting their interaction with IRF4 (see Discussion for the function of NONO and BCLAF1). After selection of these candidate proteins, we first aimed to validate their expression in BioID and TAP samples with western blot.

5.6. Validation of NONO and BCLAF1 Expression in TAP Samples

Samples of first replicate of TAP were blotted with anti-BTF (Abcam) and anti-nmt55/p54nrb (Abcam) antibodies, which detect BCLAF1 and NONO, respectively, in order to verify their expression in TAP samples.

BCLAF1 has different variants and their sizes differ from 106 kDa to 86 kDa. When TAP samples were blotted with Anti-BTF (Abcam) antibody, bands at the sizes between 100 kDa and 70 kDa were observed in the inputs, eluates of Dynabeads His-Tag Isolation and Pulldown beads and IRF4_TAP_pIRES2-eGFP eluate of Sigma Anti-FLAG M2 magnetic beads which is not present in Only_TAP_pIRES2-eGFP eluate of

Sigma Anti-FLAG M2 magnetic beads (Figure 5.13A). NONO has a molecular weight of 54 kDa and when the same samples were blotted with anti-nmt55/p54nrb (Abcam) antibody, a band at the size of NONO was observed in inputs and all eluates, there was not a difference at the amount of NONO protein between IRF4_TAP_pIRES2-eGFP eluate and Only_TAP_pIRES2-eGFP eluate of Sigma Anti-FLAG M2 magnetic beads (Figure 5.13B).

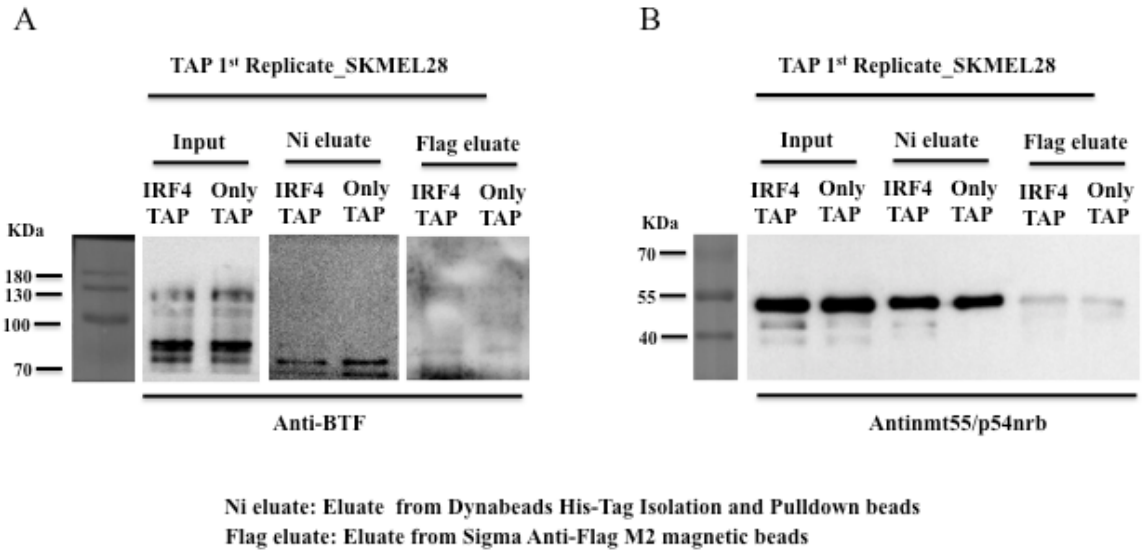

Figure 5.13 Blotting of samples of 1st replicate of TAP with anti-BTF (A) and anti-nmt55/p54nrb (B) antibodies. BCLAF 1 was observed in the eluate of IRF4_TAP_pIRES2 from Sigma Anti-FLAG M2 magnetic beads and absent in the eluate of Only_TAP_pIRES2. NONO was observed at the same level in both IRF4_TAP_pIRES2-eGFP eluate and Only_TAP_pIRES2-eGFP eluate of Sigma Anti-FLAG M2 magnetic beads.

5.7. Validation of NONO and BCLAF1 Expression n BioID Samples

In order to confirm NONO and BCLAF1 expression in BioID samples. Inputs and eluates of BioID third replicate were blotted with anti-BTF (Abcam) and Anti-nmt55/p54nrb (Abcam) antibodies.

When BioID third replicate samples were blotted with anti-BTF (Abcam) antibody, a band at the size of BCLAF1 was observed in the inputs and IRF4_BirA* eluate, it was absent in negative controls (Figure 5.14A). Unfortunately, when the same samples were blotted with anti-nmt55/p54nrb (Abcam) antibody, a band at the size of NONO was observed in inputs but it was absent in all eluates (Figure 5.14B).

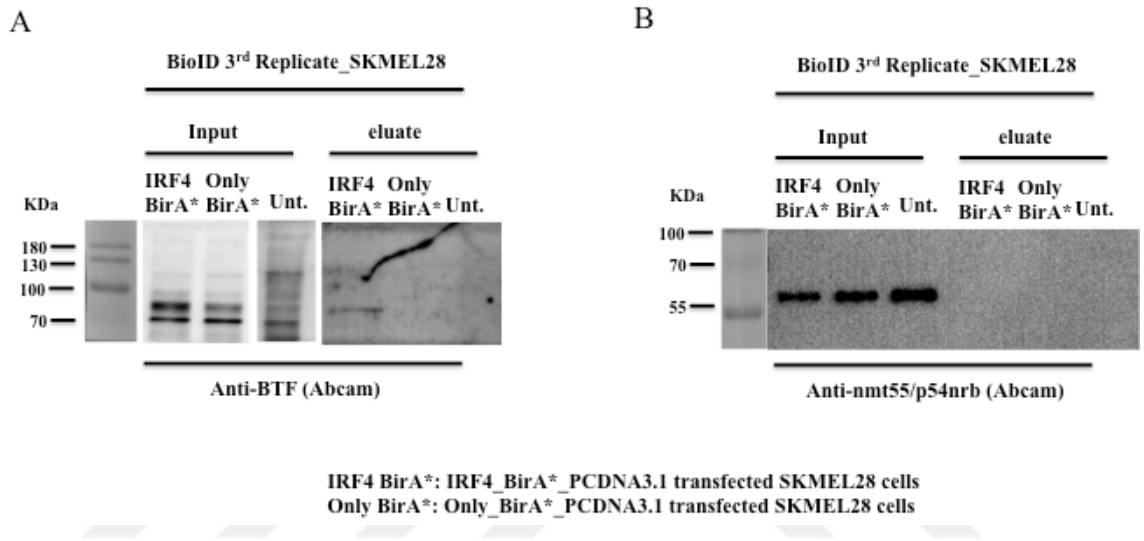

Figure 5.14 Blotting of samples of 3rd replicate of BioID with anti-BTF (A) and anti-nmt55/p54nrb (B) antibodies. BCLAF1 band was observed in the eluate of IRF4_BirA*_PCDNA3.1 and absent in negative controls. NONO band was not observed in any of the eluates.

5.8. Endogenous IRF4 Pulldown

Endogenous IRF4 Pulldown was performed to detect if the BCLAF1 and NONO proteins can be observed to interact with IRF4 with an additional method of protein purification. Melanoma cell lines, SKMEL28, SKMEL5 and G361 was used for the pulldown. SKMEL28 is the primary cell line we used also in TAP and BioID, SKMEL5 is the secondary cell line, used by our group and G361 is the cell line that shows the highest expression of IRF4. In addition to these cell lines, HBL-1, OCI-LY-3 (ABC DLBCL

cell lines) and FEPD (AACL cell line) were used as IRF4 expression is shown to be high also in lymphomas.

In order to confirm the endogenous IRF4 pulldown method, samples were first blotted with IRF4 (M-17) antibody. Goat IgG, which is the negative control as the IRF4 (M-17) antibody is a goat-origin antibody, was observed to show high background, for this reason Goat IgG was excluded from the Figure 5.14 (See Appendix I for the blotting of also Goat IgG). When the level of IRF4 protein is compared between the IRF4 (M-17) antibody and only beads control, it is concluded that endogenous IRF4 pulldown method is working. Then the samples were blotted with anti-BTF (Abcam) antibody in order to observe if BCLAF1 is co-immunoprecipitated with IRF4. For the cell lines SKMEL28, SKMEL5 and FEPD, a band at the size of BCLAF1 was observed in IRF4 (M-17) antibody pulldown but it was absent in only beads control. However, an interaction between IRF4 and BCLAF1 can not be concluded for the cell lines G361, HBL-1 and OCI-LY3 with this method (Figure 5.15).

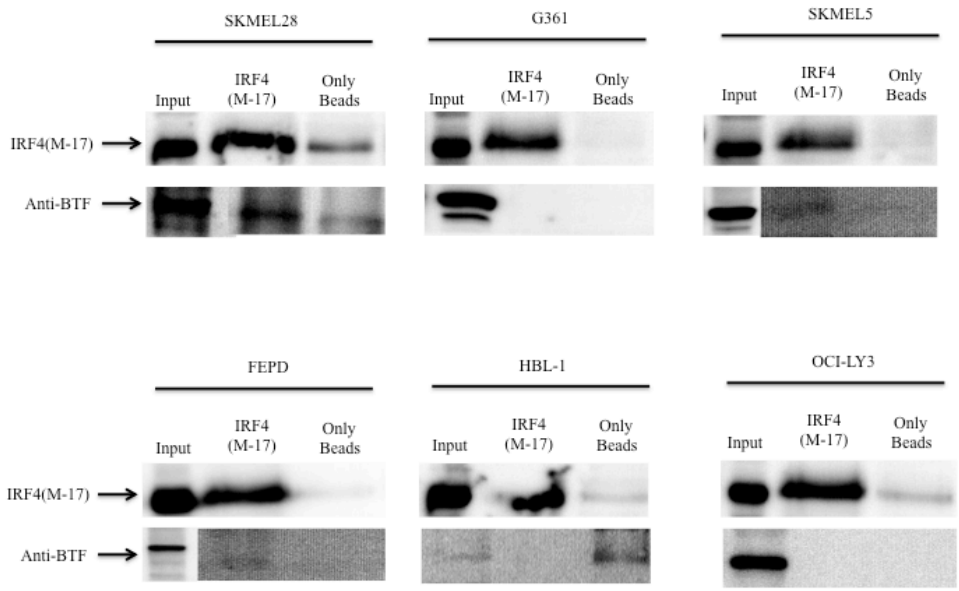

Figure 5.15 Blotting of Endogenous IRF4 Pulldown samples with IRF4 (M-17) and anti-BTF antibodies (empty wells between the samples were cropped and some parts of the membranes were examined under higher exposure to observe the bands.)

Also Endogenous IRF4 Pulldown samples were blotted with anti-nmt55/p54nrb (Abcam) antibody, but a band at the size of NONO was observed for also negative controls. Therefore, blotting of the samples with anti-nmt55/p54nrb (Abcam) antibody were excluded from the Figure 5.15

5.9. Endogenous nmt55/p54nrb/NONO Pulldown

Endogenous NONO pulldown was performed with SKMEL28 and G361 cell lines. In order to confirm the method, samples were first blotted with anti-nmt55/p54nrb (Abcam) antibody. Blotting of the samples with anti-nmt55/p54nrb (Abcam) antibody showed a band at the size of NONO for inputs and anti-nmt55/p54nrb antibody sample of SKMEL28 and G361 cell lines, as expected. However, NONO band was also present in negative controls of both cell lines, Rabbit IgG and only beads (Figure 5.16)

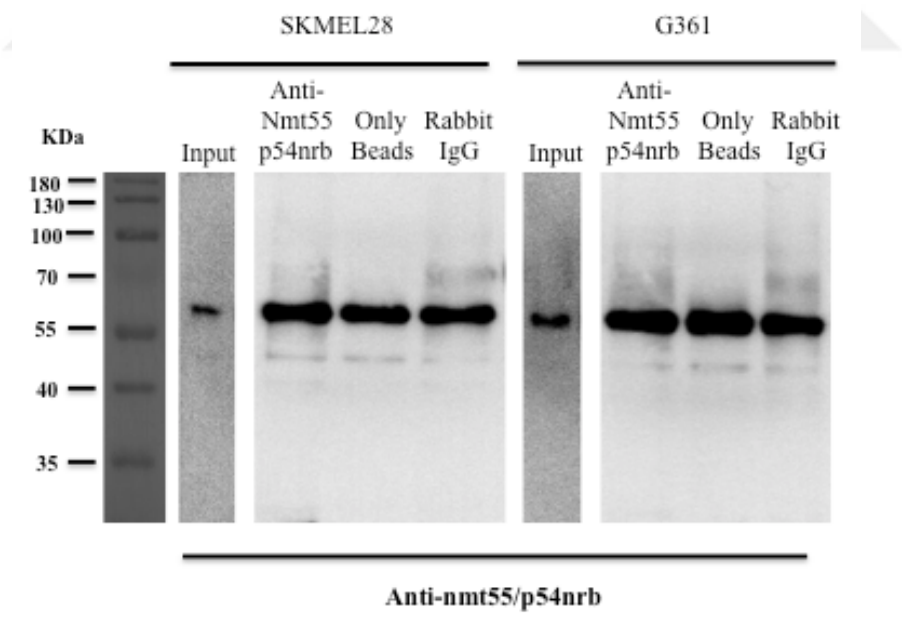

Figure 5.16 Blotting of Endogenous NONO Pulldown samples of SKMEL28 and G361 cell lines with anti-nmt55/p54nrb antibody. NONO band was observed in negative controls in addition to inputs and anti-nmt55/p54nrb antibody samples of SKMEL28 and G361 cell lines.

As a consequence of the presence of NONO protein in negative controls, endogenous NONO pulldown could not have been confirmed to be successful and samples were not blotted IRF4 (M-17) antibody.

5.10. Endogenous BTF/BCLAF1 Pulldown

For further confirmation of BCLAF1 and IRF4 interaction, Endogenous BCLAF1 pulldown was performed with SKMEL28 cell line. Pulldown with anti-BTF (Abcam) antibody and the negative controls only beads and Rabbit IgG were first blotted with anti-BTF (Abcam) antibody to see if the method is working or not. It was confirmed that endogenous BCLAF1 pulldown is working as a band at the size of BCLAF1 was observed for input and anti-BTF antibody sample and it was absent in the negative controls. Then the samples were blotted with IRF4(M-17) antibody. A band at the size of IRF4 was observed in input and anti-BTF antibody sample, whereas it was not observed in the negative controls (Figure 5.17).

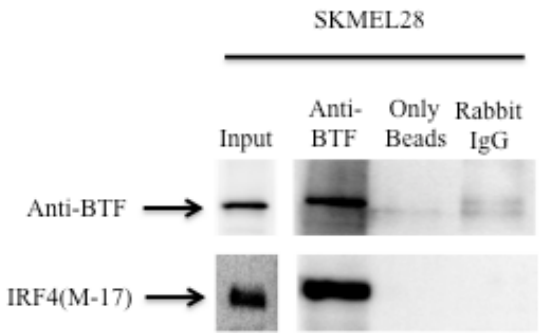

Figure 5.17 Blotting of Endogenous BCLAF1 Pulldown Samples with anti-BTF and IRF4 (M-17) antibodies. BCLAF1 and IRF4 bands were observed in input and anti-BTF antibody sample, but it was absent in negative controls.

In addition to TAP, BioID and endogenous IRF4 pulldown methods, endogenous BCLAF1 pulldown method further confirmed the interaction between IRF4 and BCLAF1.

6. DISCUSSION

IRF4 was initially shown to be involved in immune cell development; such as lymphoid-, myeloid-, and dendritic-cells (Shaffer *et al*., 2009). However, recently IRF4 was shown to be expressed in non-immune cells such as adipocytes (Eguchi *et al*., 2008), cardiac tissue (Jiang *et al*., 2013), CNS (central nervous system) neurons (Jiang *et al*., 2013, Guo *et al*., 2014) and melanocytes (Grossman *et. al*, 1996, Praetorius et al 2013). With the accumulation of genetic aberrations, melanocytes can transform into melanoma, an aggressive type of skin cancer. Melanoma cell line G361 was shown to have high IRF4 expression in the study of Grossman *et al*., 1996. Furthermore, according to the data from Cancer Cell Line encyclopedia, melanoma shows the highest IRF4 expression after multiple myeloma and different kind of lymphomas (Barretina *et al*., 2012). In addition to those, some genetic aberrations of IRF4 protein was linked to melanoma; a germline SNP in IRF4 (rs12203592) (Han *et al.*, 2011; Duffy *et al*., 2010; Nan *et al.*, 2009; Gathany *et al*., 2009) and another SNP in the enhancer region of IRF4 (Praetorius *et al*., 2013). As a consequence of these knowledge ; our group aims to characterize the function of IRF4 in melanoma.

One of the most important steps to characterize the function of a protein is the identification of its interaction partners as any protein can not take a role in a pathway without its co-activation with other proteins. As a result, two different methods were applied for the identification of IRF4-interacting proteins in melanoma cells in this project. One of them is tandem affinity purification, which benefits from the affinity of a tag that is fused to the target protein for the pulldown. The other method is BioID, in this mehod biotinylation reaction of target protein-interacting proteins is triggered via fusion of BirA* enzyme to the target protein. And in the study of Lambert *et al*., 2014, these two methods were shown to be complementary rather than resulting in the identification of similar interaction partners for a target protein. The proteins identified with TAP and BioID in this thesis are suggested to be involved mostly in RNA processing and splicing, by DAVID Functional Annotation Tool. It can be a reason of transcription and splicing occurs in proximity (Kornblihtt *et al*., 2004). Yet, IRF4 together with these proteins

could have a function in splicing. In addition, functions such as RNA transport, nucleic acid transport and histone acetylation are assigned to proteins from TAP and BioID analysis, which is reasonable as IRF4 is a transcription factor. Eventhough these biological processes are significantly assigned to the proteins from TAP and BioID, they are not present in the clusters in Figure 5.10, 5.11 and 5.12 as their significance levels are less than RNA processing and splicing and only the first clusters with highest significance levels are shown in these figures..

Bcl-2 associated transcription factor (BCLAF1 or BTF) and non-POU domain containing octamer-binding protein ($p54^{nrb}$, nmt55 or NONO) were chosen as the first proteins to be validated in melanoma cells after the analysis of TAP and BioID mass spectrometry results. BCLAF1 and NONO are present in both TAP and BioID mass spectrometry data (Table 5.2). They both have a p-value less than 0.05 in BioID mass spectrometry analysis, eventhough q-values (false discovery rate, FDR) of BCLAF1 and NONO are 25% and 11%, respectively, q values of all proteins in BioID mass spectrometry analysis are quite high (See Table 5.1 for q-values of BioID proteins). For the calculation of q-value, proteins are arranged according to their p-values in an ascending manner, then p-value of each protein is multiplied by the number of proteins in the list and divided by the rank of the protein. The large number of proteins in BioID list before the filtering causes high q-values, as a result we decided to accept false discovery rate till 25%.

Interaction of BCLAF1 with IRF4 was validated with endogenous IRF4 pulldown and endogenous BCLAF1 pulldown methods in adition to TAP and BioID methods. As a result, we can conclude BCLAF1 as an interaction partner of IRF4 in SKMEL28 cell line. Interaction of NONO with IRF4 could not have been validated with endogenous IRF4 pulldown and endogenous NONO pulldown methods. Also NONO expression could not have been confirmed in TAP and BioID samples. Thus, the interaction between IRF4 and NONO remains to be clarified.

BCLAF1 firstly identified as a proapoptotic transcription factor, and its activity is inhibited by Bcl-2 (Kasof *et al.*, 1999). Moreover, many other functions were attribut-

ed to BCLAF1, other than apoptosis (Sarras *et al*., 2010; Kong *et al*., 2011). Although BCLAF1 belongs to Bcl-2 family protein, it shows high structural similarity to THRAP3 as both of them contain arginine-serine (RS) rich domain; RS rich domain containing proteins commonly involved in pre-mRNA splicing and mRNA processing (Sarras *et al*., 2010). In furtherance of the role of BCLAF1 in pre-mRNA splicing and mRNA processing; THRAP3 and BCLAF1 were found in the composition of human mRNPs (Merz, 2007). In addition to BCLAF1, THRAP3 is also present as a possible interaction partner of IRF4 in TAP and BioID Mass Spectrometry results. These two proteins might be involved in pre-mRNA splicing and mRNA processing in melanoma cell line SKMEL28 and their interaction with IRF4 might also suggest a role for IRF4 in pre-mRNA splicing, which needs further studies to be concluded.

Different functions of BCLAF1 might be a result of different transcript variants. In the study of Zhou *et al.,* 2014 serine/arginine rich splicing factor 10 (SRSF10) was shown to be involved in the inclusion of exon5a in BCLAF1 and Exon5a containing form of BCLAF1 (BCLAF1-L) was positively correlated with colorectal cancer cell proliferation and colony formation. SRSF10 protein is also present in BioID analysis, although it is not shown in the table as it is excluded after filtering. The presence of SRSF10 in BioID samples might indicate the presence of BCLAF1-L isoform in SKMEL28 melanoma cell line. Thus, BCLAF1-L, together with IRF4 might play an essential role for the proliferation of melanoma cells.

NONO is a member of Drosophila Behavior/Human Splicing (DBHS) protein family, just as SFPQ and PSPC1 (Passon *et al*., 2012). DBHS family proteins show structural similarity, consisting of two tandem RNA recognition motif (RRM) domain, a predicted coiled-coil of 100 aa segment, and a putative protein-protein interaction motif in their core; also DBHS proteins have an uncharacterized domain, called as NONA/paraspeckle (NOPS), between the second RRM and and coiled coil. Core domains of DBHS family proteins enable their homo- or heterodimerization (Kiesler *et al*., 2003; Fox *et al*., 2005). NONO and other DBHS family proteins are involved in nuclear processes; such as mRNA splicing, retention of defective RNAs via formation of paraspeckle components and regulation of transcription (Teigelkamp *et al*., 1997; Emili

et al., 2002; Prasanth *et al*., 2005; Mathur *et al*., 2001; Hallier *et al*., 1996). NONO, SFPQ and PSPC1 exist to be potential interaction partners of IRF4 from TAP and BioID mass spectrometry data. Therefore, IRF4 might have a function together with this complex.

In addition to its function in nuclear processes, NONO was correlated with melanoma cell progression and migration, and it is suggested to have an important role in early tumor development via its regulation by melanoma inhibitory activity, MIA (Bosserhoff *et al*., 2005; Schmid *et al*., 2010; Schiffner *et al*., 2011). In melanoma cell lines tested by Schiffner *et al*., 2011, also including SKMEL28 cell line which is the cell line used for BioID and TAP methods in our study, treatment of the cells with MIA- specific small interfering RNAs caused a decrease in the expression of NONO. And knockdown of NONO, caused reduced proliferation and migration of the cells besides increased levels of apoptosis. In our study, NONO was identified to be a possible interaction partner of IRF4 as well as SFPQ and PSPC1. However, we decided to first validate the interaction of IRF4 with NONO as NONO is positively correlated with melanoma cell progression. NONO and IRF4 might be acting on melanoma cell progression together.

The positive correlation of NONO and BCLAF1 with tumorigenesis is consistent with the effect of IRF4 on some melanoma cell lines. The knockdown of IRF4 with shIRF4 treatment caused a decrease in the competitive fitness of SKMEL28 when compared to shLuc control treated cells (Ayhan *et al.,* unpublished, Figure 6.1). IRF4 can be positively affecting competitive fitness of SKMEL28 cells, in conjunction with BCLAF1 and/or NONO and the complex of DBHS family proteins, which requires further investigation to be conclusive.

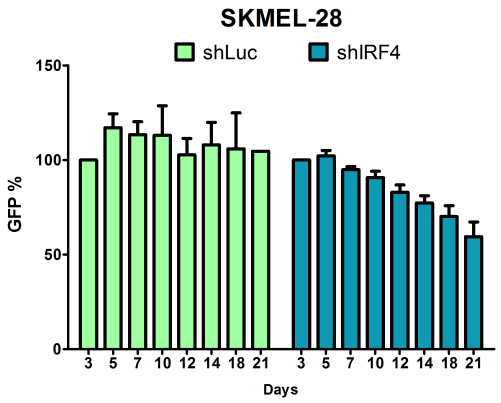

Figure 6.1 GFP competition assay results, indicating reduced competitive fitness of SKMEL28 when treated with shIRF4 (Ayhan *et al.,* unpublished).

BCLAF 1 is validated for its interaction with IRF4, yet NONO remains unclear. The protein NONO seems to be too sticky to also bind the beads alone as it is depicted from the results of endogenous NONO pulldown (Figure 5.15) . Therefore, we concluded that the endogenous pulldown with this protein requires optimization in order to be able to get conslusive results.

As future studies, the importance of the interaction between IRF4 and BCLAF1 in melanoma cell lines can be studied and some optimizations can be performed to validate the interaction between IRF4 and NONO. Even the interaction between IRF4 and NONO could not have been validated yet, NONO was observed in both TAP and BioID mass spectrometry data and found to be statistically significant in BioID mass spectrometry analysis. As a result, NONO is still a highly possible interaction partner of IRF4. NONO has been related to melanoma (Bosserhoff *et al*., 2005; Schmid *et al*., 2010; Schiffner *et al*., 2011) and also NONO is a part of the complex including also SFPQ and PSPC1. Therefore, it would be interesting to find out the functional role of IRF4 together with this complex.

Other proteins in addition to BCLAF1 and NONO can be selected from TAP and BioID analysis to study for their interaction with IRF4. Investigation of the interaction of IRF4 with other proteins could shed a light on the possible function of IRF4 in RNA

processing and splicing as well as histone acetylation, RNA and nucleic acid transport. As high q values observed in t-test of BioID samples, a different statistical test can be applied to BioID mass spectrometry data, such as SAINTexpress which is a statistical method developed for the scoring of protein-protein interaction data from affinity purification-mass spectrometry experiments (Teo *et al.,* 2014). In this manner, a more precise list of target proteins can be obtained and candidate proteins with lower FDRs can be selected to study in the future.

Finally, in order to get statistical siginifcance tests for TAP and to be able to resolve the contradictory data between the 1st and 2nd replicate of TAP, a 3rd replicate can be prepared for Mass Spectrometry analysis.

APPENDIX A: CONSTRUCTION OF IRF4_TAP FUSION PROTEIN AND ITS ONLY_TAP CONTROL EXPRESSING PLASMIDS

The construction of IRF4_TAP fusion protein was achieved by cloning of IRF4 into PCMV-FLAG-MAT tag 2 plasmid. This plasmid contains FLAG and MAT tags tandemly, which is called as TAP tag (Figure A.1).

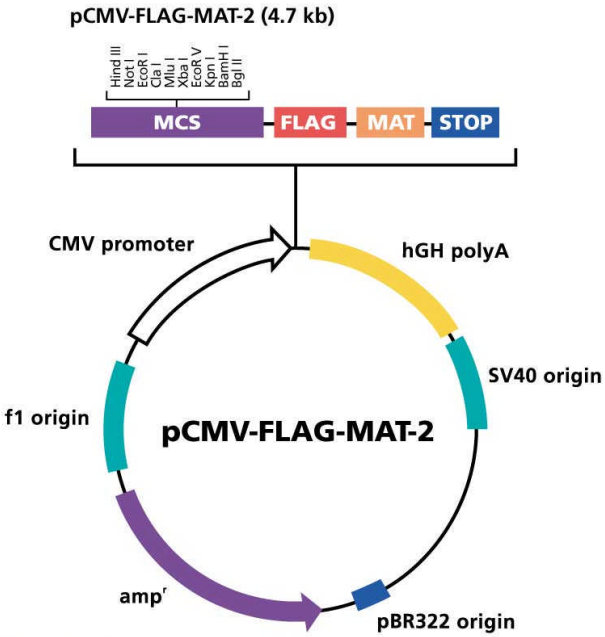

Figure A. 1 Vector map of PCMV-FLAG-MAT tag 2 plasmid (Sigma).

IRF4 insert was PCR amplified from IRF4_pDONR221 plasmid, using forward and reverse primers of IRF4 _PCMV-FLAG-MAT-2. The primers contain EcoRI and BamHI restriction sites. These sites also present in the multiple cloning site of PCMV-FLAG-MAT 2 plasmid and the plasmid was double digested with these enzymes. IRF4 insert and digested plasmid were loaded to agarose gel. IRF4 insert is 1356 bp and a proper size of band was observed for the PCR product of IRF4. PCMV-FLAG-MAT tag 2 plasmid was concluded to be digested as a linear band was observed for the digested plasmid (Figure A.2).

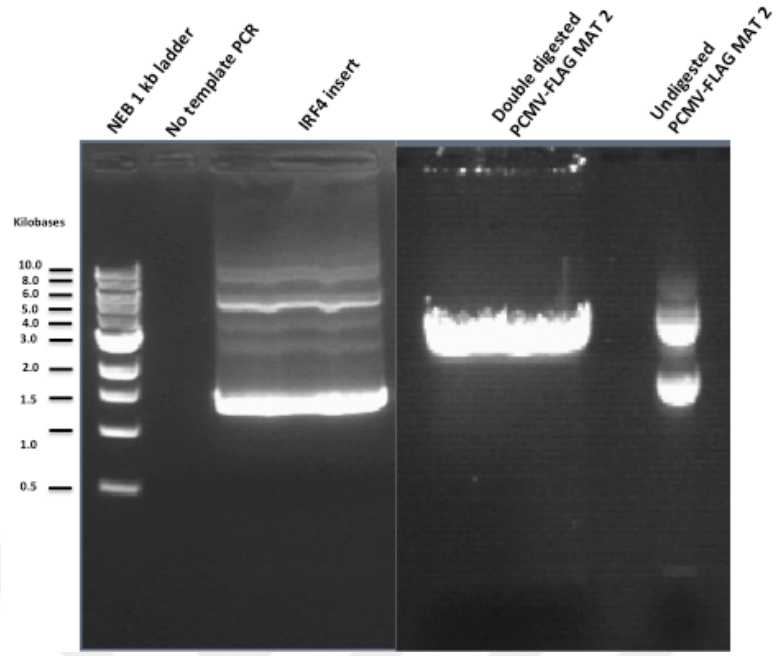

Figure A. 2 PCR product of IRF4 insert and undigested and double digested PCMV-FLAG-MAT tag 2 plasmid. A band at the size of IRF4 was observed for the PCR product and the linear band for the digested plasmid verifies the success of digestion.

PCR product of IRF4 and double digested PCMV-FLAG-MAT tag 2 plasmid were extracted from the gel and IRF4 insert was double digested with EcoRI and BamHI enzymes. Digested IRF4 insert and digested PCMV-FLAG-MAT2 plasmid were ligated and transformed into Stbl3 bacterial strain. Moreover, ligation reaction was performed with only digested plamid, as the control for the religation.Transformed bacteria was spreaded on ampicillin plates as the PCMV-FLAG-MAT tag 2 plasmid has ampicillin resistance gene. Colonies were observed on both IRF4_PCMV-FLAG-MAT tag 2 and religation plates, however the number of colonies on the religation plate were much more smaller than the number of colonies on IRF4_PCMV-FLAG-MAT tag 2 plate. Colonies of ligation were tested via Colony PCR and a band at the size of IRF4 was observed for the colonies. Colony PCR was also applied to one colony from the religation plate and no band was observed for this negative control colony (Figure A.3).

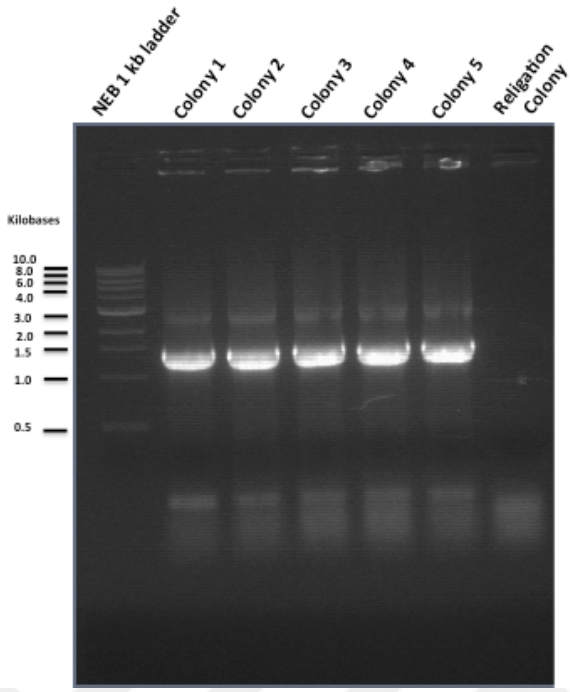

Figure A. 3 Colony PCR of IRF4_PCMV-FLAG-MAT tag 2 colonies. A band at the size of IRF4 was observed for the ligation colonies but it was absent in the religation control.

Then some of these colonies were validated for the sequence of IRF4 via sanger sequencing.

IRF4_TAP fusion protein and its negative control Only_TAP were aimed to be cloned into pIRES2-eGFP plasmid which is an episomal plasmid with green fluorescent protein marker (Figure A.4). A GFP containing plasmid was preferred to be able to trace the amount of cells that had taken the plasmid after transfection. GFP_pIRES2-eGFP plasmid was borrowed from Tuncay Şeker, in which an additional GFP had been cloned into the plasmid between EcoRI and SalI restriction sites. IRF4_TAP and Only_TAP coding sequences were cloned into the plasmid between EcoRI and SalI restriction sites in order to replace this additional GFP with IRF4_TAP or Only_TAP.

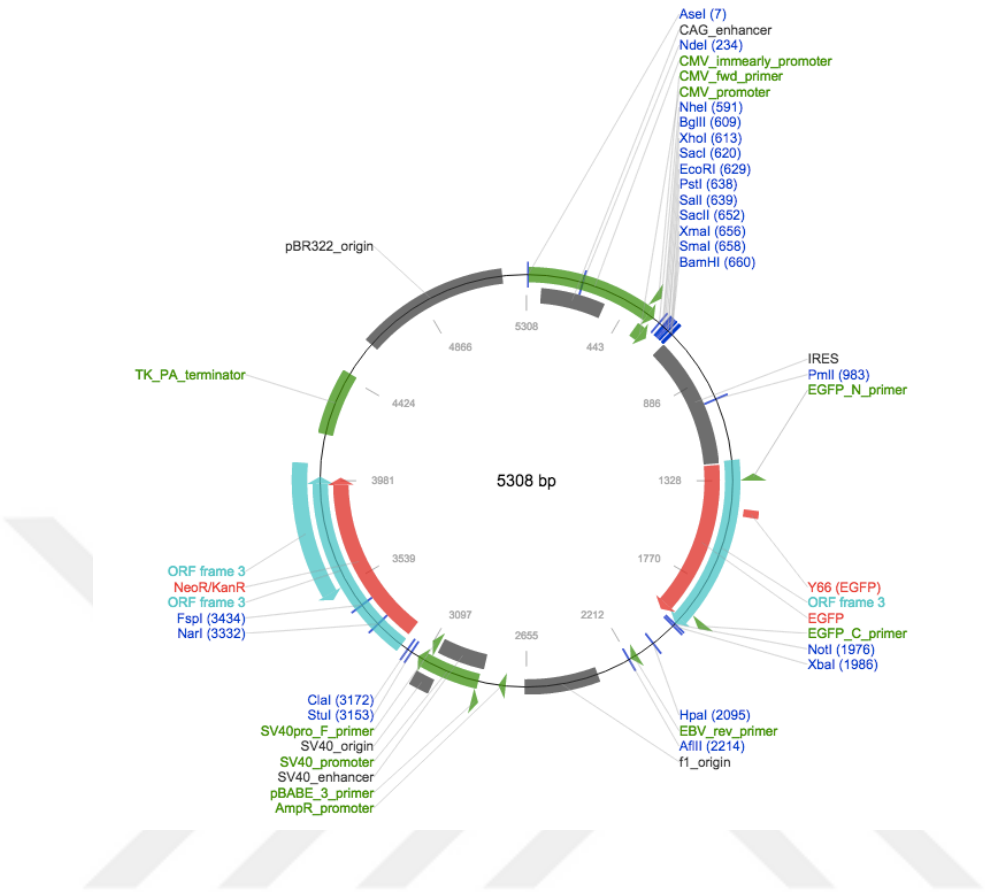

Figure A. 4 Vector map of pIRES2-eGFP (Clontech).

IRF4_TAP fusion protein from IRF4_PCMV-FLAG-MAT 2 was PCR amplified, using forward and reverse primers of IRF4_TAP_pIRES2-eGFP which contains EcoRI and SalI restriction sites. Only_TAP tag was PCR amplified from PCMV-FLAG-MAT tag 2 plasmid, using forward and reverse primers of Only_TAP_pIRES2-eGFP, containing EcoRI and SalI restriction sites. Moreover, pIRES2-eGFP plasmid was digested with again the same restriction endonucleases, EcoRI and SalI. IRF4_TAP and Only_TAP inserts and digested pIRES2-eGFP plasmid were loaded to agarose gel. Only_TAP tag is 51 bp together with the stop codon at its C-terminal and IRF4 insert becomes 1407 bp bp when it is fused to TAP tag. For the PCR products of IRF4_TAP and Only_TAP, proper sizes of bands were observed. A linear band above 5 kb was observed for the digested pIRES2-eGFP plasmid which indicates successful digestion reaction. The smaller band observed for the digested plasmid is at the size of GFP, which is expected to be released when the plasmid is digested with EcoRI and SalI enzymes (Figure A.5)

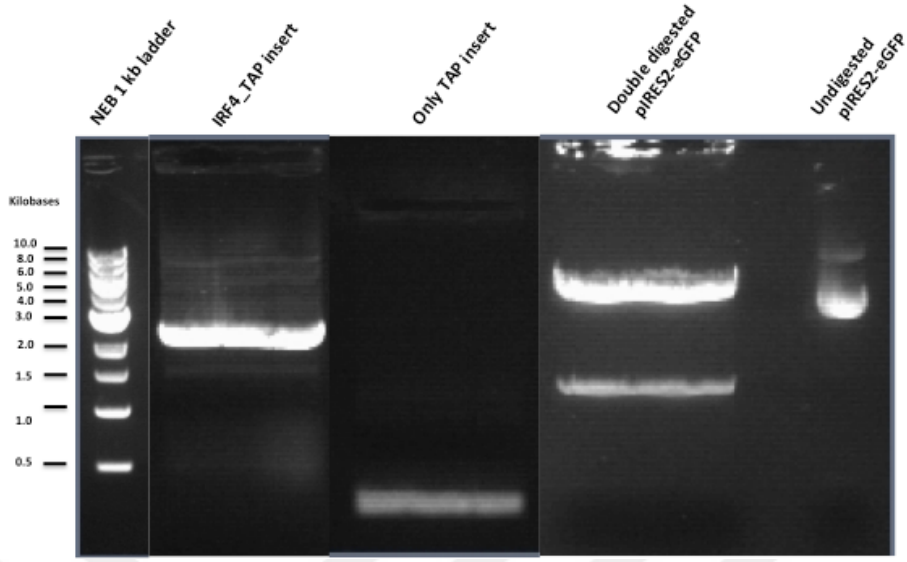

Figure A. 5 PCR products of IRF4_TAP and Only_TAP and undigested and double digested pIRES2-eGFP plasmid. Bands at the sizes of IRF4_TAP and Only_TAP were observed for the PCR products and the linear band for the digested plasmid verifies the success of digestion.

PCR products and double digested pIRES2-eGFP plasmid were extracted from the gel and IRF4_TAP insert and Only_TAP insert were double digested with EcoRI and SalI enzymes. Digested inserts and digested pIRES2-eGFP plasmid were ligated and transformed into Stbl3 bacterial strain. Moreover, ligation reaction was performed with only digested plamid, as the control for the religation.Transformed bacteria was spread-ed on kanamycin plates as the pIRES2-eGFP plasmid has kanamycin resistance gene. Colonies from the ligations of IRF4_TAP and Only_TAP were tested via colony PCR. A band at the size of IRF4_TAP was observed for ligation colonies of IRF4_TAP and a band at the size of Only_TAP was observed for ligation colonies of Only_TAP (Figure A.6).

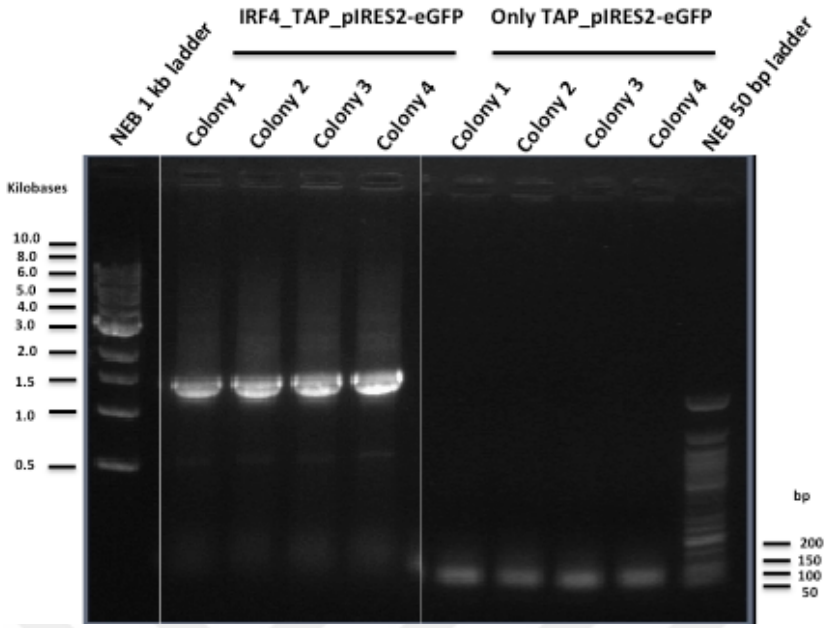

Figure A. 6 Colony PCR of IRF4_TAP_pIRES2-eGFP and Only_TAP_pIRES2-eGFP colonies. Proper sizes of bands were observed for both IRF4_TAP_pIRES2-eGFP and Only_TAP_pIRES2-EGFP colonies.

Then some of these colonies were validated for the sequence of IRF4_TAP and Only_TAP via sanger sequencing.

APPENDIX B: FIDELITY OF NUCLEAR FRACTIONATION OF SKMEL28 CELLS

Nuclear and cytoplasmic fractions were prepared from SKMEL28 cells. In order to check the fidelity of nuclear fractionation protocol, nuclear and cytoplasmic fractions of SKMEL28 cells were blotted with Anti-Histone H3 (Abcam) and Anti-Actin (Abcam) antibodies. Histone H3 has a molecular weight of 18 kDa and a band at the size of Histone H3 was observed for the nuclear fraction of SKMEL28 but it was absent in the cytoplasmic fraction of SKMEL28, which is expected as Histone H3 is a nuclear protein. Actin has a molecular weight of 42 kDa and a band at the size of Actin was observed only in the cytoplasmic fraction of SKMEL28, expectedly as Actin is a cytoplasmic protein (Figure B.1).

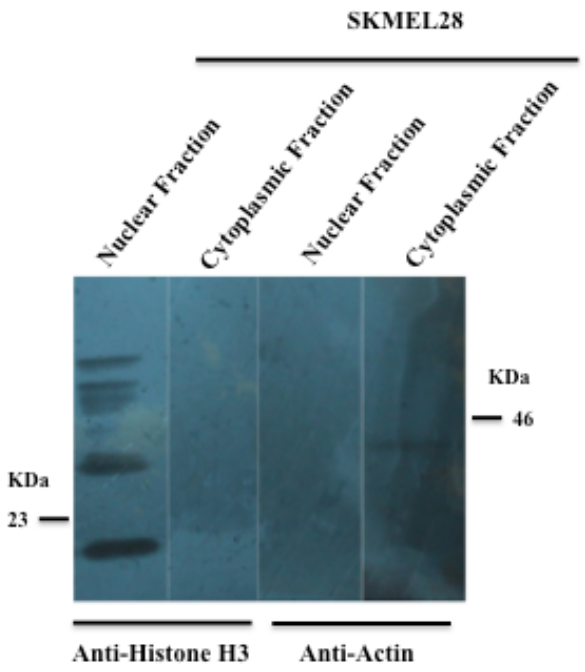

Figure B. 1 Fidelity of nuclear fractionation protocol. Histone H3 nuclear protein was observed only in the nuclear fraction of SKMEL28 and cytoplasmic Actin protein was observed on in the cytoplasmic fraction of SKMEL28, thus the blotting of the nuclear and cytoplasmic fractions validates successful fractionation.

APPENDIX C: PULLDOWN OF IRF4 AND IRF4-INTERACTING PROTEINS WITH TAP (SECOND REPLICATE)

To prepare the second replicate of TAP, SKMEL28 cells were transfected with IRF4_TAP_pIRES2-eGFP and Only_TAP_pIRES2-eGFP and cells were examined under fluorescence microscope and analyzed through FACS. IRF4_TAP_pIRES2-eGFP transfected SKMEL28 cells showed 81% transfection efficiency and Only_TAP_pIRES2-eGFP transfected cells showed 70% efficiency, the transfection efficiencies of the cells were sufficient for the TAP protocol (Figure C.1).

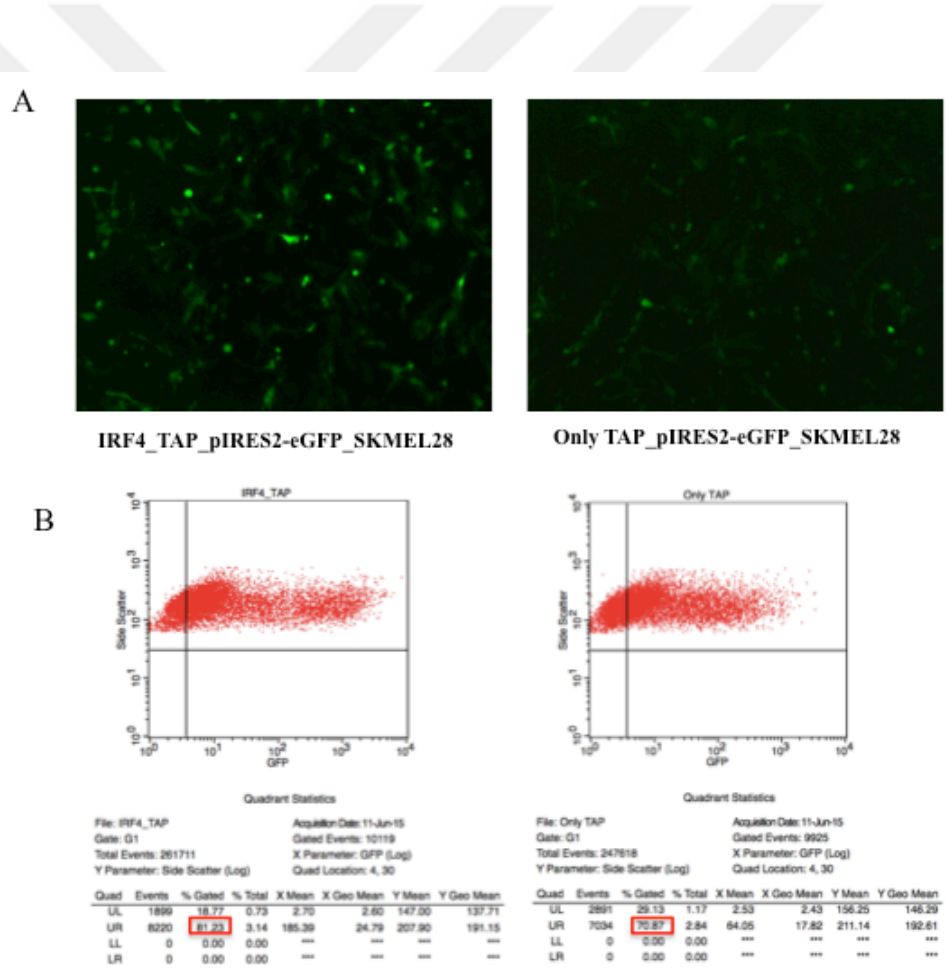

Figure C. 1 Images of IRF4_TAP_pIRES2-eGFP and Only_TAP_pIRES2-eGFP transfected SKMEL28 cells under fluorescence microscope and their analysis through Flow cytometer. Transfected cells showed sufficient transfection efficiencies for TAP.

In the second replicate of TAP, a proportion of the beads were bolied at 95°C for the elution, as the boling of beads causes the release of heavy and light chains of anti-FLAG antibody, samples were blotted only with IRF4(M-17) antibody. Anti-mouse IgG which is required for the detection of anti-FLAG antibody, would mainly detect heavy and light chains and would prevent the detection of IRF4_TAP protein. However, anti-goat IgG, which is required for the detection of IRF4(M-17) antibody, does not show high cross reactivity with mouse IgG and IRF4_TAP protein can be detected when the samples are blotted with M-17 antibody. From the western blot, IRF4_TAP protein is observable in IRF4_TAP_pIRES2-eGFP eluate of Sigma Anti-FLAG M2 magnetic beads and there is a faint band for Only_TAP_pIRES2-eGFP eluate of Sigma Anti-FLAG M2 magnetic beads, which most probably belongs to antibody heavy chain (Figure C.2.

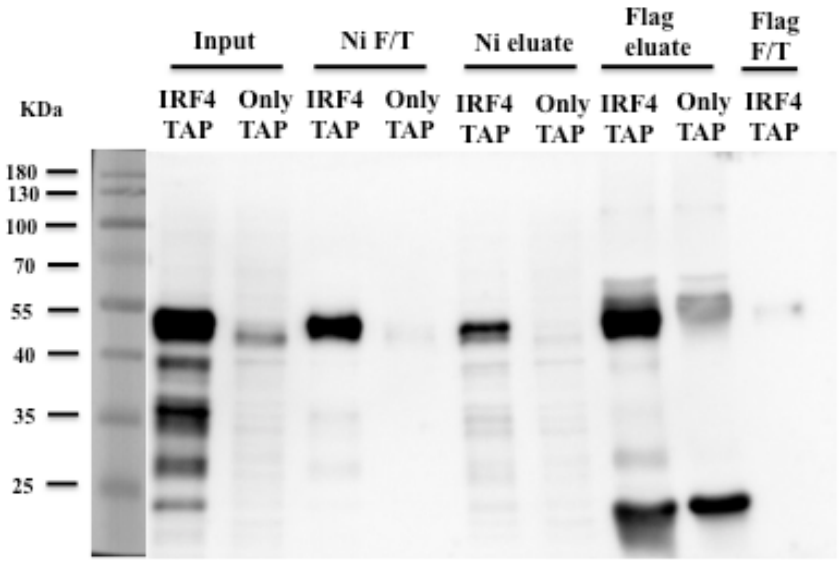

Ni F/T: Flowthrough of Dynabeads His-Tag Isolation and Pulldown beads
Ni eluate: Eluate from Dynabeads His-Tag Isolation and Pulldown beads
Flag F/T: Flowthrough of Sigma Anti-Flag M2 magnetic beads
Flag eluate: Eluate from Sigma Anti-Flag M2 magnetic beads

Figure C. 2 Confirmation of second replicate of TAP protocol. Inputs, F/Ts and eluates of second replicate of TAP were blotted with IRF4(M-17) antibody and the presence of IRF4 band in IRF4_TAP_pIRES2-eGFP eluate of Sigma Anti-FLAG M2 magnetic beads confirms the success of TAP protocol.

APPENDIX D: CONSTRUCTION OF IRF_BIRA* FUSION PROTEIN AND ITS ONLY BIRA* CONTROL EXPRESSING PLASMIDS

IRF4 was aimed to clone into PCDNA3.1 MCS-BirA(R118G)-HA plasmid. This plasmid contains the mutated form of biotin ligase (BirA*). With the fusion of BirA* to the C-terminal of IRF4, proteins that are in proximity with IRF4 can be biotinylated.

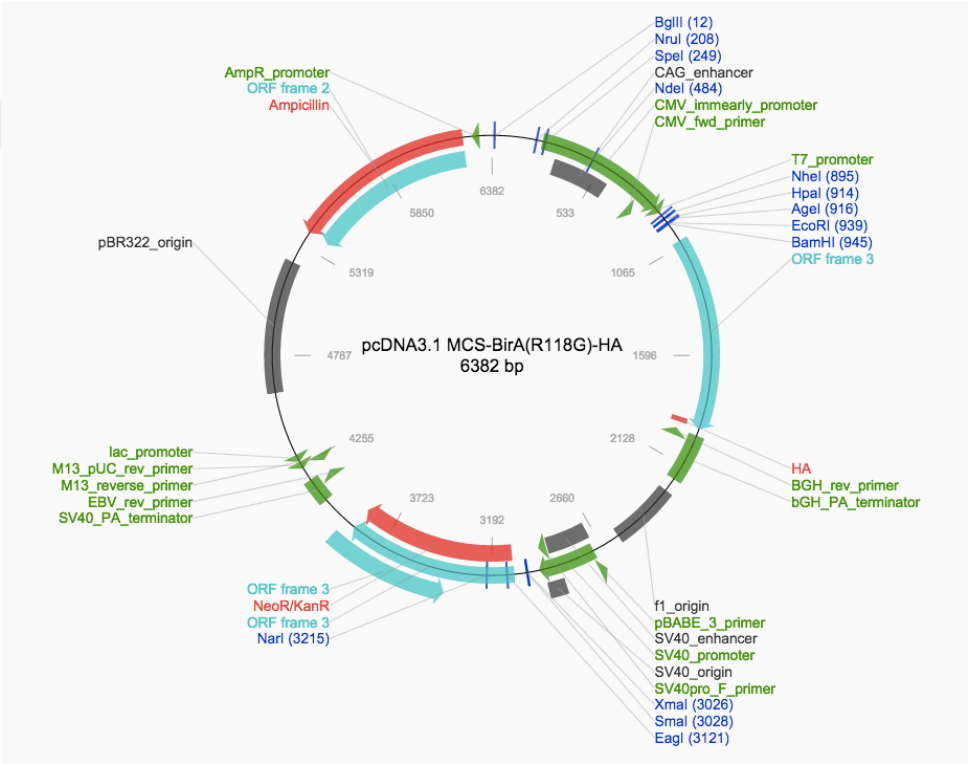

Figure D. 1 vector map of PCDNA3.1 MCS-BirA(R118G)-HA (Kyle Roux).

IRF4 insert was PCR amplified from IRF4_pDONR221 plasmid, using forward and reverse primers of IRF4_PCDNA3.1 MCS-BirA(R118G)-HA. The primers contain HpaI and BamHI restriction sites. These sites also present in the multiple cloning site of PCDNA3.1 MCS-BirA(R118G)-HA plasmid and the plasmid was double digested with these enzymes. IRF4 insert and digested plasmid were loaded to agarose gel. A proper size of band was observed for the PCR product of IRF4. Double digested PCDNA3.1 MCS-BirA(R118G)-HA plasmid showed a linear band, expectedly. Only HpaI and only

BamHI digested PCDNA3.1 MCS-BirA(R118G)-HA plasmid showed a linear band as well as the double digested plasmid. Single digestions of the plasmid were performed to check if both of the enzymes are working properly or not (Figure D.2).

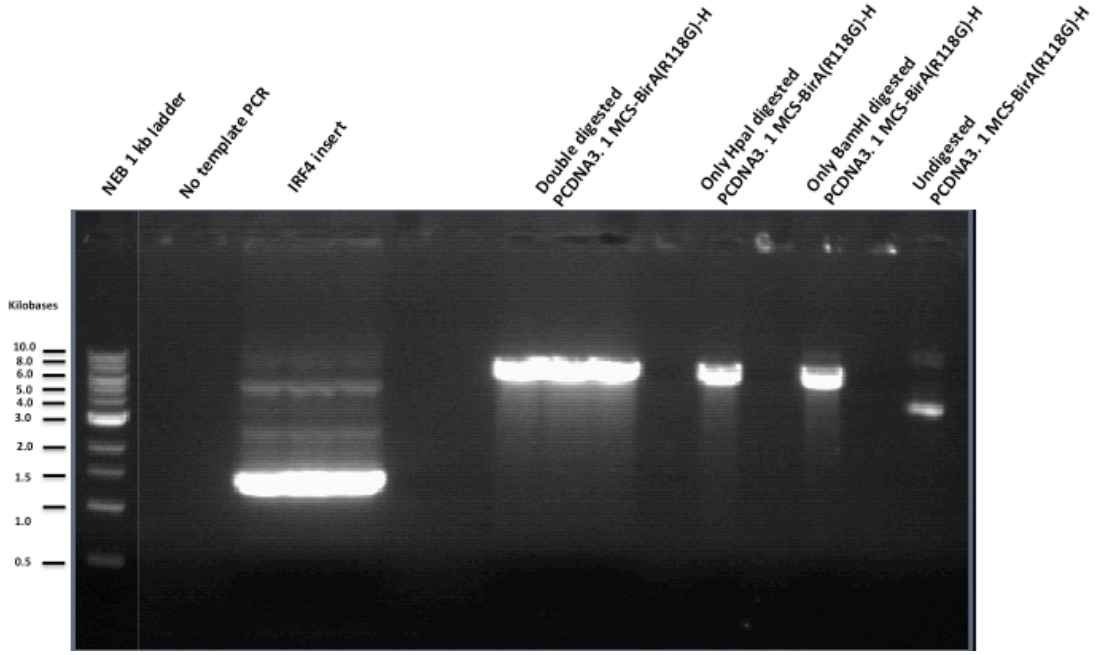

Figure D. 2 PCR product of IRF4 and undigested, single digested and double digested PCDNA3.1 MCS-BirA(R118G)-HA plasmid. A band at the size of IRF4 was observed for the PCR product and the linear band of double digested plasmid confirms successful digestion.

After the confirmation of PCR product, IRF4 insert and double digested PCDNA3.1 MCS-BirA(R118G)-HA were extracted from the gel. IRF4 insert was double digested with HpaI and BamHI enzymes. Digested IRF4 insert and digested PCDNA3.1 MCS-BirA(R118G)-HA plasmid were ligated and transformed into Stbl3 bacterial strain. Moreover, ligation reaction was performed with only digested plamid, as the control for the religation.Transformed bacteria was spreaded on ampicillin plates as the PCDNA3.1 MCS-BirA(R118G)-HA plasmid has ampicillin resistance gene. Colonies of ligation were tested via Colony PCR and a band at the size of IRF4 was observed

for some of the colonies. Colony PCR was also applied to one colony from the relegation plate and no band was observed for this negative control colony (Figure D.3).

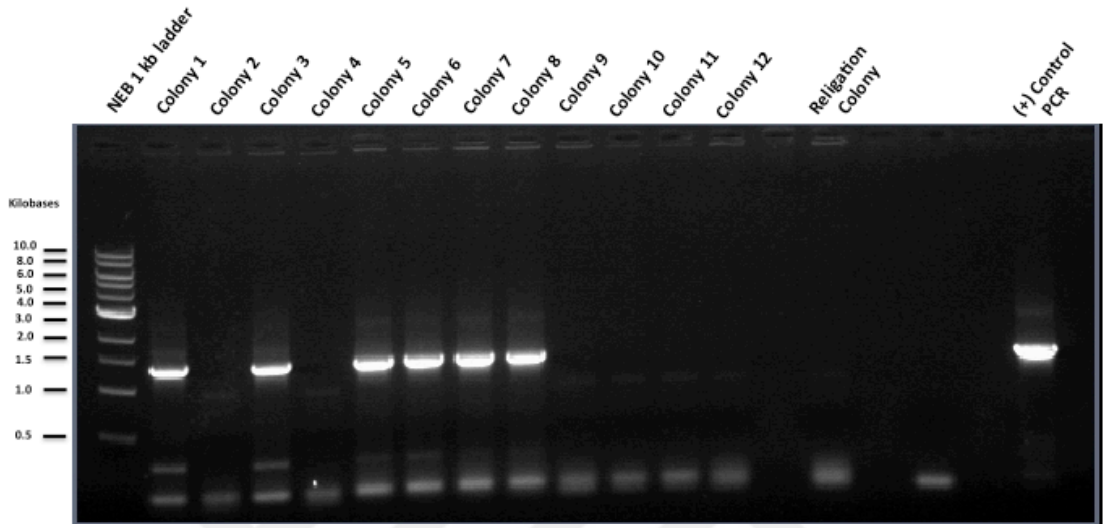

Figure D. 3 Colony PCR of IRF4_PCDNA3.1 MCS-BirA(R118G)-HA colonies. A band at the size of IRF4 was observed for some of the ligation colonies but it was absent in the religation control.

Then some of the IRF4 insert positive colonies were validated for the sequence of IRF4 via sanger sequencing.

APPENDIX E: BLOTTING OF NUCLEAR LYSATES OF IRF4_BIRA*_PCDNA3.1 AND ONLY_BIRA*_PCDNA3.1 TRANSFECTED SKMEL28 CELLS WITH ANTI-HA ANTIBODY

PCDNA3.1 MCS-BirA(R118G)-HA plasmid contains HA tag at the C-terminal of BirA*, resulting in the fusion of IRF4_BirA* and Only_BirA* proteins to HA tag. For the confirmation of the entrance of Only_BirA* protein into the nucleus, nuclear and total lysates of IRF4_BirA*_PCDNA3.1 and Only_BirA*_PCDNA3.1 transfected and biotin administered cells were blotted with Anti-HA (Abcam) antibody. Blotting of the samples with Anti-HA (Abcam) antibody, showed that Only_BirA* protein is capable of nuclear entrance as a band at the size of Only_BirA* was observed in the nuclear fraction of Only_BirA*_PCDNA3.1 transfected cells as well as it was observed in the total lysate of Only_BirA*_PCDNA3.1 transfected cells. With this result, Only_BirA* was concluded to be convenient as a negative control (Figure E.1).

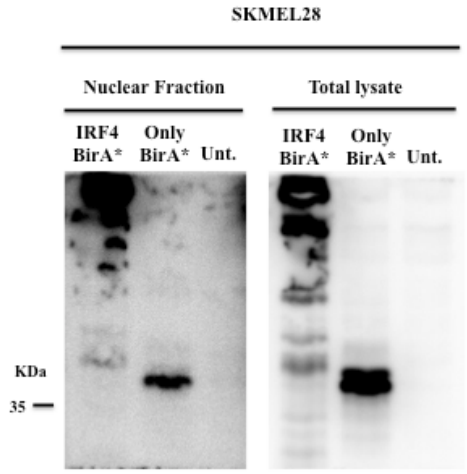

IRF4 BirA*: IRF4_BirA*_PCDNA3.1 transfected SKMEL28 cells
Only BirA*: Only_BirA*_PCDNA3.1 transfected SKMEL28 cells
Unt.: Untransfected cells

Figure E. 1 Anti-HA blotting of total and nuclear lysates of IRF4_BirA*_PCDNA3.1 and Only_BirA*_PCDNA3.1 transfected and biotin administered SKMEL28 cells. The presence of Only_BirA* band in the nuclear lysate of Only_BirA* transfected cells demonstrates the convenience of Only_BirA* as a negative control.

APPENDIX F: PULL DOWN OF BIOTINYLATED PROTEINS WITH BIOID (FIRST AND THIRD REPLICATES)

In the first replicate of BioID, untransfected and biotin treated SKMEL28 cells were not included. Inputs, F/Ts and eluates of first replicate were blotted with IRF4 (M-17) antibody and silver stained (Figure F.1A and B). Both western blot and silver staining images showed a band at the size of IRF4_BirA* for the eluate of IRF4_BirA*_PCDNA3.1 and this band was absent in the eluate of Only BirA*_PCDNA3.1.

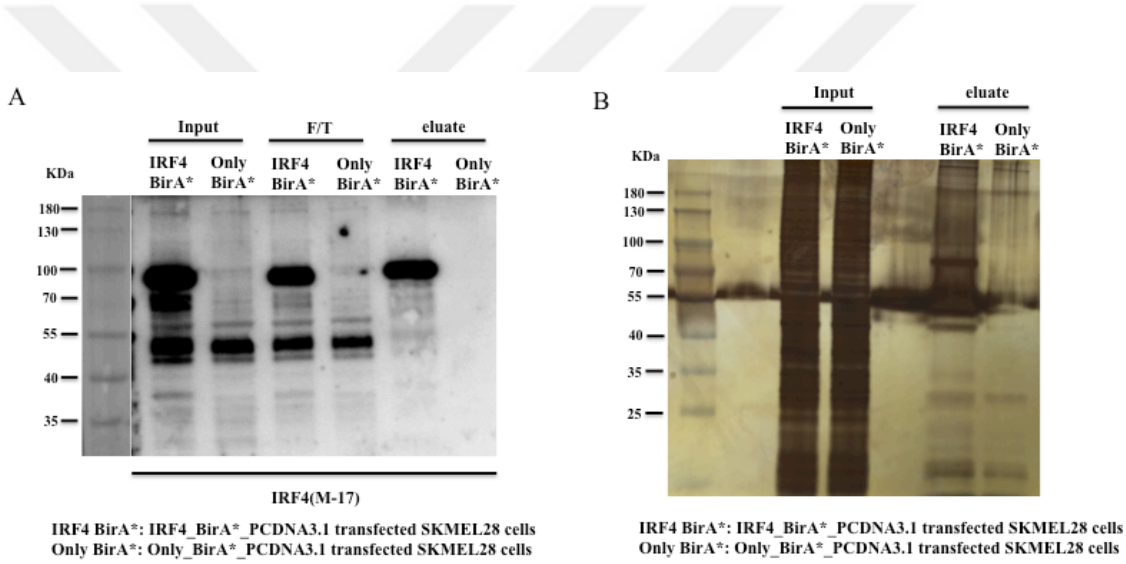

Figure F. 1 Confirmation of first replicate of BioID. Blotting of inputs, F/Ts and eluates with IRF4(M-17) antibody (A) and silver stainings of inputs and eluates (B) showed a band at the size of IRF4_BirA* for the eluate of IRF4_BirA*_PCDNA3.1 and it was absent in the eluate of Only_BirA*_PCDNA3.1.

Third replicate of BioID was prepared similarly with the second replicate, including untransfected and biotin treated SKMEL28 cells as an additional negative control. Inputs, F/Ts and eluates of third replicate were blotted with IRF4 (M-17) antibody and silver stained (Figure F.2A and B). Western blot and silver staining images showed a band at the size of IRF4_BirA* for the eluate of IRF4_BirA*_PCDNA3.1 and this band was absent in the eluates of Only BirA*_PCDNA3.1 and untransfected controls.

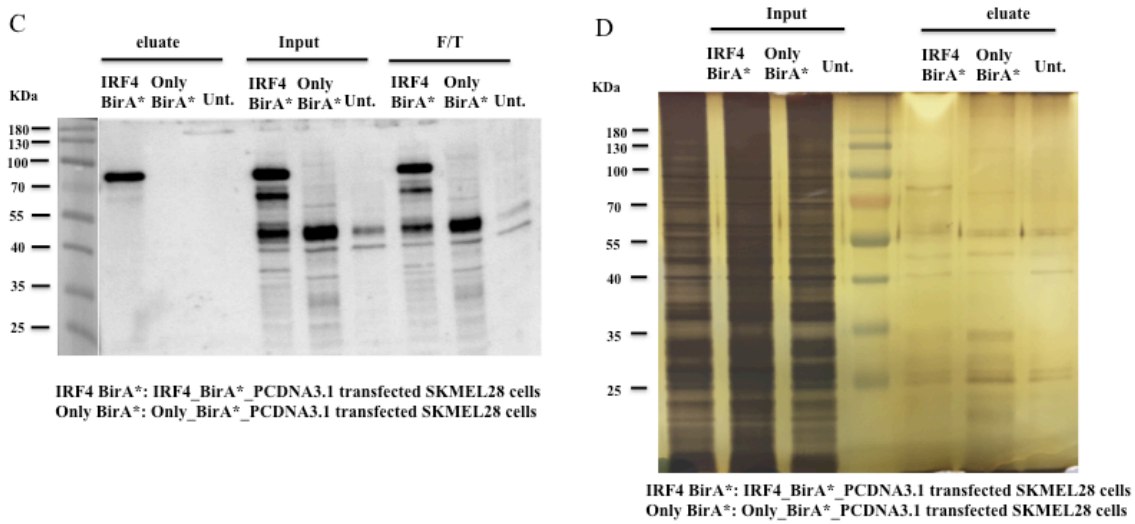

Figure F. 2 Confirmation of third replicate of BioID. Blotting of inputs, F/Ts and eluates with IRF4(M-17) antibody (A) and silver stainings of inputs and eluates (B) showed a band at the size of IRF4_BirA* for the eluate of IRF4_BirA*_PCDNA3.1 and it was absent in the negative controls.

APPENDIX G: THE LIST OF THE PROTEINS FROM TAP

The list of proteins obtained from TAP 1st replicate are shown in the table. In the table, raw spectral counts of IRF4_TAP and Only_TAP samples are shown. Proteins that show a fold change less than 1.5 are excluded from the table and they are organized according to the fold change in a descending manner. IRF4 was shaded with red, observation of the target protein in the analysis further confirms the success of TAP method (Table G.1).

Table G. 1 Proteins identified with TAP Analysis.

Identified Proteins	Gene Symbol	Molecular Weight (kDa)	IRF4 TAP	Only TAP	Fold Change
40S ribosomal protein S3a	RPS3A	30	8	0	43
40S ribosomal protein S10	RPS10	19	5	0	42
Keratin, type I cytoskeletal 16	KRT16	51	13	0	41
Keratin, type II cytoskeletal 6A	KRT6A	60	14	0	37
Keratin, type I cytoskeletal 14	KRT14	52	12	0	37
40S ribomal protein S4, X isoform	RPS4X	30	6	0	32
Dynein light chain 1, cytoplasmic	DYNLL1	10	2	0	32
DNA replication licensing factor MCM3	MCM3	91	18	0	32
Isoform 2 of Heterogeneous nuclear ribonucleoprotein K	HNRNPK	51	9	0	28
RuvB-like 2	RUVBL2	51	9	0	28
U1 small nuclear ribonucleoprotein C	SNRPC	17	3	0	28
Isoform 2 of Mitotic checkpoint protein BUB3	BUB3	37	6	0	26
40S ribosomal protein S2	RPS2	31	5	0	26
Interferon-stimulated gene 20 kDa protein	ISG20	20	3	0	24
Keratin, type II cytoskeletal 5	KRT5	62	9	0	23
Histone H2A.Z	H2AFZ	14	2	0	23
DNA replication licensing factor MCM5	MCM5	82	11	0	21
60S ribosomal protein L23	RPL23	15	2	0	21
40S ribosomal protein S15a	RPS15A	15	2	0	21
DnaJ homolog subfamily A member 1	DNAJA1	45	5	0	18
THO complex subunit 4	ALYREF	27	3	0	18
Isoform 2 of Paraspeckle component 1	PSPC1	46	5	0	17
Splicing factor U2AF 35 kDa subunit	U2AF1	28	3	0	17
CGG triplet repeat-binding protein 1	CGGBP1	19	2	0	17
RNA-binding protein 14	RBM14	69	7	0	16
U4/U6.U5 tri-snRNP-associated protein 1	SART1	90	9	0	16

Table G. 1 Proteins identified with TAP Analysis (cont.).

Isoform 2 of 60S ribosomal protein L11	RPL11	20	2	0	16
Isoform 2 of Fragile X mental retardation syndrome-related protein 1	FXR1	61	6	0	16
Isoform 2 of Splicing factor U2AF 65 kDa subunit	U2AF2	53	5	0	15
Isoform 2 of DNA-3-methyladenine glycosylase	MPG	32	3	0	15
Histone deacetylase 1	HDAC1	55	5	0	15
40S ribosomal protein SA	RPSA	33	3	0	15
60S ribosomal protein L18	RPL18	22	2	0	15
60S ribosomal protein L9	RPL9	22	2	0	15
Isoform 2 of Runt-related transcription factor 3	RUNX3	46	4	0	14
Phenylalanine--tRNA ligase alpha subunit	FARSA	58	5	0	14
ATP-dependent RNA helicase A	DHX9	141	12	0	14
Poly(rC)-binding protein 1	PCBP1	37	3	0	13
Isoform 2 of Poly(rC)-binding protein 2	PCBP2	39	3	0	12
Cleavage and polyadenylation specificity factor subunit 5	NUDT21	26	2	0	12
Polyubiquitin-B	UBB	26	2	0	12
DnaJ homolog subfamily B member 11	DNAJB11	41	3	0	12
Isoform 2 of RuvB-like 1	RUVBL1	42	3	0	11
60S ribomal protein L8	RPL8	28	2	0	11
Zinc finger CCHC domain-containing protein 9	ZCCHC9	30	2	0	11
DnaJ homolog subfamily A member 2	DNAJA2	46	3	0	10
Isoform 2 of Serine/arginine-rich splicing factor 10	SRSF10	31	2	0	10
Matrin-3	MATR3	95	6	0	10
ATP-dependent RNA helicase DDX1	DDX1	82	5	0	10
60S acidic ribomal protein P0	RPLP0	34	2	0	9
Ras GTPase-activating protein-binding protein 1	G3BP1	52	3	0	9
Isoform 2 of ATP-dependent RNA helicase DDX3X	DDX3X	71	4	0	9
Putative pre-mRNA-splicing factor ATP-dependent RNA helicase DHX15	DHX15	91	5	0	9
Isoform 2 of Protein FAM98A	FAM98A	55	3	0	9
U5 small nuclear ribonucleoprotein 200 kDa helicase	SNRNP200	245	13	0	8
Eukaryotic translation initiation factor 2 subunit 2	EIF2S2	38	2	0	8
Isoform 2 of U4/U6 small nuclear ribonucleoprotein Prp4	PRPF4	58	3	0	8
Isoform 2 of DNA-directed RNA polymerases I and III subunit RPAC1	POLR1C	39	2	0	8
Staphylococcal nuclease domain-containing protein 1	SND1	102	5	0	8
X-ray repair crs-complementing protein 5	XRCC5	83	4	0	8
Isoform Short of Cold shock domain-containing protein E1	CSDE1	86	4	0	7
116 kDa U5 small nuclear ribonucleoprotein component	EFTUD2	109	5	0	7
Splicing factor 3A subunit 1	SF3A1	89	4	0	7

Table G. 1 Proteins identified with TAP Analysis (cont.).

Isoform Alpha of LIM domain and actin-binding protein 1	LIMA1	67	3	0	7
Isoform 1 of Fragile X mental retardation protein 1	FMR1	67	3	0	7
Transcriptional repressor protein YY1	YY1	45	2	0	7
Pre-mRNA-processing-splicing factor 8	PRPF8	274	12	0	7
Isoform 2 of Putative RNA-binding protein Luc7-like 2	LUC7L2	46	2	0	7
Actin-like protein 6A	ACTL6A	47	2	0	7
Isoform 2 of DNA-directed RNA polymerase I subunit RPA2	POLR1B	122	5	0	7
Isoform 2 of Heterogeneous nuclear ribonucleoprotein M	HNRNPM	74	3	0	6
Splicing factor 3B subunit 2	SF3B2	100	4	0	6
Isoform 2 of Serrate RNA effector molecule homolog	SRRT	100	4	0	6
Luc7-like protein 3	LUC7L3	51	2	0	6
Isoform 2 of Cleavage and polyadenylation specificity factor subunit 7	CPSF7	51	2	0	6
U4/U6 small nuclear ribonucleoprotein Prp3	PRPF3	78	3	0	6
Isoform 2 of Histone-binding protein RBBP7	RBBP7	52	2	0	6
Isoform 2 of Interferon regulatory factor 4	IRF4	52	36	6	6
Isoform 2 of Gamma-interferon-inducible protein 16	IFI16	82	3	0	6
ATP synthase subunit beta, mitochondrial	ATP5B	57	2	0	6
Splicing factor 3B subunit 1	SF3B1	146	5	0	5
Isoform 2 of RNA-binding protein 39	RBM39	59	2	0	5
Isoform 2 of Heat shock protein HSP 90-alpha	HSP90AA1	98	3	0	5
Isoform 2 of 5'-3' exoribonuclease 2	XRN2	100	3	0	5
Splicing factor 3B subunit 3	SF3B3	136	4	0	5
DNA replication licensing factor MCM2	MCM2	102	3	0	5
Isoform 4 of Double-stranded RNA-specific adenine deaminase	ADAR	141	4	0	5
Procollagen galactyltransferase 1	GLT25D1	72	2	0	4
Isoform 2 of Protein SPT2 homolog	SPTY2D1	74	2	0	4
Heterogeneous nuclear ribonucleoprotein L	HNRNPL	64	17	4	4
Actin, cytoplasmic 1	ACTB	42	17	4	4
Isoform 2 of Transcription intermediary factor 1-beta	TRIM28	79	2	0	4
RNA-binding protein 27	RBM27	119	3	0	4
Coronin-1C	CORO1C	53	8	2	4
Isoform F of Constitutive coactivator of PPAR-gamma-like protein 1	FAM120A	125	3	0	4
Transducin beta-like protein 3	TBL3	89	2	0	4
ELAV-like protein 1	ELAVL1	36	7	2	4
Cell division cycle 5-like protein	CDC5L	92	2	0	3
Vigilin	HDLBP	141	3	0	3
Heterogeneous nuclear ribonucleoprotein H	HNRNPH1	49	10	3	3

Table G. 1 Proteins identified with TAP Analysis (cont.).

ATP synthase subunit alpha, mitochondrial	ATP5A1	60	10	3	3
Isoform 2 of Polypyrimidine tract-binding protein 1	PTBP1	59	10	3	3
Isoform 2 of DBIRD complex subunit KIAA1967	KIAA1967	103	2	0	3
Isoform 2 of RNA-binding protein 10	RBM10	103	2	0	3
Isoform 2 of Bcl-2-associated transcription factor 1	BCLAF1	106	2	0	3
Scaffold attachment factor B2	SAFB2	107	2	0	3
Cleavage and polyadenylation specificity factor subunit 1	CPSF1	161	3	0	3
Isoform 2 of Ataxin-2-like protein	ATXN2L	112	2	0	3
Isoform 2 of Probable ATP-dependent RNA helicase DHX36	DHX36	113	2	0	3
DNA damage-binding protein 1	DDB1	127	2	0	3
Probable ATP-dependent RNA helicase DDX23	DDX23	96	5	2	3
DNA-directed RNA polymerase I subunit RPA1	POLR1A	195	3	0	2
Isoform 2 of Probable ATP-dependent RNA helicase DDX17	DDX17	72	12	5	2
60S ribomal protein L27	RPL27	16	7	3	2
60S ribomal protein L30	RPL30	13	7	3	2
Non-POU domain-containing octamer-binding protein	NONO	54	24	12	2
Heterogeneous nuclear ribonucleoprotein R	HNRNPR	71	4	2	2
Isoform 2 of Splicing factor 1	SF1	69	4	2	2
Keratin, type I cytoskeletal 10	KRT10	59	19	10	2
Probable ATP-dependent RNA helicase DDX5	DDX5	69	13	7	2
DNA topoisomerase 1	TOP1	91	20	11	2
60S ribosomal protein L7a	RPL7A	30	7	4	2
40S ribosomal protein S19	RPS19	16	7	4	2
Splicing factor, proline- and glutamine-rich	SFPQ	76	26	15	2
Serine/arginine-rich splicing factor 3	SRSF3	19	5	3	2
40S ribosomal protein S3	RPS3	27	23	14	2
Isoform Short of Heterogeneous nuclear ribonucleoprotein U	HNRNPU	89	16	10	2
Isoform Short of Double-stranded RNA-binding protein Staufen homolog 1	STAU1	55	6	4	2
Poly [ADP-ribe] polymerase 1	PARP1	113	3	2	2
Thyroid hormone receptor-associated protein 3	THRAP3	109	3	2	2
Protein FRG1	FRG1	29	3	2	2
60S ribosomal protein L22	RPL22	15	3	2	2
60S ribosomal protein L34	RPL34	13	3	2	2
Histone H4	HIST1H4A	11	3	2	2

APPENDIX H: RAW SPECTRAL COUNTS OF BIOID SAMPLES

Raw spectral counts of the proteins for IRF4_BirA*, Only_BirA* and Unt. sample groups of 1st, 2nd and 3rd replicate of BioID are shown in Table H.1, arrangement of the proteins are same with Table 5.1.

Table H. 1 Raw spectral counts of BioID samples.

	1st replicate		2nd replicate			3rd replicate		
Gene Symbol	**IRF4 BirA***	**Only BirA***	**IRF4 BirA***	**Only BirA***	**Unt.**	**IRF4 BirA***	**Only BirA***	**Unt.**
IRF4	668	0	298	0	0	208	0	0
FUBP2	24	0	33	0	0	17	0	1
SF01	31	0	21	0	0	5	0	0
A6NEM2	20	0	13	0	0	10	0	0
SYNEM	23	0	29	0	0	12	0	2
BCLF1	7	0	27	0	0	9	0	0
TCPQ	2	0	16	0	0	21	0	0
SFPQ	35	0	55	0	0	22	2	6
RBP2	9	0	18	0	0	5	0	0
IPO7	7	0	14	0	0	7	0	0
IF4A3	4	0	12	0	0	12	0	0
CMC2	7	0	14	0	0	4	0	0
IMB1	6	0	11	0	0	7	0	0
STML2	3	0	8	0	0	14	0	0
PSPC1	11	0	7	0	0	4	0	0
NCOR1	10	0	7	0	0	5	0	0
RBM14	11	0	7	0	0	3	0	0
ADNP	4	0	12	0	0	7	0	0
HNRPM	7	0	13	0	0	9	1	2
SIN3A	7	0	10	0	0	7	2	0
MEF2D	8	0	7	0	0	3	0	0
CHAP1	4	0	11	0	0	4	0	0
ARI1A	3	0	12	0	0	3	0	0
TR150	14	0	37	6	7	20	0	0
PRPF3	3	0	12	0	0	10	0	2
BRD3	4	0	5	0	0	6	0	0
TBA1B	39	8	47	11	11	83	17	10
ZC3H4	3	0	8	0	0	3	0	0
SOX13	6	0	3	0	1	4	0	0

Table H.1 Raw spectral counts of BioID samples (cont.).

COR1B	10	0	5	3	0	4	0	0
P66B	4	0	10	0	0	3	2	0
IF4A1	8	0	16	4	5	29	8	2
UACA	4	0	18	0	0	20	8	0
FLNA	42	2	44	33	0	90	11	10
XRN2	3	0	7	0	0	3	0	0
BRD4	3	0	5	0	0	5	0	0
NONO	28	0	47	2	3	46	13	16
P66A	7	0	13	0	0	7	5	0
ROA2	10	0	41	0	0	49	16	15
ADT2	17	9	36	4	2	13	4	0
ROA1	10	2	32	0	0	22	4	10
LRC47	6	0	8	4	0	16	4	2
RBM27	4	0	4	0	0	2	0	0
RAD50	1	0	6	0	0	4	0	0
KPYM	9	0	7	0	1	3	0	3
PCBP1	2	0	4	0	0	7	2	1
LMNA	7	0	33	3	0	39	7	15
PLEC	133	22	403	22	71	545	153	163
TBB5	28	6	15	7	5	24	10	11
RS7	8	0	41	6	7	37	15	12
CAND1	2	0	5	0	0	1	0	0
DYHC1	79	2	60	5	15	38	0	33
FLNA	5	0	3	3	0	3	0	0
PDS5A	8	3	17	3	5	12	4	5
PERQ2	19	0	24	3	10	18	0	7
ZC11A	11	4	26	17	11	18	4	3
CDK12	4	0	4	0	2	6	0	2
GOGA2	3	0	10	3	4	5	0	0
EP300	13	0	11	7	9	9	1	1
SF3B1	11	2	39	3	9	36	0	16
BI2L1	4	0	5	0	0	5	5	0
KINH	2	0	3	0	0	3	2	0
TBB2A	2	0	2	0	1	2	0	0
ATX2L	6	0	13	0	4	7	0	5
NUMA1	15	0	40	19	17	23	2	10
SF3B2	4	0	10	2	0	9	0	7
VIGLN	23	0	21	2	5	34	8	24
DDX17	4	3	12	3	3	8	1	6
RS16	37	26	53	65	37	76	36	26

Table H.1 Raw spectral counts of BioID samples (cont.).

IF4A2	1	0	2	0	0	1	0	0

APPENDIX I: ENDOGENOUS IRF4 PULLDOWN (INCLUDING GOAT IGG)

IRF4(M-17) blotting showed a band at the size of IRF4 in negative control Goat IgG. However, this Goat IgG is a bit old, and we also observed before that when IgGs are old, they tend to show high background. Although, there is a background in Goat IgG, the IRF4 band observed for IRF4(M-17) sample is higher, therefore endogenous IRF4 pulldown can still be concluded to be successful (Figure I.1).

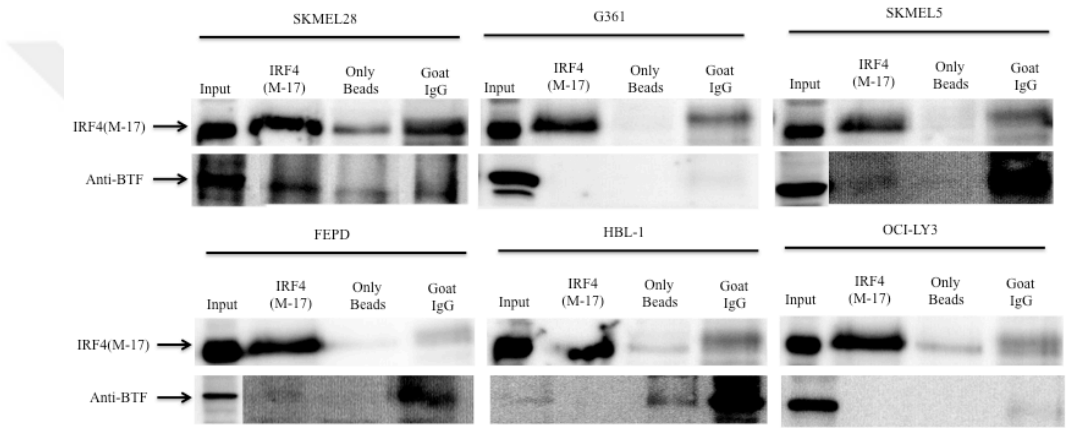

Figure I. 1 Blotting of Endogenous IRF4 Pulldown samples, including Goat IgG with IRF4(M-17) and anti-BTF (Abcam) antibodies. Eventhough Goat IgG showed IRF4 band when blotted with IRF4(M-17) antibody, still the IRF4 band in IRF4(M-17) sample is bolder.

REFERENCES

Chin, L., L. A. Garraway, and D. E. Fisher. 2006, "Malignant melanoma: genetics and therapeutics in the genomic era", *Genes Dev,* Vol. 20, No. 16, pp. 2149-2182.

Costin, G. E., and V. J. Hearing. 2007, "Human skin pigmentation: melanocytes modulate skin color in response to stress", *FASEB J,* Vol. 21, No. 4, pp. 976-994.

De Silva, N. S., G. Simonetti, N. Heise, and U. Klein. 2012, "The diverse roles of IRF4 in late germinal center B-cell differentiation", *Immunol Rev,* Vol. 247, No. 1, pp. 73-92.

Dingar, D., M. Kalkat, P. K. Chan, T. Srikumar, S. D. Bailey, W. B. Tu, E. Coyaud, R. Ponzielli, M. Kolyar, I. Jurisica, et al., 2015, "BioID identifies novel c-MYC interacting partners in cultured cells and xenograft tumors", *J Proteomics,* Vol. 118, No., pp. 95-111.

Diz, A. P., A. Carvajal-Rodriguez, and D. O. Skibinski. 2011, "Multiple hypothesis testing in proteomics: a strategy for experimental work", *Mol Cell Proteomics,* Vol. 10, No. 3, pp. M110 004374.

Duffy, D. L., M. M. Iles, D. Glass, G. Zhu, J. H. Barrett, V. Hoiom, Z. Z. Zhao, R. A. Sturm, N. Soranzo, C. Hammond, et al., 2010, "IRF4 variants have age-specific effects on nevus count and predispose to melanoma", *Am J Hum Genet,* Vol. 87, No. 1, pp. 6-16.

Edgar, R., M. Domrachev, and A. E. Lash. 2002, "Gene Expression Omnibus: NCBI gene expression and hybridization array data repository", *Nucleic Acids Res,* Vol. 30, No. 1, pp. 207-210.

Eguchi, J., Q. W. Yan, D. E. Schones, M. Kamal, C. H. Hsu, M. Q. Zhang, G. E. Crawford, and E. D. Rosen. 2008, "Interferon regulatory factors are transcriptional regulators of adipogenesis", *Cell Metab,* Vol. 7, No. 1, pp. 86-94.

Einhauer, A., and A. Jungbauer. 2001, "The FLAG peptide, a versatile fusion tag for the purification of recombinant proteins", *J Biochem Biophys Methods,* Vol. 49, No. 1-3, pp. 455-465.

Emili, A., M. Shales, S. McCracken, W. Xie, P. W. Tucker, R. Kobayashi, B. J. Blencowe, and C. J. Ingles. 2002, "Splicing and transcription-associated proteins PSF and p54nrb/nonO bind to the RNA polymerase II CTD", *RNA,* Vol. 8, No. 9, pp. 1102-1111.

Ettinger, R., G. P. Sims, A. M. Fairhurst, R. Robbins, Y. S. da Silva, R. Spolski, W. J. Leonard, and P. E. Lipsky. 2005, "IL-21 induces differentiation of human naive and memory B cells into antibody-secreting plasma cells", *J Immunol,* Vol. 175, No. 12, pp. 7867-7879.

Fox, A. H., C. S. Bond, and A. I. Lamond. 2005, "P54nrb forms a heterodimer with PSP1 that localizes to paraspeckles in an RNA-dependent manner", *Mol Biol Cell,* Vol. 16, No. 11, pp. 5304-5315.

Gathany, A. H., P. Hartge, S. Davis, J. R. Cerhan, R. K. Severson, W. Cozen, N. Rothman, S. J. Chanock, and S. S. Wang. 2009, "Relationship between interferon regulatory factor 4 genetic polymorphisms, measures of sun sensitivity and risk for non-Hodgkin lymphoma", *Cancer Causes Control,* Vol. 20, No. 8, pp. 1291-1302.

Grossman, A., H. W. Mittrucker, J. Nicholl, A. Suzuki, S. Chung, L. Antonio, S. Suggs, G. R. Sutherland, D. P. Siderovski, and T. W. Mak. 1996, "Cloning of human

lymphocyte-specific interferon regulatory factor (hLSIRF/hIRF4) and mapping of the gene to 6p23-p25", *Genomics,* Vol. 37, No. 2, pp. 229-233.

Grumont, R. J., and S. Gerondakis. 2000, "Rel induces interferon regulatory factor 4 (IRF-4) expression in lymphocytes: modulation of interferon-regulated gene expression by rel/nuclear factor kappaB", *J Exp Med,* Vol. 191, No. 8, pp. 1281-1292.

Guo, S., Z. Z. Li, D. S. Jiang, Y. Y. Lu, Y. Liu, L. Gao, S. M. Zhang, H. Lei, L. H. Zhu, X. D. Zhang, et al., 2014, "IRF4 is a novel mediator for neuronal survival in ischaemic stroke", *Cell Death Differ,* Vol. 21, No. 6, pp. 888-903.

Gupta, S., M. Jiang, A. Anthony, and A. B. Pernis. 1999, "Lineage-specific modulation of interleukin 4 signaling by interferon regulatory factor 4", *J Exp Med,* Vol. 190, No. 12, pp. 1837-1848.

Hallier, M., A. Tavitian, and F. Moreau-Gachelin. 1996, "The transcription factor Spi-1/PU.1 binds RNA and interferes with the RNA-binding protein p54nrb", *J Biol Chem,* Vol. 271, No. 19, pp. 11177-11181.

Han, J., A. A. Qureshi, H. Nan, J. Zhang, Y. Song, Q. Guo, and D. J. Hunter. 2011, "A germline variant in the interferon regulatory factor 4 gene as a novel skin cancer risk locus", *Cancer Res,* Vol. 71, No. 5, pp. 1533-1539.

Hanahan, D., and R. A. Weinberg. 2000, "The hallmarks of cancer", *Cell,* Vol. 100, No. 1, pp. 57-70.

Hu, C. M., S. Y. Jang, J. C. Fanzo, and A. B. Pernis. 2002, "Modulation of T cell cytokine production by interferon regulatory factor-4", *J Biol Chem,* Vol. 277, No. 51, pp. 49238-49246.

Huber, L. A., 2003, "Is proteomics heading in the wrong direction?", *Nat Rev Mol Cell Biol,* Vol. 4, No. 1, pp. 74-80.

Jiang, D. S., Z. Y. Bian, Y. Zhang, S. M. Zhang, Y. Liu, R. Zhang, Y. Chen, Q. Yang, X. D. Zhang, G. C. Fan, et al., 2013, "Role of interferon regulatory factor 4 in the regulation of pathological cardiac hypertrophy", *Hypertension,* Vol. 61, No. 6, pp. 1193-1202.

Kasof, G. M., L. Goyal, and E. White. 1999, "Btf, a novel death-promoting transcriptional repressor that interacts with Bcl-2-related proteins", *Mol Cell Biol,* Vol. 19, No. 6, pp. 4390-4404.

Kiesler, E., F. Miralles, A. K. Ostlund Farrants, and N. Visa. 2003, "The Hrp65 self-interaction is mediated by an evolutionarily conserved domain and is required for nuclear import of Hrp65 isoforms that lack a nuclear localization signal", *J Cell Sci,* Vol. 116, No. Pt 19, pp. 3949-3956.

Kong, S., S. J. Kim, B. Sandal, S. M. Lee, B. Gao, D. D. Zhang, and D. Fang. 2011, "The type III histone deacetylase Sirt1 protein suppresses p300-mediated histone H3 lysine 56 acetylation at Bclaf1 promoter to inhibit T cell activation", *J Biol Chem,* Vol. 286, No. 19, pp. 16967-16975.

Kornblihtt, A. R., M. de la Mata, J. P. Fededa, M. J. Munoz, and G. Nogues. 2004, "Multiple links between transcription and splicing", *RNA,* Vol. 10, No. 10, pp. 1489-1498.

Kuphal, S., and A. Bosserhoff. 2009, "Recent progress in understanding the pathology of malignant melanoma", *J Pathol,* Vol. 219, No. 4, pp. 400-409.

Kwon, H., D. Thierry-Mieg, J. Thierry-Mieg, H. P. Kim, J. Oh, C. Tunyaplin, S. Carotta, C. E. Donovan, M. L. Goldman, P. Tailor, et al., 2009, "Analysis of interleukin-21-induced Prdm1 gene regulation reveals functional cooperation of STAT3 and IRF4 transcription factors", *Immunity,* Vol. 31, No. 6, pp. 941-952.

Lambert, J. P., M. Tucholska, C. Go, J. D. Knight, and A. C. Gingras. 2015, "Proximity biotinylation and affinity purification are complementary approaches for the interactome mapping of chromatin-associated protein complexes", *J Proteomics,* Vol. 118, No., pp. 81-94.

Levy, C., M. Khaled, and D. E. Fisher. 2006, "MITF: master regulator of melanocyte development and melanoma oncogene", *Trends Mol Med,* Vol. 12, No. 9, pp. 406-414.

Mathur, M., P. W. Tucker, and H. H. Samuels. 2001, "PSF is a novel corepressor that mediates its effect through Sin3A and the DNA binding domain of nuclear hormone receptors", *Mol Cell Biol,* Vol. 21, No. 7, pp. 2298-2311.

Merz, C., H. Urlaub, C. L. Will, and R. Luhrmann. 2007, "Protein composition of human mRNPs spliced in vitro and differential requirements for mRNP protein recruitment", *RNA,* Vol. 13, No. 1, pp. 116-128.

Nagulapalli, S., and M. L. Atchison. 1998, "Transcription factor Pip can enhance DNA binding by E47, leading to transcriptional synergy involving multiple protein domains", *Mol Cell Biol,* Vol. 18, No. 8, pp. 4639-4650.

Nan, H., P. Kraft, A. A. Qureshi, Q. Guo, C. Chen, S. E. Hankinson, F. B. Hu, G. Thomas, R. N. Hoover, S. Chanock, et al., 2009, "Genome-wide association study of tanning phenotype in a population of European ancestry", *J Invest Dermatol,* Vol. 129, No. 9, pp. 2250-2257.

Osman, A., 2004, "Yeast two-hybrid assay for studying protein-protein interactions", *Methods Mol Biol,* Vol. 270, No., pp. 403-422.

Passon, D. M., M. Lee, O. Rackham, W. A. Stanley, A. Sadowska, A. Filipovska, A. H. Fox, and C. S. Bond. 2012, "Structure of the heterodimer of human NONO and paraspeckle protein component 1 and analysis of its role in subnuclear body formation", *Proc Natl Acad Sci U S A,* Vol. 109, No. 13, pp. 4846-4850.

Phizicky, E. M., and S. Fields. 1995, "Protein-protein interactions: methods for detection and analysis", *Microbiol Rev,* Vol. 59, No. 1, pp. 94-123.

Pongubala, J. M., S. Nagulapalli, M. J. Klemsz, S. R. McKercher, R. A. Maki, and M. L. Atchison. 1992, "PU.1 recruits a second nuclear factor to a site important for immunoglobulin kappa 3' enhancer activity", *Mol Cell Biol,* Vol. 12, No. 1, pp. 368-378.

Praetorius, C., C. Grill, S. N. Stacey, A. M. Metcalf, D. U. Gorkin, K. C. Robinson, E. Van Otterloo, R. S. Kim, K. Bergsteinsdottir, M. H. Ogmundsdottir, et al., 2013, "A polymorphism in IRF4 affects human pigmentation through a tyrosinase-dependent MITF/TFAP2A pathway", *Cell,* Vol. 155, No. 5, pp. 1022-1033.

Prasanth, K. V., S. G. Prasanth, Z. Xuan, S. Hearn, S. M. Freier, C. F. Bennett, M. Q. Zhang, and D. L. Spector. 2005, "Regulating gene expression through RNA nuclear retention", *Cell,* Vol. 123, No. 2, pp. 249-263.

Puig, O., F. Caspary, G. Rigaut, B. Rutz, E. Bouveret, E. Bragado-Nilsson, M. Wilm, and B. Seraphin. 2001, "The tandem affinity purification (TAP) method: a general procedure of protein complex purification", *Methods,* Vol. 24, No. 3, pp. 218-229.

Rengarajan, J., K. A. Mowen, K. D. McBride, E. D. Smith, H. Singh, and L. H. Glimcher. 2002, "Interferon regulatory factor 4 (IRF4) interacts with NFATc2 to modulate interleukin 4 gene expression", *J Exp Med,* Vol. 195, No. 8, pp. 1003-1012.

Rhodes, D. R., J. Yu, K. Shanker, N. Deshpande, R. Varambally, D. Ghosh, T. Barrette, A. Pandey, and A. M. Chinnaiyan. 2004, "ONCOMINE: a cancer microarray database and integrated data-mining platform", *Neoplasia,* Vol. 6, No. 1, pp. 1-6.

Roux, K. J., D. I. Kim, M. Raida, and B. Burke. 2012, "A promiscuous biotin ligase fusion protein identifies proximal and interacting proteins in mammalian cells", *J Cell Biol,* Vol. 196, No. 6, pp. 801-810.

Sarras, H., S. Alizadeh Azami, and J. P. McPherson. 2010, "In search of a function for BCLAF1", *ScientificWorldJournal,* Vol. 10, No., pp. 1450-1461.

Schiffner, S., N. Zimara, R. Schmid, and A. K. Bosserhoff. 2011, "p54nrb is a new regulator of progression of malignant melanoma", *Carcinogenesis,* Vol. 32, No. 8, pp. 1176-1182.

Schmid, R., S. Schiffner, A. Opolka, S. Grassel, T. Schubert, M. Moser, and A. K. Bosserhoff. 2010, "Enhanced cartilage regeneration in MIA/CD-RAP deficient mice", *Cell Death Dis,* Vol. 1, No., pp. e97.

Shaffer, A. L., N. C. Emre, P. B. Romesser, and L. M. Staudt. 2009, "IRF4: Immunity. Malignancy! Therapy?", *Clin Cancer Res,* Vol. 15, No. 9, pp. 2954-2961.

Slipicevic, A., R. Holm, M. T. Nguyen, P. J. Bohler, B. Davidson, and V. A. Florenes. 2005, "Expression of activated Akt and PTEN in malignant melanomas: relationship with clinical outcome", *Am J Clin Pathol,* Vol. 124, No. 4, pp. 528-536.

Sundram, U., J. D. Harvell, R. V. Rouse, and Y. Natkunam. 2003, "Expression of the B-cell proliferation marker MUM1 by melanocytic lesions and comparison with S100, gp100 (HMB45), and MelanA", *Mod Pathol,* Vol. 16, No. 8, pp. 802-810.

Teigelkamp, S., C. Mundt, T. Achsel, C. L. Will, and R. Luhrmann. 1997, "The human U5 snRNP-specific 100-kD protein is an RS domain-containing, putative RNA helicase with significant homology to the yeast splicing factor Prp28p", *RNA,* Vol. 3, No. 11, pp. 1313-1326.

Teo, G., G. Liu, J. Zhang, A. I. Nesvizhskii, A. C. Gingras, and H. Choi. 2014, "SAINTexpress: improvements and additional features in Significance Analysis of IN-Teractome software", *J Proteomics,* Vol. 100, No., pp. 37-43.

Vultur, A., and M. Herlyn. 2013, "SnapShot: melanoma", *Cancer Cell,* Vol. 23, No. 5, pp. 706-706 e701.

Wu, H., V. Goel, and F. G. Haluska. 2003, "PTEN signaling pathways in melanoma", *Oncogene,* Vol. 22, No. 20, pp. 3113-3122.

Yang, Y., A. L. Shaffer, 3rd, N. C. Emre, M. Ceribelli, M. Zhang, G. Wright, W. Xiao, J. Powell, J. Platig, H. Kohlhammer, et al., 2012, "Exploiting synthetic lethality for the therapy of ABC diffuse large B cell lymphoma", *Cancer Cell,* Vol. 21, No. 6, pp. 723-737.

Yang, Y., J. Wu, A. Demir, M. Castillo-Martin, R. D. Melamed, G. Zhang, M. Fukunaga-Kanabis, R. Perez-Lorenzo, B. Zheng, D. N. Silvers, et al., 2013, "GAB2 induces tumor angiogenesis in NRAS-driven melanoma", *Oncogene,* Vol. 32, No. 31, pp. 3627-3637.

Zheng, Y., A. Chaudhry, A. Kas, P. deRoos, J. M. Kim, T. T. Chu, L. Corcoran, P. Treuting, U. Klein, and A. Y. Rudensky. 2009, "Regulatory T-cell suppressor program co-opts transcription factor IRF4 to control T(H)2 responses", *Nature,* Vol. 458, No. 7236, pp. 351-356.

Zhou, X., X. Li, Y. Cheng, W. Wu, Z. Xie, Q. Xi, J. Han, G. Wu, J. Fang, and Y. Feng. 2014, "BCLAF1 and its splicing regulator SRSF10 regulate the tumorigenic potential of colon cancer cells", *Nat Commun,* Vol. 5, No., pp. 4581.

Aebersold, R., and M. Mann. 2003, "Mass spectrometry-based proteomics", *Nature,* Vol. 422, No. 6928, pp. 198-207.

Alves, G., and Y. K. Yu. 2015, "Mass spectrometry-based protein identification with accurate statistical significance assignment", *Bioinformatics,* Vol. 31, No. 5, pp. 699-706.

Barretina, J., G. Caponigro, N. Stransky, K. Venkatesan, A. A. Margolin, S. Kim, C. J. Wilson, J. Lehar, G. V. Kryukov, D. Sonkin, et al., 2012, "The Cancer Cell Line Encyclopedia enables predictive modelling of anticancer drug sensitivity", *Nature,* Vol. 483, No. 7391, pp. 603-607.

Berggard, T., S. Linse, and P. James. 2007, "Methods for the detection and analysis of protein-protein interactions", *Proteomics,* Vol. 7, No. 16, pp. 2833-2842.

Bernstein, B. E., J. A. Stamatoyannopoulos, J. F. Costello, B. Ren, A. Milosavljevic, A. Meissner, M. Kellis, M. A. Marra, A. L. Beaudet, J. R. Ecker, et al., 2010, "The NIH Roadmap Epigenomics Mapping Consortium", *Nat Biotechnol,* Vol. 28, No. 10, pp. 1045-1048.

Bornhorst, J. A., and J. J. Falke. 2000, "Purification of proteins using polyhistidine affinity tags", *Methods Enzymol,* Vol. 326, No., pp. 245-254.

Bosserhoff, A. K., 2005, "Melanoma inhibitory activity (MIA): an important molecule in melanoma development and progression", *Pigment Cell Res,* Vol. 18, No. 6, pp. 411-416.

Bosserhoff, K. a., 2009, "Recent progress in understanding the pathology of malignant melanoma", *Journal of Pathology,* Vol. 219, No. 4, pp. 400-409.

Bruckner, A., C. Polge, N. Lentze, D. Auerbach, and U. Schlattner. 2009, "Yeast two-hybrid, a powerful tool for systems biology", *Int J Mol Sci,* Vol. 10, No. 6, pp. 2763-2788.

Ch'ng, S., and S. T. Tan. 2009, "Genetics, cellular biology and tumor microenvironment of melanoma", *Front Biosci (Landmark Ed),* Vol. 14, No., pp. 918-928.